Self-gravitating Interferometry and Intrinsic Decoherence

by

David William Francisco Gooding

B.Sc., Simon Fraser University, 2008

A THESIS SUBMITTED IN PARTIAL FULFILLMENT OF
THE REQUIREMENTS FOR THE DEGREE OF

DOCTOR OF PHILOSOPHY

in

The Faculty of Graduate and Postdoctoral Studies

(Physics)

THE UNIVERSITY OF BRITISH COLUMBIA

(Vancouver)

April 2015

Abstract

To investigate the possibility that an intrinsic form of gravitational decoherence can be theoretically demonstrated within canonical quantum gravity, we develop a model of a self-gravitating interferometer, and analyze the WKB regime of its reduced phase space quantization. We search for evidence in the resulting interference pattern that general relativity necessarily places limits on coherence, due to the inherent ambiguity associated with forming superpositions of geometries. We construct the "beam" of the interferometer out of WKB states for an infinitesimally thin shell of matter, and work in spherical symmetry to eliminate the occurrence of gravitational waves. For internal consistency, we encode information about the beam optics within the dynamics of the shell itself, by arranging an ideal fluid on the surface of the shell with an equation of state that enforces beam-splitting and reflections.

The interferometric analysis is performed for single-mode inputs, and coherence is shown to be fully present regardless of gravitational self-interaction. Next we explore the role coordinate choices play in our description of the interferometer, by considering a family of generalized coordinate systems and their corresponding quantizations. Included in this family are the Painlevé-Gullstrand coordinates, which are related to a network of infalling observers that are asymptotically at rest, and the Eddington-Finkelstein coordinates, which are related to a network of infalling observers that travel at the speed of light. We then introduce another model, obtained by adding to the shell a harmonic oscillator as an internal degree of freedom. The internal oscillator evolves with respect to the local proper time of the shell, and therefore serves as a clock that ticks differently depending on the shell's position and momentum. If we focus only on the external dynamics, we must trace out the clock degree of freedom, and this results in a form of intrinsic decoherence that shares some features with a recently-proposed "universal" decoherence mechanism attributed to gravitational time dilation. We discuss some variations of this proposal, and point out a way to bootstrap the gravitational contribution to the time dilation decoherence with self-gravitation. We interpret this as a fundamentally gravitational intrinsic decoherence effect.

Preface

All of the research presented in this thesis was conducted under the supervision of Bill Unruh while the author attended UBC.

Much of the material in Chapters 1 and 2 has been published in Physical Review D under the title "Self-gravitating interferometry and intrinsic decoherence" [1]. This publication was co-authored by Bill Unruh. With Bill's direction, the author of this dissertation performed the calculations, generated the figures, and did the majority of the writing.

Some of the material in Chapter 3 was done in collaboration with Friedemann Queisser, a postdoctoral fellow at UBC. Friedemann first brought to the author's attention the generalized family of coordinates presented in [68], and contributed notes to Sections 3.4-3.5.

The content of Chapter 4 went into a paper entitled "Bootstrapping Time Dilation Decoherence," co-authored by Bill Unruh, that was submitted on Jan. 25th, 2015 as an invited contribution to a special issue of Foundations of Physics ("Probing the limits of quantum mechanics: theory and experiment"). The material was written entirely by the author of this dissertation, with guidance from Bill.

Table of Contents

Table of Contents

List of Figures

Acknowledgements

Dedication

To Ashley, for her encouragement and support.

Chapter 1

Introduction

1.1 Preliminary Considerations

Ever since the discovery by Hawking in the early 1970s that black holes emit thermal radiation due to quantum effects [2], it has been a major goal in theoretical physics to understand the connections between general relativity, quantum theory, and thermodynamics. The four laws of black hole mechanics [3] themselves closely resemble thermodynamic laws, with horizon area playing the role of an entropy (as pointed out by Bekenstein [4]), and Hawking's discovery of black hole evaporation indicated that this was more than just a resemblance: a black hole was shown to have a temperature equal to $1/2\pi$ times its surface gravity, and an entropy of $1/4$ times the area of its event horizon (in natural units, $c = G = \hbar = 1$).

There still remain many open questions about the role of entropy in gravitational systems, as well as possible quantum-mechanical origins. One might hope that a complete theory of quantum gravity would answer such questions, but until such a theory is formulated we have to settle for partial pictures coming from approximation schemes. Black hole radiation, for instance, was demonstrated within the framework of quantum field theory in curved spacetime, which approximates the spacetime as being fixed and the quantum field as being a negligible perturbation that does not significantly affect the curvature of the spacetime.

One of the major goals of this thesis is to determine the consequences of eliminating the assumption of a fixed background spacetime on the application of quantum theory to gravitational systems. It is not possible to accomplish this in general, so we will find an appropriate (idealized) arena for our exploration, and work within a particular approximation scheme in order to formulate tractable problems. Though it may be incorrect to simply "quantize" general relativity, as the Einstein equation could emerge from an underlying theory as an equation of state [5], for the purposes of this thesis we will consider the spacetime metric a fundamental degree of freedom, and work within canonical quantum gravity.

Apart from the specific issues raised by quantum field theory in curved

spacetimes, it is in general becoming more and more important to understand systems for which both quantum and general relativistic effects are important (see [6]-[8] for some recent experimental examples, though an exhaustive discussion of such systems is beyond the scope of this thesis). It has also become increasingly clear that our current conceptual understanding of quantum gravitational systems is severely lacking. This lack of understanding inspires us to study such systems, and the clash between quantum theory (QT) and general relativity (GR), in hope that we may find guidance towards a resolution of the many technical and conceptual problems one faces when attempting to unify these two pillars of physics.

1.2   The Universe of this Nutshell

The specific purpose of this work is to explore an ambiguity that results from taking both QT and GR seriously: quantum superpositions of different matter states are associated with different spacetime geometries, and hence different definitions of time evolution; how, then, can we use a single time-evolution operator to evolve superpositions of distinct spacetimes? Since the 1980s, Roger Penrose has been arguing that this ambiguity results in an instability, and that in turn this instability leads to a type of "decay" that reduces the system to a state with a single well-defined geometry [9].

Let us sketch the line of reasoning Penrose uses to reach this conclusion [10]. Suppose we have two quantum states, $|\psi\rangle$ and $|\chi\rangle$, which represent two static mass distributions, each with the same energy E but localized in different places. Neglecting gravity, both of these states will be "stationary," meaning that each will be an eigenfunction of the appropriate Hamiltonian operator H. Accordingly, we will have $H|\psi\rangle = E|\psi\rangle$ and $H|\chi\rangle = E|\chi\rangle$, and by the superposition principle we will also have

$$H\left(\alpha|\psi\rangle + \beta|\chi\rangle\right) = E\left(\alpha|\psi\rangle + \beta|\chi\rangle\right), \tag{1.1}$$

for any (complex) α, β. This tells us that the arbitrary superposition $\alpha|\psi\rangle + \beta|\chi\rangle$ is also stationary, as it is an eigenstate of the Hamiltonian H with energy E.

In GR, gravity is a consequence of the manner in which a distribution of mass/energy curves space and time. Thus, to incorporate gravity into our description, we associate each mass distribution with a spacetime geometry, and therefore each of the states $|\psi\rangle$ and $|\chi\rangle$ a geometry state (denoted by $|G_\psi\rangle$ and $|G_\chi\rangle$, respectively). The superposed state then takes the form

$$\alpha|\psi\rangle|G_\psi\rangle + \beta|\chi\rangle|G_\chi\rangle. \tag{1.2}$$

2

Is *this* superposition "stationary"? One should keep in mind that in GR, a spacetime is considered stationary if there exists a timelike Killing vector T, which generates time-translations. Penrose then regards this T as the differential operator $\partial/\partial t$ for the spacetime, and interprets quantum states that are eigenstates of T to be stationary states, since they have well-defined energies. Explicitly, $|\Psi\rangle$ is considered stationary if

$$T|\Psi\rangle = -iE_\Psi|\Psi\rangle, \tag{1.3}$$

for some energy E_Ψ.

One then faces a problem, when trying to understand the superposed state (1.2): there is no longer a specific timelike Killing vector, since there is no longer a specific spacetime. GR tells us that we cannot in general compare two spacetimes unambiguously through point-wise identification, so we therefore do not have an unambiguous differential operator with which to define time-translation. This also prevents us from defining "stationary states" as the eigenvectors of such an operator.

If the states $|\psi\rangle$ and $|\chi\rangle$ are very similar, then we can identify points in the corresponding spacetimes in an approximate way. In the Newtonian limit, for instance, we can identify the time coordinate t of the two spacetimes, but even then we can not identify individual points of the spatial geometries. In other words, there is a correspondence between the spatial slices of one spacetime with the spatial slices of the other, but not between the points of a spatial slice of one spacetime with the points of a spatial slice of the other. This ambiguity in point-wise identification of spatial slices directly implies an essential ill-definedness in the notion of a time-translation, since although the time coordinates of the two spacetimes can be identified, it is the structure of the remaining (spatial) coordinates that defines the time-translation operator.

Penrose then suggests that we can quantify the difference between two (similar) spacetimes with the scalar quantity

$$(\boldsymbol{f}_\psi - \boldsymbol{f}_\chi)^2 = (\boldsymbol{f}_\psi - \boldsymbol{f}_\chi) \cdot (\boldsymbol{f}_\psi - \boldsymbol{f}_\chi), \tag{1.4}$$

with $\boldsymbol{f}_\psi$ and $\boldsymbol{f}_\chi$ being the acceleration 3-vectors of geodesic (free-fall) motions of the associated spacetimes. From a Newtonian perspective, $\boldsymbol{f}_\psi$ and $\boldsymbol{f}_\chi$ represent the Newtonian gravitational force-per-unit-test-mass (also called simply the gravitational field), at a particular point, in each space-time [10].

The *total* measure of incompatibility (or "uncertainty," as Penrose calls it) can be obtained by integrating (1.4) over a spatial slice. We will call the

resulting quantity Δ_G. For concreteness, Penrose uses a flat spatial metric for the integration, in which case the spatial integral of (1.4) yields

$$\Delta_G = -4\pi \int \int d^3x \, d^3y \, \frac{(\rho_\psi(\boldsymbol{x}) - \rho_\chi(\boldsymbol{x}))\,(\rho_\psi(\boldsymbol{y}) - \rho_\chi(\boldsymbol{y}))}{|\boldsymbol{x} - \boldsymbol{y}|}, \qquad (1.5)$$

with the mass density ρ connected to the gravitational field $\boldsymbol{f}$ via the Newtonian gravitational equation (Gauss's law) $\nabla \cdot \boldsymbol{f} = -4\pi\rho$. The quantity Δ_G is effectively the gravitational self-energy of the difference between the two mass distributions. Penrose thinks of Δ_G as an energy uncertainty associated with the superposition of geometries, and hypothesizes that this energy uncertainty makes the superposition *unstable*. In analogy with a radioactive nucleus, or any other unstable particle, we can use the time-energy uncertainty principle to estimate the lifetime of the superposition, $\Delta t \sim 1/\Delta_G$, after which there is a significant probability that the superposition will "decay" into one geometry or the other. A consequence of this lifetime estimate is that as the geometries associated with each element of the superposition become arbitrarily different, the superposition becomes arbitrarily unstable, and decays after an arbitrarily short time.

It is not clear from Penrose's work, however, whether some sort of "collapse" occurs, or whether there is simply a form of "intrinsic" decoherence that removes phase correlations between states associated with sufficiently different geometries. In this thesis, we consider the latter, and discuss whether or not a direct application of both QT and GR is enough to demonstrate the existence of this new type of "intrinsic" decoherence.

By "intrinsic" decoherence, we mean a decoherence effect that arises solely out of the internal behaviour of an isolated system, and not due to its interaction with the external world. For example, if we use a buckyball in a double-slit experiment, and prepare one of the slits to excite internal degrees of freedom of the buckyball, then the internal degrees of freedom carry "which-way" information and decohere the center-of-mass degree of freedom [11]. More generally, if a system carries an internal clock and is in a superposition of states corresponding to two paths that have different proper times associated with them, then again the internal clock read at the interference screen could provide which-way information, and decohere the center-of-mass [12]-[14].

Whereas the decoherence produced by entangling internal degrees of freedom to a center-of-mass coordinate could be considered "third-party" decoherence [15], what we are primarily concerned with here is whether or not there is something about the quantum effect of a system's gravity on the system itself that could lead to such intrinsic decoherence. Penrose's

intuition says yes: the path a mass takes alters the associated spacetime and especially the flow of time. Since the quantum phase is determined by the flow of time, the phase evolution is also altered by which path the mass takes. When one tries to interfere the two paths, these "random" phases (because it is impossible to uniquely map one spacetime onto another) cause decoherence. It is this *gravitational* intrinsic decoherence that we explore here.

There are several proposals in the literature for a mechanism to describe intrinsic forms of gravitational decoherence [16]-[18], and other proposals for intrinsic decoherence mechanisms that are merely inspired by tension between QT and GR [19]-[21]. Many of these approaches incorporate alterations to known physics, such as adding stochastic [21] or nonlinear [22]-[24] terms to the Schrödinger equation, in order to achieve the desired decoherence effect. Such alterations are often ad hoc, and have historically faced difficulties maintaining consistency with experimental constraints; nonlinear additions to the Schrödinger equation, for instance, have been shown under a wide range of conditions to lead to either superluminal signal propagation or to communication between different branches of the wavefunction [25]. While it may be possible to obtain a sensible theory that allows communication between different wavefunction branches [26], it remains to be seen whether a consistent interpretation results from this alteration. Instead, we take Penrose's initial arguments at face value, and entertain the possibility that a consistent combination of QT and GR can explain (gravitational) intrinsic decoherence without any assumptions about new physics.

Now, it is well-known that gravitational waves can carry away information from a system in a manner analogous to standard decoherence [27], [28]. Penrose's suggestion is independent of such standard gravitational-wave-induced decoherence, so to distinguish between the two we will work in spherical symmetry. The restriction to spherical symmetry is not only a technical simplification, but avoids the occurrence of gravitational waves altogether.

Because this exploration requires both QT and GR, we will naturally be faced with some serious difficulties, which we will have to either overcome, sidestep, or ignore [29]. For instance, we will avoid issues with the factor-ordering ambiguity by working in the WKB[1] regime (as in [30]), and we will avoid issues with perturbative non-renormalizability by working in minisuperspace (i.e. enforcing spherical symmetry) and employing a reduced

---

[1]By "WKB," we mean "Wentzel-Kramers-Brillouin."

phase space approximation (as in [31])[2]. It is still unclear what the exact connection is between the reduced phase space approximation, obtained by solving the GR constraints classically and then quantizing the reduced theory, and the standard Dirac quantization, obtained by quantizing the theory in the full kinematical Hilbert space and then enforcing the constraints at the quantum level. Following Hawking's path integral approach to quantum gravity [32], Halliwell has made some progress elucidating the connection between reduced phase space minisuperspace quantization and the standard Dirac approach in special cases [33], but in general the connection is not well understood. Nonetheless, the limit we will work in has a rich structure, and in this thesis we will explore whether or not it has a rich enough structure to contain evidence of intrinsic decoherence caused by gravity.

Since we aim to test whether or not gravity places a fundamental limit on the coherence of quantum systems, we develop a model of a self-gravitating interferometer. Interferometers are ideal for studying coherence, because interference is a key feature of coherent systems. We describe how the same interferometer would behave in the absence of gravity, and then we investigate the consequences of general relativistic corrections to this behaviour. In an interferometric setting, the intrinsic decoherence we seek to understand manifests itself as a phase-scrambling along different interferometer arms (for a general discussion see [34]), which in this case is attributed to gravity. According to Penrose, we should expect that the (interferometric) coherence should decay as the arm-length increases indefinitely, since this would correspond to a superposition of arbitrarily different spacetimes. We focus on the possibility that no collapse occurs, so we will simply analyze the interference pattern and search for departures from non-gravitational behaviour that indicate coherence loss. Conceptually, we are testing the idea that when one forms superpositions of geometries in the interferometer, the nature of time in GR leads at the quantum level to an imprint of which-way information, which is accompanied by a loss of fringe visibility [35].

Still, an objection may be raised that if one describes the interferometer as a closed quantum system without tracing out over any physical degrees of freedom, then QT implies that coherence must prevail, regardless of whether the system is general relativistic. This objection was raised by Banks, Susskind, and Peskin [36] in the context of black hole evaporation,

---

[2]As we will see in Chapter 2, the combination of the minisuperspace restriction and the reduced phase space approximation reduce the number of (continuous) degrees of freedom from infinity to one, thus sidestepping any renormalization issues.

but it was later pointed out not only that the arguments in [36] were inconclusive, and that we have reason to support the possibility that pure states can effectively evolve into mixed states in black hole systems [37].

The more radical idea entertained here is that one might find pure states evolving to mixed states in gravitational systems without horizons. In general, this "dissipationless" type of decoherence has been explored to some degree [38]-[42], but even the fact that it is possible has not been widely appreciated. Nonetheless, one can observe that the thermal character of acceleration radiation is approximately present even without the involvement of Rindler horizons (for recent analyses see [43]-[46]), and by the equivalence principle one might expect to find a gravitational analog of this thermal behaviour. This means, then, that one might expect that gravity generates an intrinsic form of entropy, even in systems without the horizon structure that one usually associates with entropy in black hole thermodynamics.

With this in mind, we will construct our interferometer, theoretically, out of a self-gravitating, spherically symmetric, infinitesimally thin shell of matter. The interferometer "optics" are encoded internally, by adding tangential pressure to the fluid that lives on the surface of the shell. The resulting model is reminiscent of an idea Einstein first proposed in 1939 [47], but in our case, the tangential pressure satisfies an equation of state that produces a beam-splitter and perfect reflectors. The fluid is ideal, in the sense that one obtains a perfect-fluid stress-energy tensor, if one projects the full four-dimensional spacetime stress-energy tensor onto the three-dimensional history of the shell. This approach ensures that at the classical level, the interferometric setup is manifestly invariant under coordinate transformations.

The configuration we construct resembles that of a Michelson interferometer in optics. Thus, we will send initial states at a beam-splitter, at which point the transmitted and reflected components travel in opposite directions until they encounter "mirrors." The components will then reflect, travel back towards each other, and encounter the splitter once more. There will be two possible outputs, corresponding to final transmission and final reflection, which are comprised of different combinations of the initially split wave components.

What we mean by (interferometric) coherence, in this system, is the sustained phase relationships between different wave components that can allow us, for instance, to completely cancel either of the final outputs. In other words, if we are unable to obtain complete constructive or destructive interference in our interferometer (as predicted by Penrose), we can conclude that coherence is being limited in the system. The goal of our current

investigation is to determine whether or not general relativistic effects could demonstrably produce such a limitation.

1.3   Outline

Our investigation begins in the following chapter (Chapter 2) with the construction of our self-gravitating interferometer model, followed by an analysis of the resulting interference for single-mode input states, in the WKB regime. The stationary nature of the probability distributions for the single-mode states makes the notion of a *probability current* very useful, and we will exploit this usefulness to study the interference patterns in our system.

Chapter 2 makes use of a specific coordinate choice during the process of phase space reduction. The reduced phase space is classically equivalent to the full phase space, modulo coordinate transformations. Does this property hold at the quantum level? Chapter 3 generalizes the original coordinate choice to a family of similar coordinate choices, at which point we can determine which aspects of our system (if any) depend on the coordinate choice. Along the way, we will encounter several serious obstacles that obscure the answers to these questions, and discuss what we can learn from the difficulties that arise.

We then turn our attention to a more complicated model, presented in Chapter 4, obtained by adding an internal degree of freedom to the shell. The internal degree of freedom is chosen to be a harmonic oscillator that evolves with respect to the proper time of the shell. As such, the oscillator behaves as a local clock, and evolves differently depending on the shell's (external) motion due to time dilation. If one is only interested in making a measurement of the external properties of the shell, it is necessary to take the partial trace over the clock degree of freedom. We show that even in the (gravity-free) limit of flat spacetime, this leads to the type of intrinsic decoherence previously referred to as "third-party" decoherence [15], due to the acceleration produced by the tangential pressure on the surface of our shell. Though in this limit the system exhibits "third-party" decoherence, it does not result from a fundamental limit to coherence brought about by general relativity, and is thus not the type of intrinsic decoherence studied in the earlier chapters. However, by incorporating gravitational self-interaction, we can demonstrate that the system exhibits "third-party" decoherence even when the tangential pressure vanishes, because of the gravitational influence of the system on itself. We interpret this "third-party decoherence without the third party" as a fundamentally gravitational intrinsic decoher-

ence effect.

The thesis then finishes in Chapter 5 with a reflection on the results of the previous chapters: the implications, remaining questions, and overall lessons that can be learned from this work.

Chapter 2

Self-gravitating Interferometry

2.1 Introduction

This chapter introduces the model we use to construct our self-gravitating interferometer. To remind the reader, this model has spherical symmetry, to avoid gravitational wave decoherence, and involves an infinitesimally thin shell of matter, so that we only have a single (continuous) physical degree of freedom to work with. The physical degree of freedom in this case is the "areal" radial coordinate of the shell, defined as the square root of the shell area divided by 4π. This "areal" radius is closely connected with the shell's energy density.

In our construction of the interferometer, we will embed "mirrors" and a beam-splitter into the dynamics of the shell itself, to avoid any artificial external influences on the system. This can be accomplished by adding tangential pressure to the surface of the shell, with an equation of state that has the necessary features to describe reflections and beam-splitter. Thus, the "mirrors" and beam-splitter are designed to be triggered by internal features of the shell, like energy density, rather than being located at particular coordinate points; this removes all possible coordinate dependence from the motion of the shell and the locations of the interferometer's optical components. Since we are using an "areal" radial coordinate to describe the shell position, the correspondence between the shell area and the energy density fixes the optical components at specific radial coordinate values.

The reduced Hamiltonian treatment of a spherically symmetric system was originally done by Berger, Chitre, Moncrief and Nutku [48] and was corrected by Unruh [49], who also applied the technique to a spherical shell [private communication]. This is similar to Kraus and Wilczek [50]-[52] who used it to quantize a pressureless spherical shell. The coordinate choices they made (the Painlevé-Gullstrand form) simplified the Hamiltonian equations significantly, and left the Hamiltonian that of a single degree of freedom (the

position of the shell). This approach also works for a shell with tangential pressure, which is what we will use in this thesis.

Much of this chapter will focus on the construction of a general relativistic action principle for our model, followed by the Hamiltonian formulation of the system, and subsequent phase space reduction. Once in its reduced form, the system is simple enough to be analyzed as an interferometer. We will first describe this interferometer in the flat spacetime limit, and point out how coherence manifests itself in the interference pattern. Finally, we will calculate general relativistic corrections to the flat spacetime behaviour, to search for evidence of a fundamental limitation on the system caused by gravity.

2.2 Theory of Self-gravitating Spherical Shells

2.2.1 Action Principle

The perfect-fluid shell model we now develop is a generalization of the dust shell model used by Kraus and Wilczek in their attempt to calculate self-interaction corrections to standard Hawking radiation [50]-[52]. Generalizing the Kraus and Wilczek approach to include the required pressure effects is not without complications, even in the classical theory. In contrast to the approach to thin-shells pioneered by Israel that involves stitching two spacetimes together along the shell's history [53], the starting point for our theoretical considerations is an action that is composed of a gravitational part given by the Einstein-Hilbert action, plus some action for the shell that we can initially leave unspecified, written (in natural units) as

$$I = \frac{1}{16\pi} \int d^4x \, \sqrt{-g^{(4)}} \, \mathcal{R}^{(4)} + I_{shell}. \tag{2.1}$$

The superscripts on the metric determinant g and the Ricci scalar $\mathcal{R}$ indicate that these quantities are constructed from the full $(3+1)$-dimensional spacetime metric components $\{g_{\mu\nu}\}$, with $\mu, \nu \in \{0, 1, 2, 3\}$.

We will express the metric in Arnowitt-Deser-Misner (ADM) form [54], which in spherical symmetry is given by

$$g_{\mu\nu}dx^\mu dx^\nu = -N^2 dt^2 + L^2 \left(dr + N^r dt\right)^2 + R^2 d\Omega^2, \tag{2.2}$$

where N is the lapse function, N^r is the radial component of the shift vector, and L^2 and R^2 are the only nontrivial components of the spatial metric.

The angular variables are taken to be the polar angle θ and the azimuthal angle ϕ, such that the angular metric takes the form $d\Omega^2 = d\theta^2 + \sin^2\theta d\phi^2$.

The shell action studied by Kraus and Wilczek takes the form

$$I_{dust} = -m \int d\lambda \sqrt{-g_{\mu\nu} \frac{dx^\mu}{d\lambda} \frac{dx^\nu}{d\lambda}}, \tag{2.3}$$

with m being the rest-mass of the shell and all metric quantities evaluated on the shell history. The arbitrary parameter λ can be chosen to coincide with the coordinate time t, which simplifies the integrand for the shell action.

To describe a more general fluid than dust, we need a more general action. There are well-established variational principles for regular perfect fluids in GR [55], but the authors are unaware of any satisfactory variational principles for the perfect fluid shells we wish to describe. The stress-energy tensor for a perfect fluid with density σ and pressure p is given by

$$S^{ab} = \sigma u^a u^b + p(\gamma^{ab} + u^a u^b), \tag{2.4}$$

where u^a are the components of the fluid proper velocity in coordinates that cover the fluid history. For our purposes, the geometry along the fluid history of our shell is described by an induced metric $\gamma_{ab} dy^a dy^b = -d\tau^2 + \hat{R}^2 d\Omega^2$, with τ being the shell proper time. This induced metric obeys the relation

$$\gamma_{ab} = e_a^\mu e_b^\nu g_{\mu\nu}, \tag{2.5}$$

with the introduction of projectors onto the shell history given by

$$e_a^\mu = \frac{\partial x^\mu}{\partial y^a} = u^\mu \delta_a^\tau + \delta_\Omega^\mu \delta_a^\Omega. \tag{2.6}$$

Here and elsewhere, the repeated Ω denotes a sum over angular coordinates. These projectors allow us to express the full spacetime stress-energy tensor of our perfect fluid shell as

$$T^{\mu\nu} = S^{ab} e_a^\mu e_b^\nu \delta(\chi), \tag{2.7}$$

where we have introduced a Gaussian normal coordinate χ in the direction of the outward-pointing space-like unit normal $\boldsymbol{\xi}$, with the shell location defined by $\chi = 0$.

We want to obtain an action, expressed in terms of the full spacetime quantities, that yields the tensor (2.4) in the intrinsic coordinates of the shell history. To convert derivative expressions from the intrinsic coordinates to the ADM coordinates given in equation (4.3), we can write infinitesimal changes in r and t as

$$dt = u^t d\tau + \xi^t d\chi, \quad dr = u^r d\tau + \xi^r d\chi. \tag{2.8}$$

Taking advantage of the fact that $\boldsymbol{\xi}$ satisfies $u^\mu \xi_\mu = 0$ and $\xi^\mu \xi_\mu = 1$, and suppressing the (vanishing) angular components for brevity, the outward normal can be written as

$$\xi_\alpha = \sqrt{g_{tr}^2 - g_{tt}g_{rr}}\left(-u^r, u^t\right) = N^2 L^2 \left(-u^r, u^t\right). \tag{2.9}$$

For radial integration within an ADM slice, one has $dt = 0$, and in this case we can solve for $\frac{dr}{d\chi}$ in equation (2.8) to obtain [56]

$$\frac{dr}{d\chi} = \xi^r - \frac{u^r}{u^t}\xi^t. \tag{2.10}$$

Also, since $u^\mu = (dt/d\tau)(1, \dot{X}, 0, 0)$, the 4-velocity normalization $u^\mu u_\mu = -1$ (evaluated on the shell) implies

$$\left(\frac{dt}{d\tau}\right)^2 = (u^t)^2 = \left(N^2 - L^2(N^r + \dot{X})^2\right)^{-1}. \tag{2.11}$$

This allows conversion of the delta function appearing in our expression (2.7) for the full spacetime stress-energy tensor:

$$\delta(\chi) = \frac{dr}{d\chi}\delta(r - X) = \frac{\sqrt{N^2 - L^2(N^r + \dot{X})^2}}{NL}\delta(r - X). \tag{2.12}$$

Using equation (2.7), we find that our stress-energy tensor takes the form

$$T^{\mu\nu} = \left(\sigma u^\mu u^\nu + p g^{\Omega\Omega}\delta_\Omega^\mu\delta_\Omega^\nu\right)\delta(\chi), \tag{2.13}$$

where the repeated Ω indices denote a single sum over angular coordinates. In expression (2.13), the "tangential" nature of the pressure is manifest, since the projection of this tensor onto the space-like normal $\boldsymbol{\xi}$ clearly vanishes.

The action we seek, then, yields (2.13) upon taking variations with respect to the metric, in accordance with the definition

$$\delta I = \frac{1}{2}\int d^4x \sqrt{-^4g}T^{\mu\nu}\delta g_{\mu\nu}. \tag{2.14}$$

We are especially interested in the contribution from the tangential pressure, which takes the form

$$\delta I_p = 8\pi \int dt\, dr\, NL\delta\left(\chi\right)pR\delta R. \tag{2.15}$$

13

By inspection, we find that the action

$$I_{shell} = -\int d\lambda \sqrt{-g_{\mu\nu}\frac{dx^\mu}{d\lambda}\frac{dx^\nu}{d\lambda}}M(R), \qquad (2.16)$$

with all quantities evaluated on the shell history, yields the appropriate stress-energy tensor: the relevant variational derivative of (4.1) with respect to the metric is

$$\delta I_{shell,p} = -\int dt\, dr\, NL\delta\left(\chi\right)M'(R)\delta R, \qquad (2.17)$$

from which it follows that one has the pressure identification $p = -M'(R)/8\pi R$, along with the usual density identification $\sigma = M(R)/4\pi R^2$. We will use the freedom in choosing the function $M(R)$ to parametrize an equation of state that relates the density and pressure of our fluid. It should be noted that R is not a coordinate, but a metric component that serves as a measure of the shell's internal energy.

The action (4.1) is reparametrization-invariant, as well as invariant under general (spherically symmetric) coordinate transformations, even with the inclusion of an R-dependent 'mass'. As mentioned above, this is because R, when evaluated on the shell, is nothing more than the reduced area of the shell, and this area is independent of coordinate choices.

2.2.2 Hamiltonianization

Following the canonical formalism [54], one can perform a Legendre transformation $\mathcal{H} = P\dot{X} - \mathcal{L}$, for the shell variables. Here $\mathcal{L}$ is the Lagrangian defined by (4.1), subject to the condition that the shell history is parametrized by t. One then finds

$$\mathcal{L} = -\int dr \sqrt{N^2 - L^2(N^r + \dot{X})^2}M(R)\delta(r - X), \qquad (2.18)$$

and it follows that the momentum conjugate to the shell position X for the unreduced problem is given by

$$P = \frac{\partial\mathcal{L}}{\partial\dot{X}} = \int dr\, \frac{L^2(N^r + \dot{X})M(R)}{\sqrt{N^2 - L^2(N^r + \dot{X})^2}}\delta(r - X). \qquad (2.19)$$

Explicitly, we can determine the Hamiltonian $\mathcal{H}$ to be

$$\mathcal{H} = P\dot{X} - \mathcal{L} = \int dr\ (NH_0^s + N^r H_r^s), \qquad (2.20)$$

14

with the definitions

$$
\begin{aligned}
H_0^s &= \sqrt{L^{-2}P^2 + M(R)^2}\,\delta(r - X), \\
H_r^s &= -P\delta(r - X).
\end{aligned}
\tag{2.21}
$$

Similarly, we can Hamiltonianize the gravitational action, and express the total action as

$$
I = \int dt\, P\dot{X} + \int dt\, dr\, \left(\pi_R \dot{R} + \pi_L \dot{L} - NH_0 - N^r H_r \right),
\tag{2.22}
$$

for $H_0 = H_0^s + H_0^G$ and $H_r = H_r^s + H_r^G$, such that

$$
\begin{aligned}
H_0^G &= \frac{L\pi_L^2}{2R^2} - \frac{\pi_L \pi_R}{R} + \left(\frac{RR'}{L} \right)' - \frac{(R')^2}{2L} - \frac{L}{2}, \\
H_r^G &= R'\pi_R - L\pi_L'.
\end{aligned}
\tag{2.23}
$$

2.2.3 Equations of Motion

Once in Hamiltonian form, the equations of motion for the system are obtained by varying the action with respect to the variables N, N^r, π_L, π_R, L, and R. Explicitly, these variations (respectively) lead to

$$
\begin{aligned}
H_0 &= 0, \\
H_r &= 0, \\
\dot{L} &= \frac{N}{R}\left(\frac{L\pi_L}{R} - \pi_R \right) + (N^r L)', \\
\dot{R} &= -\frac{N\pi_L}{R} + N^r R', \\
\dot{\pi}_L &= \frac{N}{2}\left(1 - \frac{\pi_L^2}{R^2} - \frac{(R')^2}{L^2} \right) - \frac{N'RR'}{L^2} \\
&\quad + N^r \pi_L' + \frac{NP^2\delta(r - X)}{L^2\sqrt{P^2 + L^2M^2}}, \\
\dot{\pi}_R &= \frac{N\pi_L}{R^2}\left(\frac{L\pi_L}{R} - \pi_R \right) - N\left(\frac{R'}{L} \right)' - \left(\frac{N'R}{L} \right)' \\
&\quad + (N^r \pi_R)' - \frac{NM\frac{dM}{dR}\delta(r - X)}{\sqrt{L^{-2}P^2 + M^2}}.
\end{aligned}
\tag{2.24}
$$

The first two equations are the Hamiltonian and momentum constraints, whereas the next four are the dynamical equations of motion for the gravitational variables.

For the shell variables, the equation of motion for X can be easily obtained by varying the action with respect to P, or simply by solving equation (2.19) for $\dot{X}$. The result is

$$
\begin{aligned}
\dot{X} &= \int dr \left(\frac{NP}{L\sqrt{P^2 + L^2 M^2}} - N^r \right) \delta(r - X) \\
&= \frac{\hat{N}P}{\hat{L}\sqrt{P^2 + \hat{L}^2 \hat{M}^2}} - \hat{N}^r,
\end{aligned}
\tag{2.25}
$$

with hats indicating that one evaluates the quantities at $r = X$.

The equation of motion for P is more subtle, since a standard variation of the action with respect to X is formally ambiguous, as noted in [57]. The ambiguity arises because one must evaluate quantities on the shell (L', $(N^r)'$, N' and R') that are (possibly) discontinuous at $r = X$:

$$
\dot{P} = \left(N^r P - N\sqrt{L^{-2}P^2 + M^2} \right)'_{shell}.
\tag{2.26}
$$

However, it has been demonstrated in [58] that this ambiguity can be removed by requiring consistency with the constraints and the gravitational equations of motion (2.24), at least for the case of a dust shell. The argument described in [58] shows that one must average the discontinuous quantities when interpreting the equation of motion for the shell momentum, and similar reasoning leads to the same conclusion for the arbitrary perfect fluid shell described here. One then has the equation of motion

$$
\dot{P} = (\bar{N}^r)'P - \frac{\bar{N}'}{\hat{L}}\sqrt{P^2 + \hat{L}^2\hat{M}^2} + \frac{\hat{N}\left(P^2\bar{L}' - \hat{L}^3\hat{M}\bar{M}'\right)}{\hat{L}^2\sqrt{P^2 + \hat{L}^2\hat{M}^2}},
\tag{2.27}
$$

with the average taken over $(N^r)'$ in the first term of the right-hand-side, and the last term containing the factor $\bar{M}'$ defined as $\bar{M}' = \frac{d\hat{M}}{dR}\bar{R}'$.

Let us briefly sketch the argument that leads to this result. To start, we take the time derivative of the (integrated and rearranged) momentum constraint:

$$
\dot{P} = -\Delta\pi_L \frac{d}{dt}\left(\hat{L}\right) - \hat{L}\frac{d}{dt}\left(\Delta\pi_L\right).
\tag{2.28}
$$

Then, by continuity of $\dot{L}$, we have

$$
\frac{d}{dt}L(X) = L'(X \pm \epsilon)\dot{X} + \dot{L}(X \pm \epsilon) = \bar{L}'\dot{X} + \bar{\dot{L}}.
\tag{2.29}
$$

Averaging the equation of motion for L, noting that $\frac{d}{dt}(\Delta\pi_L) = \Delta(\pi'_L)\dot{X} + \Delta(\dot{\pi}_L)$, and calculating $\Delta(\dot{\pi}_L)$ from the equation of motion for π_L, we obtain

$$\dot{P} = \dot{\mathcal{P}} + \Phi, \tag{2.30}$$

with $\dot{\mathcal{P}}$ representing the right side of equation (2.27), and Φ defined such that

$$
\begin{aligned}
\Phi = \quad & - \quad P\frac{\hat{N}}{\hat{R}\hat{L}}\bar{\pi}_R + \frac{\hat{N}\Delta R'\bar{R}'}{\hat{L}} + \Delta N'\frac{\bar{R}'\hat{R}}{\hat{L}} \\
& - \quad \hat{L}\Delta\pi'_L(\hat{N}^r + \dot{X}) + \frac{\hat{N}\hat{M}\frac{d\hat{M}}{dR}\bar{R}'}{\sqrt{\hat{L}^{-2}P^2 + \hat{M}^2}}.
\end{aligned}
\tag{2.31}
$$

To then demonstrate that Φ vanishes, one needs to take the jump of the momentum constraint across the shell to obtain $\hat{L}\Delta\pi'_L = \bar{R}'\Delta\pi_R + \bar{\pi}_R\Delta R'$, then integrate the equation of motion for π_R across the shell, and use the result, combined with the fact that the delta contribution to $\dot{\pi}_R$ is given by $-\dot{X}(\Delta\pi_R)\delta(r - X)$ [57].

2.2.4   Phase Space Reduction

We now seek a description of the system in terms of only the shell coordinate X and a conjugate momentum P_c. Note that it is not necessarily true that P_c will coincide with the conjugate momentum P for the unreduced problem, as will become clear in what follows.

   To proceed with the Hamiltonian reduction, we will make use of the Liouville form $\mathcal{F}$ and the symplectic form Ω, which on the full phase space (denoted by Γ) can be written as

$$\mathcal{F} = P\boldsymbol{\delta}X + \int dr \, (\pi_L\boldsymbol{\delta}L + \pi_R\boldsymbol{\delta}R) \tag{2.32}$$

and

$$\Omega = \boldsymbol{\delta}P \wedge \boldsymbol{\delta}X + \int dr \, (\boldsymbol{\delta}\pi_L \wedge \boldsymbol{\delta}L + \boldsymbol{\delta}\pi_R \wedge \boldsymbol{\delta}R), \tag{2.33}$$

respectively, with $\boldsymbol{\delta}$ denoting an exterior derivative in the associated functional space (see [57] for more details). The reduced phase space $\bar{\Gamma}$ is defined as the set of equivalence classes in Γ under changes of coordinates, and each (permissible) choice of coordinates defines a hypersurface $\bar{H} \subseteq \Gamma$ that is transversal to the orbits generated by coordinate transformations; this ensures that there exists an isomorphism between $\bar{\Gamma}$ and the representative hypersurface $\bar{H}$.

At this point we can determine the symplectic form $\bar{\Omega}$ induced on $\bar{H}$ as follows: first, consider the pullback of $\mathcal{F}$ to $\bar{H}$; this yields a quantity which we denote by $\mathcal{F}_{\bar{H}}$. Then, the symplectic form $\Omega_{\bar{H}}$ on the representative hypersurface $\bar{H}$ (corresponding to $\bar{\Omega}$) takes the form

$$\Omega_{\bar{H}} = \delta \mathcal{F}_{\bar{H}}. \tag{2.34}$$

This quantity defines the canonical structure of the reduced phase space.

To explicitly determine the (nonlocal) contribution of the gravitational variables to the dynamics on the reduced phase space, we can solve the GR constraints for the gravitational momenta, insert the solutions into the Liouville form on the full phase space, and perform the integration to express the gravitational contribution solely in terms of the (local) shell variables. Away from the shell, take the following linear combination of the constraints:

$$-\frac{R'}{L}H_0 - \frac{\pi_L}{RL}H_r = \mathcal{M}', \tag{2.35}$$

for

$$\mathcal{M}(r) = \frac{\pi_L^2}{2R} + \frac{R}{2} - \frac{R(R')^2}{2L^2}. \tag{2.36}$$

The quantity $\mathcal{M}(r)$ corresponds to the ADM mass H when evaluated outside of the shell, and vanishes inside the shell. This enables us to solve for the gravitational momenta π_L, π_R away from the shell. The result is

$$\pi_L = \pm R\sqrt{\left(\frac{R'}{L}\right)^2 - 1 + \frac{2\mathcal{M}}{R}}, \quad \pi_R = \frac{L}{R'}\pi_L'. \tag{2.37}$$

One then makes a coordinate choice, to pick out a representative hypersurface $\bar{H}$. The coordinates we will use resemble the flat-slice coordinates $\{L = 1, R = r\}$ described in [51] (also known as Painlevé-Gullstrand coordinates), though we will have a deformation region $X - \epsilon < r < X$ explicitly included, in order to both satisfy the constraints and yield a continuous spatial metric. The deformation region is related to a jump in R' across the shell. This can be seen by first integrating the Hamiltonian and momentum constraints across the shell. Doing so yields, respectively,

$$\Delta R' = -\frac{\hat{V}}{\hat{R}}, \quad \Delta \pi_L = -\frac{P}{\hat{L}}, \tag{2.38}$$

where $V = \sqrt{P^2 + M^2 L^2}$ and Δ indicates the jump of a quantity across the shell. We therefore take

$$L = 1, \quad R(r,t) = r - \frac{\epsilon}{X}\hat{V}\mathcal{G}\left(\frac{X - r}{\epsilon}\right), \tag{2.39}$$

18

for a function $\mathcal{G}$ having support in the interval $(0,1)$ with the property $d\mathcal{G}(z)/dz \to 1$ as $z \searrow 0$. Outside of the deformation region, these coincide with flat-slice coordinates. For concreteness, let us suppose $\mathcal{G}(z)$ takes the form

$$\mathcal{G}(z) = z e^{-z^2/(1-z^2)} \tag{2.40}$$

for all $z \in (0,1)$.

In what follows, it will be useful to note that $\hat{M} = M(\hat{R}) = M(X)$, and that now P is considered to be a function of X and H, as a consequence of the gravitational constraints. We can implicitly determine this function by inserting the gravitational momentum solutions away from the shell given by equation (4.22) into the jump equations (2.38) and squaring. We are then left with

$$H = \hat{V} + \frac{\hat{M}^2}{2X} - P\sqrt{\frac{2H}{X}}. \tag{2.41}$$

With this coordinate choice, the only gravitational contribution to the Liouville form comes from the π_R term, and only from within the deformation region. Keeping in mind that we only care about terms that remain nonzero in the $\epsilon \to 0$ limit, we have, in the deformation region,

$$\pi_R = \frac{X R''}{\sqrt{(R')^2 - 1}} + \mathcal{O}(1), \tag{2.42}$$

since $R = X + \mathcal{O}(\epsilon)$ and $R'' = \mathcal{O}\left(\epsilon^{-1}\right)$. One can also note that $\boldsymbol{\delta} R = (1 - R')\boldsymbol{\delta} X + \mathcal{O}(\epsilon)$, and express the gravitational contribution to the Liouville form as

$$\int_{X-\epsilon}^{X} dr\, \pi_R \boldsymbol{\delta} R = X \boldsymbol{\delta} X \int_{X-\epsilon}^{X} dr\, \frac{R''\,(1 - R')}{\sqrt{(R')^2 - 1}} + \mathcal{O}(\epsilon). \tag{2.43}$$

To evaluate this integral, one can change the integration variable from r to $v = R'$:

$$\int_{X-\epsilon}^{X} dr\, \pi_R \boldsymbol{\delta} R = X \boldsymbol{\delta} X \int_{1}^{R'_-} dv\, \frac{(1 - v)}{\sqrt{v^2 - 1}} + \mathcal{O}(\epsilon), \tag{2.44}$$

with R'_- being R' evaluated just inside the shell. The integration is then straightforward, and after applying (2.41) and making some rearrangements one arrives at

$$X \boldsymbol{\delta} X \left[-\frac{P}{X} - \sqrt{\frac{2H}{X}} + \ln\left(1 + \sqrt{\frac{2H}{X}} + \frac{\hat{V} + P}{X} \right) \right], \tag{2.45}$$

plus terms that vanish as $\epsilon \to 0$. This completes the calculation of $\mathcal{F}_{\bar{H}}$, the pullback of the full Liouville form $\mathcal{F}$ to $\bar{H}$:

$$\mathcal{F}_{\bar{H}} = P_c \boldsymbol{\delta} X, \tag{2.46}$$

with the reduced canonical momentum evidently given by

$$P_c = -\sqrt{2HX} + X \ln\left(1 + \sqrt{\frac{2H}{X}} + \frac{\hat{V} + P}{X}\right). \tag{2.47}$$

This result agrees with [57] in the limit of a dust shell ($\hat{M}' = 0$).

To connect this with the expression derived by Kraus and Wilczek, we need only apply the expression (2.41) to the argument of the logarithm, which leads to

$$P_c = -\sqrt{2HX} - X \ln\left(\frac{X + \hat{V} - P - \sqrt{2HX}}{X}\right). \tag{2.48}$$

This form of the reduced momentum coincides with [50] in the dust-shell limit.

2.2.5   Boundary Terms

To obtain a well-defined variational principle for the reduced problem, we must be careful with boundary terms, as first noted in [59] and [49]. In [50], it is observed that for asymptotically-flat spacetimes, we simply need to subtract the ADM mass (denoted suggestively by H) from our reduced Lagrangian. Specifically, as mentioned in [57], a nonzero boundary variation results from integrating the term $\int dt dr N^r L(\delta \pi_L)'$ (which is part of the momentum constraint) by parts. The only contribution comes from infinity, and in this case we have $N^r \to N\sqrt{2H/r}$, $N \to 1$, and

$$\delta(\pi_L) \to \delta(\sqrt{2Hr}) = \sqrt{\frac{r}{2H}} \delta H, \tag{2.49}$$

so the variation of the boundary term is cancelled if we add to the action the term

$$I_{bdry} = -\int dt\, H. \tag{2.50}$$

Including the boundary term in the action defined by $\mathcal{F}_{\bar{H}}$, one obtains the reduced action

$$I_{reduced} = \int dt\, \left(P_c \dot{X} - H\right), \tag{2.51}$$

with the reduced momentum given by (2.48). From the form of the reduced action (2.51), we can see that the ADM mass is the reduced Hamiltonian, defined implicitly by (2.48) and (2.41).

Since (2.41) has more than one solution $P = P(X, H)$, our conjugate momentum P_c in turn becomes a multi-valued function of X and H, as one expects from a theory that allows the degree of freedom to either increase or decrease. Explicitly, P is given by

$$
\begin{aligned}
P \;=\; & \frac{1}{1 - \frac{2H}{X}} \left(\sqrt{\frac{2H}{X} \left(H - \frac{\hat{M}^2}{2X} \right)} \right) \\
& \pm \frac{1}{1 - \frac{2H}{X}} \left(\sqrt{\left(H - \frac{\hat{M}^2}{2X} \right)^2 - \hat{M}^2 \left(1 - \frac{2H}{X} \right)} \right),
\end{aligned}
\tag{2.52}
$$

while the combination $\hat{V} - P$ that appears in the reduced momentum (2.48) is

$$
\hat{V} - P = \frac{H - \frac{\hat{M}^2}{2X} \mp \sqrt{\left(H - \frac{\hat{M}^2}{2X} \right)^2 - \hat{M}^2 \left(1 - \frac{2H}{X} \right)}}{1 + \sqrt{\frac{2H}{X}}}.
\tag{2.53}
$$

2.2.6 Constructing Classical Spacetime

Suppose one can find a solution $X(t)$ to the classical equations of motion for the reduced system (2.51). Then, the gravitational constraints and equations of motion (2.24) can be solved to determine all the metric components $g_{\mu\nu}$. Therefore, from the reduced system solution $X(t)$ one can construct the classical spacetime structure, as we will now demonstrate.

By inserting the gravitational momenta solutions (4.22) into the gravitational equations of motion (2.24), one can obtain the lapse function N and the radial shift component N^r that correspond to our coordinate choice (2.39).

Outside of the shell, one finds the familiar Schwarzschild structure, in flat-slice coordinates. The lapse function is constant, and unity if we want a time coordinate that increases towards the future, while the radial shift is given by

$$
N^r(r \geq X) = \pm \sqrt{\frac{2H}{r}}.
\tag{2.54}
$$

The $\pm$ here indicates two possible time-slicings, though we will often take the upper sign (this means that the gravitational momenta solution (4.22) should take the upper sign as well, to ensure $N \to 1$ as $r \to \infty$).

Along with the expression (2.41) for P in terms of X and H, we now have enough information to determine the classical path $X(t)$, since H is constant along such paths. Specifically, the equation of motion for X becomes

$$\dot{X} = \frac{P}{\sqrt{P^2 + \hat{M}^2}} - \sqrt{\frac{2H}{X}}, \qquad (2.55)$$

which leads to the expression

$$\frac{dt}{dX} = \frac{\sqrt{2HX}}{X - 2H}$$

$$\pm \frac{H - \frac{\hat{M}^2}{2X}}{\left(1 - \frac{2H}{X}\right)\sqrt{\left(H - \frac{\hat{M}^2}{2X}\right)^2 - \hat{M}^2\left(1 - \frac{2H}{X}\right)}}. \qquad (2.56)$$

Therefore, finding the classical path $X(t)$ has been reduced to quadrature and inversion.

With the classical path known, one can also calculate the classical action, as done for the case of dust in [50]:

$$S(t, X(t)) = S(0, X(0)) + \int_0^t d\tilde{t}\left[P_c(\tilde{t})\dot{X}(\tilde{t}) - H\right], \qquad (2.57)$$

with

$$P_c(0) = \frac{\partial S}{\partial X}(0, X(0)). \qquad (2.58)$$

Unlike the (massless) dust case, however, our classical path $X(t)$ is not a null geodesic of the flat-slice metric

$$ds^2 = -dt^2 + \left(dr + \sqrt{\frac{2H}{r}}\,dt\right)^2, \qquad (2.59)$$

and so we cannot so easily determine explicit expressions for our shell trajectories.

2.3   Single-mode Interferometry

2.3.1   Equation of State Determination

Up until this point, the function $M(X)$ has been left unspecified, though we have established the identifications $\sigma = M(X)/4\pi X^2$ for the density and

$p = -M'(X)/8\pi X$ for the pressure. We would like to exploit this freedom for the purposes of interferometry. To maintain internal consistency, there should be a relationship $p = p(\sigma)$, which represents an equation of state for our fluid shell. The function $M(X)$ parametrizes this relationship, though not every choice of $M(X)$ yields a consistent (let alone physical) equation of state.

The interferometric setup resembles that of Michelson, except we only have one spatial dimension to work with, since our system is spherically symmetric. Still, we would like the equation of state to produce two 'reflectors' - one to reflect the shell outward if it gets too small, and one to reflect the shell inward if it gets too large. Also, we would like the equivalent of a 'half-silvered mirror' to be in between the two reflectors, to act as a beam-splitter. This is depicted schematically in Figure 2.1, with $X_{\pm}$ being the shell radii that correspond to the reflectors, and X_{δ} the radius corresponding to the splitter. Accordingly, our equation of state $p = p(\sigma)$ must have a large positive peak for some large density, a large negative peak for some small density, and an intermediate peak (serving as the beam-splitter) for some intermediate density.

It would be convenient to use delta functions for these purposes, but due to the conversion between $\delta(\sigma - \sigma_0)$ and $\delta(X - X_0)$ and the resulting appearance of products of delta functions, this possibility seems problematic. Therefore, we have been considering the simplest alternative one could think of: rectangular barriers. These can be described with the use of step functions, which we will define such that $\Theta(x < 0) = 0$ and $\Theta(x > 0) = 1$.

The equation of state, then, takes the form

$$
\begin{aligned}
p \;=\; & p_1 \left(\Theta(\sigma - \sigma_1) - \Theta(\sigma - \sigma_2) \right) \\
& + p_2 \left(\Theta(\sigma - \sigma_3) - \Theta(\sigma - \sigma_4) \right) \\
& + p_3 \left(\Theta(\sigma - \sigma_5) - \Theta(\sigma - \sigma_6) \right),
\end{aligned}
\tag{2.60}
$$

with $\sigma_{i+1} > \sigma_i$, $p_1 < 0$, and $p_2, p_3 > 0$. We may as well take $p_1 = -p_3$, since both of these peaks serve the same purpose of reflecting, but we will not yet impose this condition.

One would now like to find the function $M(X)$ that parametrizes the equation of state (2.60). If we could express (2.60) as $p = \sum_i \tilde{p}_i \Theta(X - X_i)$, then the identification $p = -M'(X)/8\pi X$ would imply

$$
M(X) = M_0 + 4\pi \sum_i \tilde{p}_i \left(X_i^2 - X^2 \right) \Theta(X - X_i),
\tag{2.61}
$$
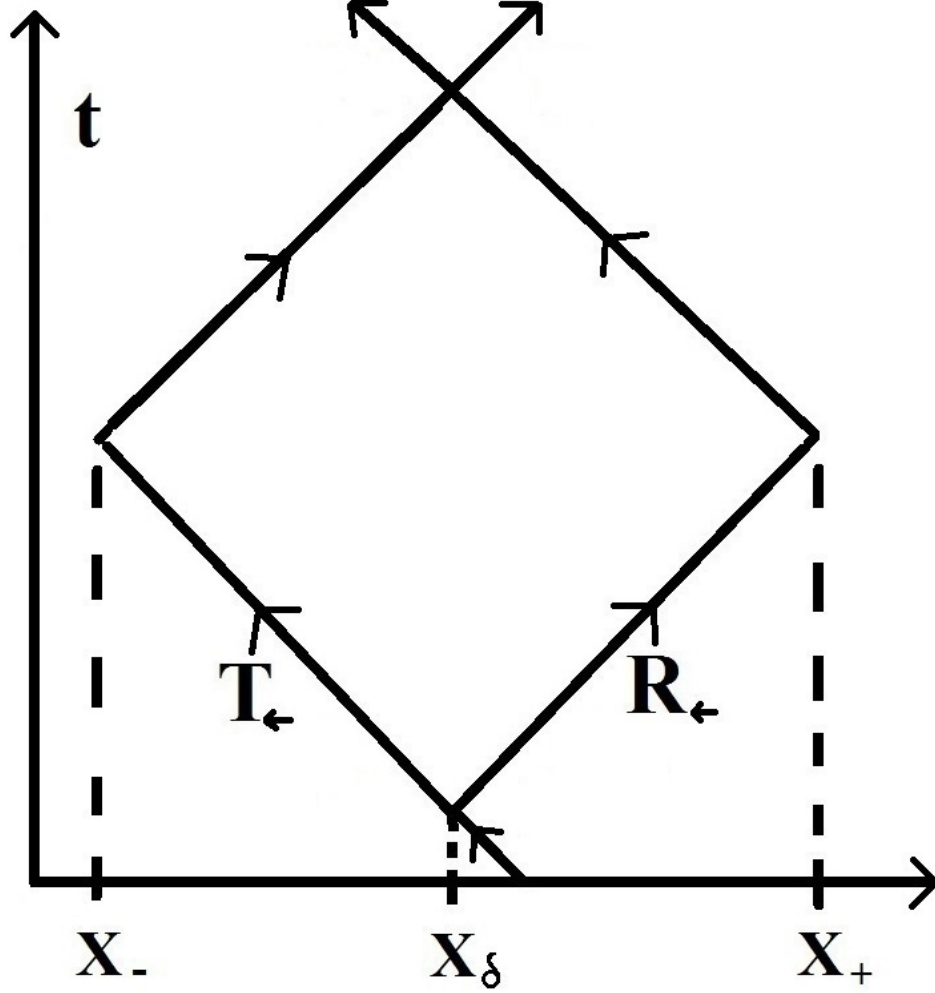
Figure 2.1: Schematic representation of the splitting, reflecting, and recombining that occur in our shell interferometer. The inner and outer mirrors are located at X_- and X_+, respectively, and the beam-splitter is located at X_δ. The initial split, depicted near the bottom of the diagram, is characterized by a transmission coefficient $T_\leftarrow$ and a reflection coefficient $R_\leftarrow$. These coefficients determine the amplitudes of the transmitted and reflected components of the initial state, which propagate along the different interferometer arms. The two arrows at the top of the diagram represent the final interferometer outputs, after recombination.
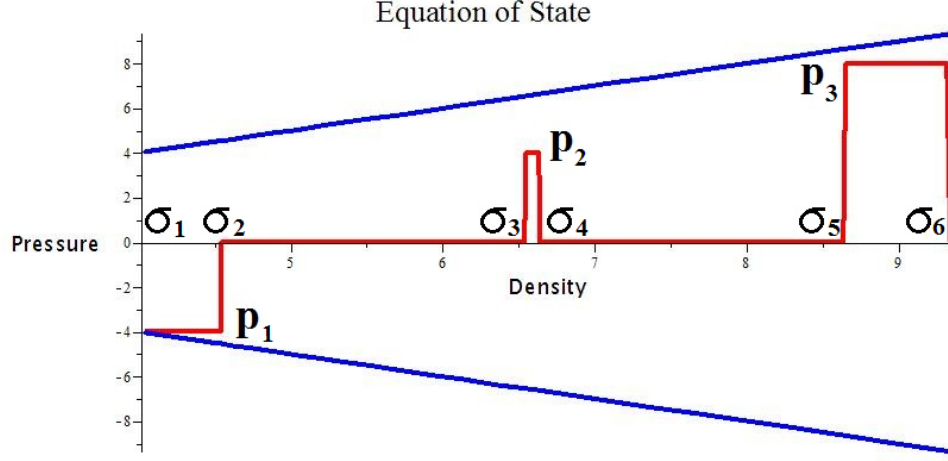
Figure 2.2: A sample equation of state represented by (2.60). There is a negative pressure peak p_1 for some low density σ_2 that causes the shell to reflect inwards whenever X gets sufficiently large, there is a positive pressure peak p_2 for some high density σ_5 to reflect the shell outwards whenever X gets sufficiently small, and there is an intermediate pressure peak p_2 that serves as a beam-splitter for our interferometer.

which would yield a density given by

$$\sigma = \frac{M_0}{4\pi X^2} + \sum_i \tilde{p}_i \left(\frac{X_i^2}{X^2} - 1 \right) \Theta(X - X_i). \qquad (2.62)$$

The problem with this possibility is that, in general, it isn't necessarily true that $\Theta(X - X_i)$ produces the same (reversed) ordering as $\Theta(\sigma - \sigma_i)$, given that $\sigma_i = M(X_i)/4\pi X_i^2$. This problem can be avoided by making sure that the density σ is a monotonically decreasing function of X. This leads to the condition

$$\frac{M_0}{4\pi} \geq - \sum_i \tilde{p}_i X_i^2 \Theta(X - X_i). \qquad (2.63)$$

Figure 2.2 illustrates the desired step function peaks, to enable our system to operate as an interferometer.

To understand what this means in terms of the pressure peaks in our equation of state (2.60), we first note that if σ monotonically decreases in X, then step functions can be converted by $\Theta(\sigma - \sigma_i) = 1 - \Theta(X - X_i)$. This allows us to conclude that $\tilde{p}_2 = -\tilde{p}_1 = p_1$, $\tilde{p}_4 = -\tilde{p}_3 = p_2$, and

$\tilde{p}_6 = -\tilde{p}_5 = p_3$. Then, one finds that monotonicity is maintained as long as

$$\frac{M_0}{4\pi} > max\{p_3 X_{5,6}^2, p_3 X_{5,6}^2 + p_2 X_{3,4}^2,$$
$$p_3 X_{5,6}^2 + p_2 X_{3,4}^2 - p_1 X_2^2\}, \tag{2.64}$$

where the notation $X_{i,j}^2 = X_i^2 - X_j^2$ was introduced, for brevity.

Since an equation of state (2.60) is described by the pressure as a function of density, one should translate the conditions for monotonicity in terms of the step locations $\{\sigma_i\}$ and the step amplitudes $\{p_i\}$. To convert between the $\{X_i\}$ and the $\{\sigma_i\}$, one can use the relations

$$
\begin{aligned}
X_6^2 &= \frac{M_0}{4\pi\sigma_6}, \\
X_5^2 &= \frac{M_0}{4\pi\sigma_6} \frac{(\sigma_6 + p_3)}{(\sigma_5 + p_3)}, \\
X_4^2 &= \frac{M_0}{4\pi\sigma_6} \frac{(\sigma_6 + p_3)}{(\sigma_5 + p_3)} \frac{\sigma_5}{\sigma_4}, \\
X_3^2 &= \frac{M_0}{4\pi\sigma_6} \frac{(\sigma_6 + p_3)}{(\sigma_5 + p_3)} \frac{\sigma_5}{\sigma_4} \frac{(\sigma_4 + p_2)}{(\sigma_3 + p_2)}, \\
X_2^2 &= \frac{M_0}{4\pi\sigma_6} \frac{(\sigma_6 + p_3)}{(\sigma_5 + p_3)} \frac{\sigma_5}{\sigma_4} \frac{(\sigma_4 + p_2)}{(\sigma_3 + p_2)} \frac{\sigma_3}{\sigma_2}, \\
X_1^2 &= \frac{M_0}{4\pi\sigma_6} \frac{(\sigma_6 + p_3)}{(\sigma_5 + p_3)} \frac{\sigma_5}{\sigma_4} \frac{(\sigma_4 + p_2)}{(\sigma_3 + p_2)} \frac{\sigma_3}{\sigma_2} \frac{(\sigma_2 + p_1)}{(\sigma_1 + p_1)}.
\end{aligned} \tag{2.65}
$$

With these expressions, one can write the monotonicity conditions in the much simpler form

$$\{\sigma_5 > 0, \sigma_3 > 0, \sigma_1 + p_1 > 0\}. \tag{2.66}$$

Thus, as long as we keep the density σ positive, it will be monotonic in X provided $\sigma_1 + p_1 > 0$.

2.3.2   The WKB Approximation

Now that we have fully defined the reduced action (2.51) of our interferometer, we can seek a quantum description of the system. As mentioned above, there are immediate complications that one is faced with: the Hamiltonian is only implicitly defined, which makes even writing down an explicit Schrödinger equation impossible, and even if we could write down an explicit Schrödinger equation we would have to deal with factor-ordering ambiguities. Fortunately, both of these issues are for the most part avoided by

focusing one's attention on the parameter space region of validity of the WKB approximation (the so-called "WKB regime"). Let us now clarify what we mean by this.

First, we will consider the time-independent Schrödinger equation,

$$H\Psi = E\Psi, \tag{2.67}$$

for a Hamiltonian that is quadratic in momentum:

$$H(X, P) = H_0(X) + H_1(X)P + H_2(X)P^2. \tag{2.68}$$

For our purposes, we will approximate a general Hamiltonian $H(X, P)$ by the first three terms in a Taylor expansion in P, given by

$$H_w = H(X, 0) + \left(\frac{\partial H}{\partial P}\right)P + \frac{1}{2}\left(\frac{\partial^2 H}{\partial P^2}\right)P^2, \tag{2.69}$$

with the P-derivatives evaluated at $P = 0$.

To make sure this Hamiltonian becomes Hermitian in the quantum theory, we must order the operators appropriately. We can symmetrize the term linear in P, such that

$$\left(\frac{\partial H}{\partial P}\right)P \rightarrow \frac{1}{2}\left(\left(\frac{\partial \hat{H}}{\partial P}\right)\hat{P} + \hat{P}\left(\frac{\partial \hat{H}}{\partial P}\right)\right), \tag{2.70}$$

as well as ordering the quadratic term as

$$\left(\frac{\partial^2 H}{\partial P^2}\right)P^2 \rightarrow \hat{P}\left(\frac{\partial^2 \hat{H}}{\partial P^2}\right)\hat{P}. \tag{2.71}$$

In the weak field limit, i.e. X large compared to the Schwarzschild radius $2E$, the WKB Hamiltonian for our shell system is given by

$$H_w \sim \left(\hat{M} - \frac{\hat{M}^2}{18X}\right) - \frac{2}{3}\sqrt{\frac{2\hat{M}}{X}}P + \left(\frac{1}{2\hat{M}} + \frac{1}{3X}\right)P^2. \tag{2.72}$$

We will postpone the derivation of the WKB Hamiltonian (2.72) until Section 3.5, as it will be instructive to consider the details in a more general setting. For brevity, we have dropped the subscript c on the reduced momentum here and for the rest of the chapter.

The WKB approximation we seek is obtained by considering the $\hbar \rightarrow 0$ limit of (2.67). We will rewrite the wavefunction Ψ as

$$\Psi = e^{\frac{i}{\hbar}\sum_{n=0}^{\infty}\hbar^n S_n(X)}, \tag{2.73}$$

where for the purposes of keeping track of asymptotic orders we are explicitly writing the "$\hbar$"s. If we take the usual coordinate representation of the momentum operator $\hat{P} = -i\hbar\frac{d}{dX}$, it follows that

$$\hat{P}\Psi = -i\hbar\frac{d}{dX}\Psi = \left(\sum_{n=0}^{\infty}\hbar^n S_n'\right)\Psi \tag{2.74}$$

and

$$\hat{P}^2\Psi = \left(-i\hbar\frac{d}{dX}\right)^2\Psi = \left(-i\hbar\sum_{n=0}^{\infty}\hbar^n S_n''\right)\Psi + \left(\sum_{n=0}^{\infty}\hbar^n S_n'\right)^2\Psi. \tag{2.75}$$

Equation (2.67) then tells us that

$$E = H_0 + H_1\sum_{n=0}^{\infty}\hbar^n S_n' - \frac{i\hbar H_2'}{2} - i\hbar H_2'\sum_{n=0}^{\infty}\hbar^n S_n'$$

$$+ H_2\left(\sum_{n=0}^{\infty}\hbar^n S_n'\right)^2 - i\hbar H_2\left(\sum_{n=0}^{\infty}\hbar^n S_n''\right). \tag{2.76}$$

At order $\hbar^0$, equation (2.76) yields

$$E = H_0 + H_1 S_0' + H_2\left(S_0'\right)^2. \tag{2.77}$$

Upon comparison with the classical Hamiltonian form (2.68), we can deduce that $S_0' = P_\pm(E, X)$, with $P_\pm$ being the two momentum solutions to equation (2.68) with the value $H = E$. We have thus arrived at the standard WKB phase,

$$S_0 = \int dX\, P_\pm(E, X). \tag{2.78}$$

By inspection, one can also see that this WKB phase holds for an arbitrary Hamiltonian $H(X, P)$, as long as it is possible to expand $H(X, P)$ in powers of P.

At order $\hbar$, we have

$$H_1 S_1' - \frac{1}{2}iH_1' - iH_2' S_0' - iS_0'' H_2 + 2H_2 S_0' S_1' = 0, \tag{2.79}$$

from which we can obtain

$$S_1' = \frac{i}{2}\frac{\frac{d}{dX}\left(H_1 + H_2 S_0'\right)}{H_1 + H_2 S_0'} = \frac{i}{2}\frac{d}{dX}\ln\left|H_1 + H_2 S_0'\right|. \tag{2.80}$$
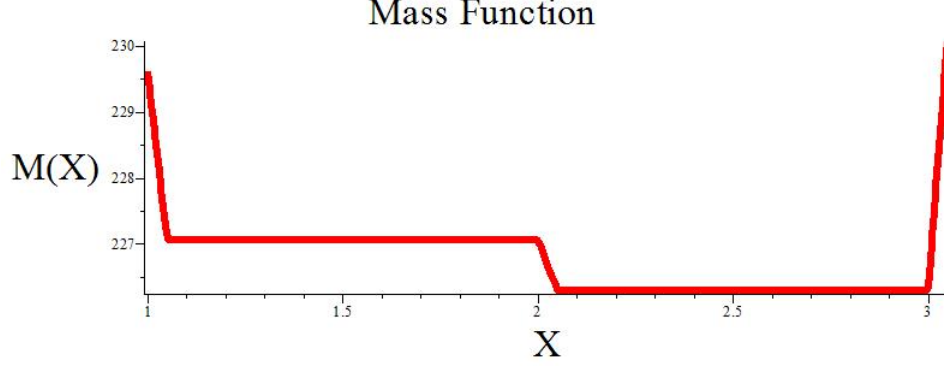
Figure 2.3: A sample mass function $\hat{M}$ is plotted with respect to the shell radius X. The mass function $\hat{M}$ serves to parametrize an equation of state of the form depicted in Figure 2.2. The approximate step function near $X = 2$ serves as a beam-splitter, and the steep quadratic sides correspond to the inner and outer reflectors of the interferometer.

Comparing again with the classical Hamiltonian form (2.68), we can write $H_1 + H_2 S_0' = \partial H / \partial P$ (evaluated at $H = E$), and up to an irrelevant constant the next term in the WKB expansion for Ψ can be written as

$$S_1 = \frac{i}{2} \ln \left| \frac{\partial H}{\partial P} \right|. \tag{2.81}$$

If we only include contributions from S_0 and S_1, we arrive at the form of the WKB approximation used to describe modes in our interferometer:

$$\Psi_E = \frac{e^{\frac{i}{\hbar} \int dX \, P_\pm(E,X)}}{\sqrt{\left| \frac{\partial E}{\partial P} \right|}}. \tag{2.82}$$

2.3.3 Flat Spacetime Limit

To determine whether or not gravity produces some form of decoherence in our interferometer, let us first clarify the manner in which coherence manifests itself in the absence of gravity. In this case spacetime is flat, and along the arms of the interferometer defined by (2.61) the shell behaves as a free particle.

As evident from Figure 2.3, the mass of the "free" shell is different on each interferometer arm. Let us call the inner mass M_-, and the outer mass

M_+, such that $M_- > M_+$. For simplicity, suppose the reflectors are perfect, which for this system means that the quadratic walls of the mass function are large and steep. Similarly, let the quadratic beam-splitter interval be approximated by a step function, to ensure that only constant mass function basis states need to be used in the quantum analysis.

Further, let us treat each element of the interferometer separately, in a similar manner to that which is done in optical systems. The initial state will first encounter the splitter, at which point each incoming mode will transform into a reflected mode with a factor $R_\leftarrow$ and a transmitted mode with a factor $T_\leftarrow$ (subscripts are used here because the reflection/transmission coefficients depend on the direction the incoming state encounters the splitter from).

The split initial state components will then perfectly reflect off of the outer/inner reflectors, and travel back towards one another to the beam-splitter. Upon recombination there will be further splitting of the components coming from each direction of the splitter, which produces two outputs (one going in each direction from the splitter) that are themselves composed of two parts; it is the interference between these two parts of each output that we are interested in.

Let us now describe the process in detail. For the purposes of this section, we will restrict our attention to a single-mode input, since the multi-mode analysis is more involved and will be discussed in Appendix B. As mentioned in Section 2.3.2, we will approximate the single-mode input by an ingoing WKB state:

$$\Psi_0 = \frac{e^{i \int dX P_{-+}}}{\sqrt{|\partial E/\partial P_{-+}|}} \equiv \psi_{-+}, \tag{2.83}$$

where the first set of plus/minuses of the reduced momentum P indicating outgoing/ingoing, and the second set indicating evaluations of P as X approaches X_δ from above/below. We will define the integration such that the lower bound in X is X_δ.

Treating the first splitting on its own, let us consider the wavefunction

$$\Psi = \begin{cases} \psi_{-+} + R_\leftarrow \psi_{++} & : X > X_\delta \\ T_\leftarrow \psi_{--} & : X < X_\delta \end{cases}$$

The (classical) flat spacetime Hamiltonian satisfies $H = \sqrt{P^2 + \hat{M}^2}$, which in the nonrelativistic limit yields $H \approx \hat{M} + P^2/2\hat{M}$. Applying wavefunction continuity at X_δ, and integrating the nonrelativistic Schrödinger equation

$$i\frac{\partial \psi}{\partial t} = \hat{M}\psi - \frac{1}{2}\frac{\partial}{\partial X}\left(\frac{1}{\hat{M}}\frac{\partial \psi}{\partial X}\right) \tag{2.84}$$

30

across X_δ, one can obtain the reflection and transmission amplitudes $R_\leftarrow$ and $T_\leftarrow$. The equations take a simpler form after transforming to the variables $\bar{R}_\leftarrow$ and $\bar{T}_\leftarrow$, which are defined by

$$\bar{R}_\leftarrow \equiv \sqrt{\left|\frac{\left|\frac{\partial E}{\partial P_{-+}}\right|}{\left|\frac{\partial E}{\partial P_{++}}\right|}\right|} R_\leftarrow, \ \ \bar{T}_\leftarrow \equiv \sqrt{\left|\frac{\left|\frac{\partial E}{\partial P_{-+}}\right|}{\left|\frac{\partial E}{\partial P_{--}}\right|}\right|} T_\leftarrow. \tag{2.85}$$

One can then easily solve for the new variables:

$$\bar{R}_\leftarrow = \frac{M_- P_{-+} - M_+ P_{--}}{M_+ P_{--} - M_- P_{++}}, \ \ \bar{T}_\leftarrow = \frac{M_-(P_{++} - P_{-+})}{M_- P_{++} - M_+ P_{--}}. \tag{2.86}$$

For convenience, we can also derive the reflection and transmission amplitudes from the left, which are found to be

$$\bar{R}_\rightarrow = \frac{M_- P_{++} - M_+ P_{+-}}{M_+ P_{--} - M_- P_{++}}, \ \ \bar{T}_\rightarrow = \frac{M_+(P_{+-} - P_{--})}{M_- P_{++} - M_+ P_{--}}, \tag{2.87}$$

using the similar definitions

$$\bar{R}_\rightarrow \equiv \sqrt{\left|\frac{\left|\frac{\partial E}{\partial P_{+-}}\right|}{\left|\frac{\partial E}{\partial P_{--}}\right|}\right|} R_\rightarrow, \ \ \bar{T}_\rightarrow \equiv \sqrt{\left|\frac{\left|\frac{\partial E}{\partial P_{+-}}\right|}{\left|\frac{\partial E}{\partial P_{++}}\right|}\right|} T_\rightarrow. \tag{2.88}$$

Let us call the outgoing state after the split $\Psi_+^{(i)}$ and the ingoing state $\Psi_-^{(i)}$. We then can consider the first splitting a transformation of the wavefunction such that

$$\Psi_0 = \psi_{-+} \rightarrow \begin{pmatrix} \Psi_+^{(i)} \\ \Psi_-^{(i)} \end{pmatrix} = \begin{pmatrix} R_\leftarrow \psi_{++} \\ T_\leftarrow \psi_{--} \end{pmatrix}. \tag{2.89}$$

This splitting should preserve the probability current, for consistency. In the nonrelativistic, flat spacetime limit, the probability current J satisfies the continuity equation

$$\frac{\partial}{\partial t}\left(|\psi|^2\right) + \frac{\partial}{\partial X}J = 0 \tag{2.90}$$

and is given by the usual quantum mechanics expression

$$\frac{1}{2im}\left(\psi^*\psi' - \psi\psi^{*\prime}\right). \tag{2.91}$$

Therefore, in this limit we have an input probability current of

$$J_0 = |\Psi_0|^2 \frac{P_{-+}}{M_+}. \tag{2.92}$$

After first encountering the beam-splitter, the probability current (2.92) splits into reflected and transmitted components

$$
\begin{aligned}
|J_+^{(i)}| &= \frac{1}{2iM_+} \left(\Psi_+^{(i)*} \left(\Psi_+^{(i)} \right)' - \Psi_+^{(i)} \left(\Psi_+^{(i)} \right)^{*\prime} \right) \\
&= |J_0| \bar{R}_\leftarrow^2 \tag{2.93}
\end{aligned}
$$

and

$$
\begin{aligned}
|J_-^{(i)}| &= \frac{1}{2iM_-} \left(\Psi_-^{(i)*} \left(\Psi_-^{(i)} \right)' - \Psi_-^{(i)} \left(\Psi_-(i) \right)^{*\prime} \right) \\
&= |J_0| \left(\frac{M_+ P_{--}}{M_- P_{-+}} \right) \bar{T}_\leftarrow^2. \tag{2.94}
\end{aligned}
$$

The splitting preserves probability current, as can be confirmed by observing that $\left| \frac{J_+^{(i)}}{J_0} \right| + \left| \frac{J_-^{(i)}}{J_0} \right|$ is unity. The terms $\left| \frac{J_+^{(i)}}{J_0} \right|$ and $\left| \frac{J_-^{(i)}}{J_0} \right|$ are usually called the reflection and transmission coefficients, respectively.

The second transformation propagates the modes along the interferometer arms, such that

$$
\begin{pmatrix} \Psi_+^{(i)} \\ \Psi_-^{(i)} \end{pmatrix} \to \begin{pmatrix} \Psi_+^{(ii)} \\ \Psi_-^{(ii)} \end{pmatrix} = \begin{pmatrix} (E_{,++})^{-1/2} R_\leftarrow e^{i\Phi_{++}} \\ (E_{,--})^{-1/2} T_\leftarrow e^{i\Phi_{--}} \end{pmatrix}. \tag{2.95}
$$

For brevity, the notation $E_{,\pm\pm}$ was used to denote $\partial E / \partial P_{\pm\pm}$, and it is understood that we are evaluating these quantities at the outer walls of the interferometer. We have also introduced the quantities $\Phi_{\pm\pm} = \phi_{\pm\pm} - E t_{\pm\pm}$, for $\phi_{\pm\pm} = \int_{X_\delta}^{X_\pm} dX P_{\pm\pm}$, where t_{++} and t_{--} denote the travel times from the splitter to X_+ and X_-, respectively.

The modes then reflect off of the outer walls, as

$$
\begin{pmatrix} \Psi_+^{(ii)} \\ \Psi_-^{(ii)} \end{pmatrix} \to \begin{pmatrix} \Psi_+^{(iii)} \\ \Psi_-^{(iii)} \end{pmatrix} = \begin{pmatrix} (E_{,-+})^{-1/2} R_\leftarrow e^{i\Phi_{++}} R^\rightarrow \\ (E_{,+-})^{-1/2} T_\leftarrow e^{i\Phi_{--}} R^\leftarrow \end{pmatrix}. \tag{2.96}
$$

The outer wall reflection amplitudes $(R^\rightarrow, R^\leftarrow)$ only depend on continuity of the wavefunction. To obtain the reflection amplitude from the left, for instance, consider the wavefunction

$$
\Psi = \psi_{++} \to \begin{cases} 0 & : X > X_+ \\ (\psi_{++} + R^\rightarrow \psi_{--}) & : X < X_+ \end{cases}
$$

By applying wavefunction continuity at X_+, one immediately obtains $R^\rightarrow$. $R^\leftarrow$ can be similarly determined, and the results are

$$\bar{R}^\rightarrow = -e^{i(\phi_{++}+\phi_{-+})}, \quad \bar{R}^\leftarrow = -e^{i(\phi_{+-}+\phi_{--})}, \tag{2.97}$$

with help of the simplifying definitions

$$\bar{R}^\rightarrow \equiv \sqrt{\left|\frac{\frac{\partial E}{\partial P_{++}}}{\frac{\partial E}{\partial P_{-+}}}\right|} R^\rightarrow, \quad \bar{R}^\leftarrow \equiv \sqrt{\left|\frac{\frac{\partial E}{\partial P_{--}}}{\frac{\partial E}{\partial P_{+-}}}\right|} R^\leftarrow. \tag{2.98}$$

The phases are defined such that $\phi_{\pm\mp} = \int_{X_\mp}^{X_\delta} dX P_{\pm\mp}$ (signs chosen together). We will refer to the modes after reflection from the outer walls as $\Psi_\pm^{(iii)}$.

Propagation along the arms back to the splitter then proceeds as

$$\begin{pmatrix} \Psi_+^{(iii)} \\ \Psi_-^{(iii)} \end{pmatrix} \rightarrow \begin{pmatrix} \Psi_+^{(iv)} \\ \Psi_-^{(iv)} \end{pmatrix}, \tag{2.99}$$

for

$$\begin{pmatrix} \Psi_+^{(iv)} \\ \Psi_-^{(iv)} \end{pmatrix} = \begin{pmatrix} (E_{,-+})^{-1/2} R_\leftarrow e^{i\Phi_{++}} R^\rightarrow e^{i\Phi_{-+}} \\ (E_{,+-})^{-1/2} T_\leftarrow e^{i\Phi_{--}} R^\leftarrow e^{i\Phi_{+-}} \end{pmatrix}. \tag{2.100}$$

In this expression, the quantities $E_{,-+}$ and $E_{,+-}$ are evaluated at the splitter, and we have used the definitions $\Phi_{\pm\mp} = \phi_{\pm\mp} - Et_{\pm\mp}$ (signs again chosen together). Here t_{-+} and t_{+-} denote the travel times from X_+ to the splitter and from X_- to the splitter, respectively.

The second encounter with the splitter occurs as it did before, as

$$\begin{pmatrix} \Psi_+^{(iv)} \\ \Psi_-^{(iv)} \end{pmatrix} \rightarrow \begin{pmatrix} \Psi_+^{(v)} \\ \Psi_-^{(v)} \end{pmatrix} = \begin{pmatrix} \bar{R}_\leftarrow & \bar{T}_\rightarrow \\ \bar{T}_\leftarrow & \bar{R}_\rightarrow \end{pmatrix} \begin{pmatrix} \Psi_+^{(iv)} \\ \Psi_-^{(iv)} \end{pmatrix}. \tag{2.101}$$

At the order we are working at in $\hbar$, the derivatives of our final outputs satisfy

$$\frac{d}{dX} \Psi_\pm^{(v)} = iP_{\pm\pm}\Psi_\pm^{(v)}, \tag{2.102}$$

and so the currents for our final outputs are given by

$$\begin{aligned} J_\pm^{(v)} &= \frac{1}{2iM_\pm} \left(\Psi_\pm^{(v)*} \left(\Psi_\pm^{(v)}\right)' - \Psi_\pm^{(v)} \left(\Psi_\pm^{(v)}\right)^{*'} \right) \\ &= \frac{P_{\pm\pm}}{M_\pm} \left|\Psi_\pm^{(v)}\right|^2. \end{aligned} \tag{2.103}$$

We then have enough information to calculate the final reflected and transmitted probability currents, which can be written

$$|J_+^{(v)}| = |J_0| \left[1 - 4\bar{R}_\leftarrow^2 \left(1 - \bar{R}_\leftarrow^2 \right) \sin^2 \varphi \right] \qquad (2.104)$$

and

$$|J_-^{(v)}| = |J_0| 4\bar{R}_\leftarrow^2 \left(1 - \bar{R}_\leftarrow^2 \right) \sin^2 \varphi, \qquad (2.105)$$

where we have defined $\varphi = \phi_{++} + \phi_{-+} - \phi_{+-} - \phi_{--}$ and made use of the identity $\bar{R}_\leftarrow^2 + \frac{M_+ P_{--}}{M_- P_{-+}} \bar{T}_\leftarrow^2 = 1$. The flat-spacetime interferometer thus manifestly conserves probability current in all regions of the parameter space.

One can now search for a nice region in the parameter space that cancels one of the outputs. First, we would like to avoid regions of the parameter space that don't describe splitting, i.e. complete initial reflection or transmission by the beam-splitter. We can accomplish this in a simple way by enforcing an equal splitting condition, $\bar{R}_\leftarrow^2 = 1/2$. This leads to compact expressions for the final reflection and transmission coefficients, given by

$$R_f \equiv \frac{|J_+^{(v)}|}{|J_0|} = \cos^2 \varphi \qquad (2.106)$$

and

$$T_f \equiv \frac{|J_-^{(v)}|}{|J_0|} = \sin^2 \varphi, \qquad (2.107)$$

respectively.

We should also make sure that our shell velocity doesn't approach the speed of light, since we are working in the nonrelativistic limit. For small shell speeds, given an outer mass M_+ and an initial speed v_+, the initial splitting will be equal provided the inner mass satisfies

$$M_- \approx M_+ \left[1 + \left(6\sqrt{2} - 8 \right) v_+^2 - \left(99\sqrt{2} - 140 \right) v_+^4 \right]. \qquad (2.108)$$

In the quantum context, the "speed" v_+ is defined such that $E = M_+ + \frac{1}{2} M_+ v_+^2$, for a WKB state with energy E.

If we denote the interferometer arm lengths by $L_\pm \equiv \pm (X_\pm - X_\delta)$, we can see from the form of the reflection and transmission coefficients that one of the outputs will be completely cancelled if

$$\begin{aligned} \varphi &= 2L_+ \sqrt{2M_+ (E - M_+)} - 2L_- \sqrt{2M_- (E - M_-)} \\ &= 2L_+ M_+ v_+ - 2L_- M_- v_- \\ &= \frac{n\pi}{2}, \end{aligned} \qquad (2.109)$$

for $n \in \mathbb{Z}$. Thus, as the outer arm length is increased or decreased, the outputs are alternately cancelled out for each value of n (odd values cancel the transmitted output, and even values cancel the reflected output), with partial interference for intermediate arm lengths that don't correspond to solutions of (2.109). This behaviour is a direct reflection of coherence in the flat spacetime interferometer.

2.3.4 General Relativistic Picture

The current framework was designed to facilitate the inclusion of general relativistic corrections. Several expressions become messier once one includes gravity, and some expressions fundamentally change in structure. For instance, the standard probability current $J_s = \frac{1}{2im}\left(\psi^*\psi' - \psi\psi^{*\prime}\right)$ given by (2.91) is no longer conserved in systems with more general Hamiltonians. In fact, a probability current for an arbitrary Hamiltonian system has never been constructed; only special cases are known, such as the standard current J_s for the nonrelativistic Hamiltonian $H = P^2/2m + V(X)$. For any other Hamiltonian, the current J_s does not satisfy the continuity equation (2.90), and therefore does not conserve probability.

A special case that is less well-known is for the first relativistic correction to the nonrelativistic Hamiltonian $H = P^2/2m + V(X)$, which is of the form αP^4 (with $\alpha = -1/8m^3$, to match the next term in the Taylor expansion of $\sqrt{P^2 + m^2}$ in P). The Schrödinger equation $i\partial\psi/\partial t = H\psi$, along with its conjugated counterpart $-i\partial\psi^*/\partial t = H^\dagger\psi^*$, imply that

$$\frac{\partial\rho}{\partial t} = i\left[\psi\left(H^\dagger\psi^*\right) - \psi^*\left(H\psi\right)\right], \tag{2.110}$$

and so linearity in H allows us to determine the correction to the current J_s coming from the extra term αP^4 independently of the first terms in the Hamiltonian. If one observes that

$$\psi\frac{\partial^4\psi^*}{\partial X^4} - \psi^*\frac{\partial^4\psi}{\partial X^4} = -\frac{\partial}{\partial X}\left(\psi^*\frac{\partial^3\psi}{\partial X^3} - \frac{\partial\psi^*}{\partial X}\frac{\partial^2\psi}{\partial X^2} + \frac{\partial^2\psi^*}{\partial X^2}\frac{\partial\psi}{\partial X} - \frac{\partial^3\psi^*}{\partial X^3}\psi\right) \tag{2.111}$$

then one can deduce that the current correction takes the form

$$i\alpha\left(\psi^*\frac{\partial^3\psi}{\partial X^3} - \frac{\partial\psi^*}{\partial X}\frac{\partial^2\psi}{\partial X^2} + \frac{\partial^2\psi^*}{\partial X^2}\frac{\partial\psi}{\partial X} - \frac{\partial^3\psi^*}{\partial X^3}\psi\right). \tag{2.112}$$

Similar (somewhat more complex) constructions exist for Hamiltonians with higher powers of the momentum, but our system of interest has

position-dependent coefficients when expanded in powers of the momentum. If we take the operator ordering of the approximate form (2.69) as an exact Hamiltonian, we end up with a more general quadratic Hamiltonian than $H = P^2/2m + V(X)$, since now we have a term linear in momentum with a function of X as a coefficient, as well as another function of X as a coefficient of the term quadratic in momentum. As demonstrated in Appendix A, we can find a probability current J for this more general Hamiltonian that satisfies the continuity equation (2.90). We can express this probability current as

$$J = \left(\frac{\partial H}{\partial P}\right)|\Psi|^2 + \frac{1}{2i}\left(\frac{\partial^2 H}{\partial P^2}\right)\left(\Psi^*\Psi' - \Psi\Psi^{*\prime}\right). \qquad (2.113)$$

The P-derivatives in this expression are again evaluated at $P = 0$, and for the special case of $\{\left(\frac{\partial H}{\partial P}\right) = 0, \left(\frac{\partial^2 H}{\partial P^2}\right) = 1/m\}$, we are left with the nonrelativistic, flat spacetime limit described by (2.91).

If we use the WKB Hamiltonian (2.72), we find that the generalized probability current is given by

$$J \sim -\frac{2}{3}\sqrt{\frac{2\hat{M}}{X}}|\Psi|^2 + \left(1 + \frac{2\hat{M}}{3X}\right)J_s, \qquad (2.114)$$

with J_s being the standard (nonrelativistic) expression (2.91) for the probability current. Note that although the functional form of J_s with respect to Ψ is the same as the nonrelativistic current (2.91), in the above expression we are inserting the general relativistic WKB wavefunction Ψ.

Since our Schrödinger equation now takes the asymptotic form

$$H_w\Psi = i\frac{\partial}{\partial t}\Psi, \qquad (2.115)$$

taking the operator ordering mentioned above, we no longer have the simple reflection and transmission amplitudes obtained in the previous section. For instance, integrating (2.115) across X_δ yields

$$\left[\left(\frac{3}{2\hat{M}} + \frac{1}{X}\right)\Psi'\right]_\delta = i\sqrt{\frac{2}{X_\delta}}\left[\sqrt{\hat{M}}\right]_\delta \Psi(X_\delta). \qquad (2.116)$$

Here, $[\cdot]_\delta$ represents the jump of a quantity across X_δ.

To the order we are working at in $\hbar$, the new reflection and transmission amplitudes for scattering from the right are given by

$$\bar{R}_\leftarrow = \frac{\sqrt{\frac{2}{X_\delta}}\left[\sqrt{\hat{M}}\right]_\delta + \left(\frac{3}{2M_-} + \frac{1}{X_\delta}\right)P_{--} - \left(\frac{3}{2M_+} + \frac{1}{X_\delta}\right)P_{-+}}{-\sqrt{\frac{2}{X_\delta}}\left[\sqrt{\hat{M}}\right]_\delta - \left(\frac{3}{2M_-} + \frac{1}{X_\delta}\right)P_{--} + \left(\frac{3}{2M_+} + \frac{1}{X_\delta}\right)P_{++}} \qquad (2.117)$$

36

and

$$\bar{T}_{\leftarrow} = \frac{\left(\frac{3}{2M_+} + \frac{1}{X_\delta}\right)(P_{++} - P_{-+})}{-\sqrt{\frac{2}{X_\delta}}\left[\sqrt{\hat{M}}\right]_\delta - \left(\frac{3}{2M_-} + \frac{1}{X_\delta}\right)P_{--} + \left(\frac{3}{2M_+} + \frac{1}{X_\delta}\right)P_{++}}. \quad (2.118)$$

Similarly, for scattering from the left we have

$$\bar{R}_{\rightarrow} = \frac{\sqrt{\frac{2}{X_\delta}}\left[\sqrt{\hat{M}}\right]_\delta + \left(\frac{3}{2M_-} + \frac{1}{X_\delta}\right)P_{+-} - \left(\frac{3}{2M_+} + \frac{1}{X_\delta}\right)P_{++}}{-\sqrt{\frac{2}{X_\delta}}\left[\sqrt{\hat{M}}\right]_\delta - \left(\frac{3}{2M_-} + \frac{1}{X_\delta}\right)P_{--} + \left(\frac{3}{2M_+} + \frac{1}{X_\delta}\right)P_{++}} \quad (2.119)$$

and

$$\bar{T}_{\rightarrow} = \frac{\left(\frac{3}{2M_-} + \frac{1}{X_\delta}\right)(P_{+-} - P_{--})}{-\sqrt{\frac{2}{X_\delta}}\left[\sqrt{\hat{M}}\right]_\delta - \left(\frac{3}{2M_-} + \frac{1}{X_\delta}\right)P_{--} + \left(\frac{3}{2M_+} + \frac{1}{X_\delta}\right)P_{++}}. \quad (2.120)$$

Reflection from the outer walls is again described by (2.98), though it should be noted that since the partial derivatives in (2.98) now have X-dependence, they are to be evaluated at the outer walls (X_+ for $R^{\rightarrow}$ and X_- for $R^{\leftarrow}$).

Given the definition of probability current in this (more general) setting, we have

$$J_{\pm}^{(v)} = \left(\left(1 + \frac{2M_{\pm}}{3X_\delta}\right)\frac{P_{\pm\pm}}{M_{\pm}} - \frac{2}{3}\sqrt{\frac{2M_{\pm}}{X_\delta}}\right)\left|\Psi_{\pm}^{(v)}\right|^2. \quad (2.121)$$

Just as in the flat spacetime limit, the final output states are given by (2.101), except that now the reflection/transmission amplitudes and the WKB phases are more complicated.

The initial current can be expressed as

$$J_i = \left(1 - \frac{2M_+}{3P_{-+}}\sqrt{\frac{2M_+}{X_\delta}} + \frac{2M_+}{3X_\delta}\right)J_0, \quad (2.122)$$

with J_0 being the nonrelativistic initial current (2.92), and so the final reflection and transmission coefficients $R_f \equiv \frac{|J_+^{(v)}|}{|J_i|}$ and $T_f \equiv \frac{|J_-^{(v)}|}{|J_i|}$ (respectively) are fully determined.

Another similarity to the flat spacetime limit is that the oscillatory part of the final reflection and transmission coefficients is defined by $\varphi = \phi_{++} +$

Final Reflection and Transmission Coefficients
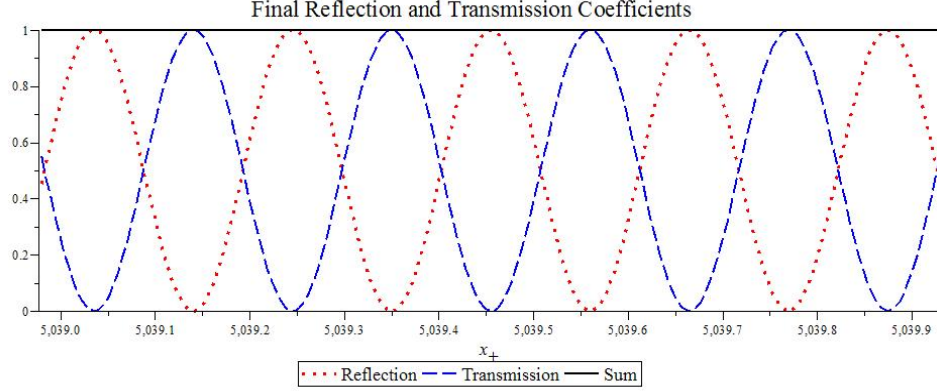
Figure 2.4: Sample interference pattern, for $M_+ = 15$, $v_+ = 0.003$, $X_- = 5000$, $L_- = 20$, and M_- chosen to satisfy (2.108), plotted against the outer mirror position, X_+. The alternating pattern from 0 to 1 of both the final reflection and final transmission coefficients indicates that complete constructive/destructive interference occurs in this parameter region, from which we can conclude that coherence is fully present.

Final Reflection and Transmission Coefficients
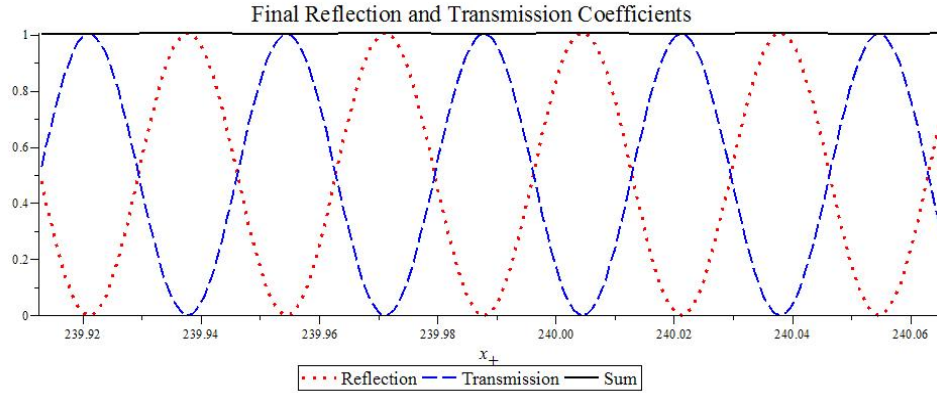
Figure 2.5: Sample interference pattern, for $M_+ = 15$, $v_+ = 0.01$, $X_- = 200$, $L_- = 20$, and M_- chosen to satisfy (2.108), plotted against the outer mirror position, X_+. As in the previous figure, there is an alternating pattern of the final reflection/transmission coefficients from 0 to 1 as the outer arm length changes, indicating that coherence is still fully present as we bring the interferometric range closer to the Schwarzschild radius of the shell. In this region of the parameter space, we begin to see the sum of the final reflection and transmission coefficients fail to add up to exactly unity, due to the gradual breakdown of our approximation to the probability current.

$\phi_{-+} - \phi_{+-} - \phi_{--}$, with the various ϕ terms involving integrals of the general relativistic momentum (2.48). In the weak-field limit, the initial ingoing momentum is given by

$$P_{-+} \sim -\sqrt{H^2 - M_+^2} + \frac{2}{3}\sqrt{\frac{2H}{X}}H$$
$$-\frac{\left(H^2 - M_+^2/2\right)H}{\sqrt{H^2 - M_+^2}X}, \tag{2.123}$$

to second order in $1/\sqrt{X}$. Care should be taken with these approximations, however, because our probability current (2.113) is exactly conserved only in the quadratic momentum limit, which for the shell system is defined by (2.72). Also, the WKB solutions only approximately satisfy the Schrödinger equation. Because of this, in order to control the errors involved in the approximations we find it useful to consider the "WKB momentum," which we define by solving (2.72) for P, and expanding to second order in $1/\sqrt{X}$. For the initial ingoing momentum, the WKB momentum takes the form

$$P_{w-+} \sim -\sqrt{2M_+\left(H - M_+\right)} + \frac{2}{3}\sqrt{\frac{2M_+}{X}}M_+$$
$$-\sqrt{\frac{2M_+}{\left(H - M_+\right)}}\frac{\left(7M_+ - 4H\right)}{12X}. \tag{2.124}$$

To understand the interference pattern described by R_f and T_f, let us consider what φ looks like in the weak-field limit, for slow speeds ($v_\pm \to 0$):

$$\varphi \quad \sim \quad 2L_+M_+v_+ - 2L_-M_-v_-$$
$$+\frac{M_+^2}{v_+}\ln\left(\frac{X_+}{X_\delta}\right) - \frac{M_-^2}{v_-}\ln\left(\frac{X_\delta}{X_-}\right). \tag{2.125}$$

Let us further imagine that we vary the outer arm length L_+, while keeping all other parameters constant. If the phase condition (2.109) from flat space-time still approximately holds, then the corresponding expression (2.125) in the weak-field limit tells us that successive values of n (say, n to $n + 1$) are associated with outer arm length values L_{+n} and $L_{+(n+1)}$. Subtracting $\varphi_n = n\pi/2$ from $\varphi_{n+1} = (n+1)\pi/2$ yields

$$\frac{\pi}{2} = 2M_+v_+\Delta L_n + \frac{M_+^2}{v_+}\ln\left(\frac{X_{+n} + \Delta L_n}{X_{+n}}\right), \tag{2.126}$$
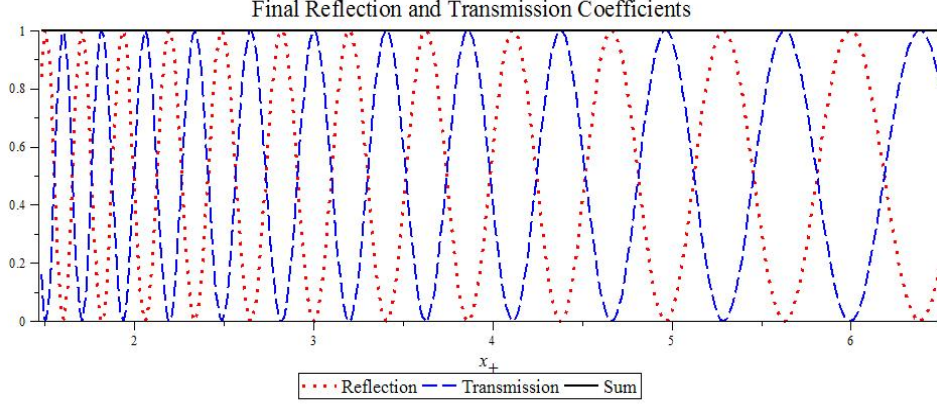
Figure 2.6: Sample interference pattern, for $M_+ = 0.05$, $v_+ = 0.0001$, $X_- \approx 1$, $L_- \approx 0.997$, and M_- chosen to satisfy (2.108), plotted against the outer mirror position, X_+. The node spacing decreases as the interferometric range is pushed closer to the Schwarzschild radius of the shell, and asymptotes to a fixed value $\Delta L_n = \pi/4M_+v_+$ as we approach spatial infinity. This "gravitational node squeezing" was present, though not visually detectable, in the previous interference patterns.

with the definitions $X_{+n} = X_\delta + L_{+n}$ and $\Delta L_n = L_{+(n+1)} - L_{+n}$. The distance between nodes of the interference pattern, denoted by ΔL_n, is somewhat less than the outer mirror radius X_+, for the cases we are interested in; thus, we can expand the logarithm and solve for ΔL_n, which gives us

$$\Delta L_n \approx \frac{\pi}{4M_+ \left(v_+ + \frac{M_+}{2v_+ X_{+n}}\right)}. \tag{2.127}$$

This result shows that gravity causes the node spacing in the interference pattern to increase with increasing outer arm length. In the flat space limit (i.e. as $X_\pm \to \infty$), we obtain the equal node spacing $\Delta L_n = \pi/4M_+v_+$, for all $n \in \mathbb{Z}$.

One can see from Figures 2.4 and 2.5 that as we go from the essentially flat limit ($X_\pm \to \infty$) to less than 10 Schwarzschild radii, we can still alternately cancel the reflection and transmission coefficients, even though the approximations lead to a probability current that is not fully conserved (note that the sum of the final probability currents differs from the initial current by about 1%). We take this as a direct indication that coherence is fully present in the single-mode system even with general relativistic corrections taken into account.

It is not clear from Figures 2.4 and 2.5, but the node spacing is indeed changing as (2.127) suggests. The reason it is not visible from these plots is that the node spacing changes noticeably only over a range of many wavelengths. Under more extreme circumstances, as depicted in Figure 2.6, there are visible changes in node spacing, though this represents a situation that is of less physical interest, since the de Broglie wavelength of the shell is larger than the interferometer arms.

2.4 Discussion

There are two problems with taking this result of no loss of coherence as the definitive answer to whether or not gravity, by itself, could decohere a system. The first is that these single-mode states correspond in some sense to energy eigenstates; one might expect it is only a superposition of energies that leads to decoherence, since from the above analysis one can see that the time-dependence cancels out of the final expressions for output probabilities in the interferometer. As mentioned above, we discuss how wave-packets behave in this model in Appendix B.

The second problem is that Penrose's intuition ties the loss of coherence to the inability to map one spacetime in any unique way onto a different spacetime. By our coordinate choice we have, in effect, chosen a unique way: two spacetime points are the same if they have the same coordinates. However, this is of course arbitrary and depends on the coordinate choice made. While the Painlevé-Gullstrand coordinates have many advantageous features, they are not the only possible choice. Do all coordinate choices produce the same maxima and minima in the interference pattern? The full classical action that describes our interferometer is independent of the coordinate choice, but it is not obvious whether this is enough to ensure coordinate independence in the reduced phase space quantization. These issues will be examined in Chapter 3.

It could also be argued that the reduced phase space approximation leads to an artificial form of time-evolution that is not entirely consistent with the "timeless" structure of canonical quantum gravity. For instance, the lack of a satisfactory interpretation of reduced phase space minisuperspace quantum cosmology was discussed in [60]. One might then be drawn to the conclusion that in the limited setting of our approximations, the evolution will necessarily be unitary (by construction), and we will escape Hawking's original arguments about pure states evolving into mixed states [61] by virtue of our approximation scheme.

Certainly, our simple model does not have the features often associated with nonunitary modifications to standard Hamiltonian evolution (such as the inclusion of microscopic wormhole interactions [62]), but there is still reason to believe the evolution defined by (2.48) could in principle exhibit decoherence. For one thing, we have in some places used an approximate Hamiltonian (2.72) that is quadratic in momenta and strictly Hermitian, but it may not be possible to define a Hermitian Hamiltonian operator that exactly corresponds to the solution of (2.48) (which is transcendental). For another, even if one could solve (2.48), the resulting Hamiltonian would be non-polynomial in both the momenta and the coordinate X. This means that the time evolution of the wavefunction at X is not described by a finite number of derivatives at X, and is thus nonlocal, in the sense that the evolution equation is equivalent to an integro-differential equation with finitely-many derivatives [63]-[66]. While some systems can be nonlocal in this way and yet maintain coherence (such as in the case of relativistic particles in flat spacetime [63], [64]), in other such systems there can be unexpected behaviour such as "nonlocally-induced randomness" [65], [66], which would in our case be attributable to gravity. These studies are still in their infancy, so it remains an open question whether or not this type of nonlocal behaviour can be connected with gravitational intrinsic decoherence.

Chapter 3

The Meaning of Time in Reduced Phase Space

3.1 Coordinate Generalizations and Time Transformations

In Section 2.2.4, we chose a specific coordinate system when we carried out the Hamiltonian reduction. One naturally wonders whether there is coordinate dependence in any of the results we have presented. The canonical momentum in the reduced system certainly depends on the coordinate choice, but one can show that a broad set of choices lead to the same reduced classical action [58].

What about the quantization associated with the specific coordinate choice we made? It is often claimed that different choices of a time variable lead to unitarily inequivalent quantizations (see [67], for instance). Does this imply that different coordinate choices lead to fundamentally different interference patterns? For each choice of coordinates, we can uniquely define a (classical) network of observers whose worldlines span the spacetime, so a different coordinate choice produces a reduced phase space quantization defined with respect to a different observer network. Which features of each quantization reflect properties of the shell system itself, and which features are due entirely to the properties of the observer network?

We will investigate differences that may arise due to different coordinate choices by considering a family of coordinate systems that generalize the Painlevé-Gullstrand coordinates used in the previous chapter. We will repeat many of the previous calculations, this time for an arbitrary member of the family of coordinate systems. In doing so, we will face some serious difficulties interpreting the results and connecting the generalized calculations with the previous ones.

Let us now describe the infinite family of coordinate systems that generalized our previous coordinates: in terms of the metric variables defined above, we can define the coordinate family (as demonstrated by Martel and

Poisson [68]) by

$$L = \lambda, \quad R = r, \quad N = \frac{1}{\lambda}, \quad N^r = \pm\frac{\sqrt{1 - \lambda^2 f}}{\lambda^2}, \quad f = 1 - \frac{2\mathcal{M}}{r}, \quad (3.1)$$

with $\mathcal{M}$ being the (enclosed) ADM mass and $0 < \lambda \leq 1$ corresponding to the set of Painlevé family members. In the $\lambda \to 0$ limit, the coordinates defined by (3.1) become the familiar (null) Eddington-Finkelstein coordinates [3]. In the upper limit, $\lambda \to 1$, the coordinates (3.1) reduce to the Painlevé-Gullstrand coordinates used in the previous chapters. We will choose the positive sign for the shift vector N^r, for simplicity.

The line element in these coordinates then takes the form

$$ds^2 = \frac{1}{\lambda^2}dt_\lambda^2 + \lambda^2\left(dr + \frac{1}{\lambda^2}\sqrt{1 - \lambda^2 f}dt_\lambda\right)^2 + r^2 d\Omega^2. \quad (3.2)$$

This generalized Painlevé-Gullstrand coordinate system still possesses the connection between coordinate lines and infalling observers, as with the standard $\lambda = 1$ coordinates. The quantity λ is related to the "initial velocity at infinity"[4] of an infalling observer:

$$\lambda = \sqrt{1 - v_\infty^2}. \quad (3.3)$$

This initial velocity is in turn related to the geodesic observer's energy per unit rest mass $\tilde{E}$ through the standard expression $\tilde{E} = 1/\sqrt{1 - v_\infty^2}$ [68]. Any particular generalized coordinate system in the family can therefore be interpreted as a network of geodesic observers, each with the same energy per unit rest mass. Any such network has the property that its observers all have proper 4-velocities equal to a constant times the gradient of a time function t_λ, with the time function given by

$$t_\lambda = T + \int dr\, \frac{\sqrt{1 - \lambda^2 f}}{f}. \quad (3.4)$$

Here T is the Schwarzschild time, which is related to the standard ($\lambda = 1$) Painlevé-Gullstrand time t by

$$t = T + 4\mathcal{M}\left(\sqrt{\frac{r}{2\mathcal{M}}} + \frac{1}{2}\ln\left|\frac{\sqrt{\frac{r}{2\mathcal{M}}} - 1}{\sqrt{\frac{r}{2\mathcal{M}}} + 1}\right|\right). \quad (3.5)$$

---

[3]Also known as Penrose-Eddington-Finkelstein coordinates, due to Penrose's explicit initial use of them [69].

[4]Following the convention from [68], we define positive observer velocity to be radially inward, such that v_∞ takes on values from 0 to 1 as λ varies from 1 to 0. This is the opposite convention as the one used for the shell velocity.

The time transformation (3.4) also implies that the relationship between the time coordinates (at the shell) specified by two different choices of λ is

$$t_\lambda - t_{\lambda'} = F_\lambda - F_{\lambda'}, \qquad (3.6)$$

such that

$$
\begin{aligned}
F_\lambda &= \int dX \, \frac{\sqrt{1 - \lambda^2 f}}{f} \\
&= 4H \left[\frac{X}{4H} \sqrt{1 - \lambda^2 f} + \ln\left(\frac{\sqrt{f}}{1 + \sqrt{1 - \lambda^2 f}} \right) \right. \\
&\quad \left. + \frac{\left(1 - \frac{\lambda^2}{2}\right)}{\sqrt{1 - \lambda^2}} \ln\left(\sqrt{\frac{X}{2H}} \left(\sqrt{1 - \lambda^2} + \sqrt{1 - \lambda^2 f} \right) \right) \right] \qquad (3.7)
\end{aligned}
$$

and $f = 1 - 2H/X$. This expression differs from the corresponding (incorrect) expression presented by Martel and Poisson in [68], though one need only perform some simple differentiation to see that (3.7) is the correct one.

In the context of investigating the connections between quantizations for different time choices, the transformation defined by (3.6) and (3.7) has some peculiar features. Most notably, the relation between two time coordinates involves both the shell position X and the Hamiltonian H. This makes it unclear under what conditions this transformation can be implemented; at the quantum level, both X and H are operators, which implies that either the relation between different time choices is operator-valued, or that we may only be able to perform the transformation at the classical level. Then it is no simple matter connecting the evolution operators for different time choices, since each operator takes the form

$$U_\lambda(t_\lambda) = e^{-iHt_\lambda}. \qquad (3.8)$$

Will the quantization for one choice of λ be interpreted from a different choice λ' as having an operator-valued time "parameter"?

To explore this issue, among others, we will quantize the shell system for an arbitrary time choice in the reduced phase space approximation. Before we can do this, we need to determine the reduced Hamiltonian structure in the generalized coordinates, which we will now focus our attention on.

3.2 Phase Space Reduction in a Family of Coordinate Systems

The starting point in the phase space reduction associated with the generalized Painlevé-Gullstrand coordinates (3.1) is again to consider the Liouville form $\mathcal{F}$ on the full phase space Γ; just as in Chapter 2, this is given by

$$\mathcal{F} = P\boldsymbol{\delta}X + \int dr\,(\pi_L\boldsymbol{\delta}L + \pi_R\boldsymbol{\delta}R). \tag{3.9}$$

We can then pull this back to the representative hypersurface $\bar{H}_\lambda \subseteq \Gamma$ associated with the particular coordinate choice for a given λ. The pulled-back Liouville form $\mathcal{F}_\lambda$ induces a Liouville form on the reduced phase space through the isomorphism between the reduced phase space $\bar{\Gamma}$ and the representative hypersurface $\bar{H}_\lambda \subseteq \Gamma$ mentioned in Chapter 2. The induced Liouville form on $\bar{\Gamma}$ yields the canonical structure of our reduced system. As usual, the reduced phase space $\bar{\Gamma}$ is defined as the set of equivalence classes in Γ under changes of coordinates.

To avoid repetition with Section 2.2.4, we will just sketch the steps involved in the calculation of $\mathcal{F}_\lambda$.

As with our previous coordinate choice, we must take care to include a deformation region (in R) near the shell ($X - \epsilon < r < X$), in order to satisfy the gravitational constraints. Away from the shell, the gravitational momenta solutions (4.22) evaluated in our new coordinates (3.1) are given by

$$\pi_L = \pm R\sqrt{\left(\frac{R'}{\lambda}\right)^2 - 1 + \frac{2\mathcal{M}(r)}{R}}, \quad \pi_R = \frac{\lambda}{R}\pi'_L, \tag{3.10}$$

with $\mathcal{M}(r)$ being a function that equals the ADM mass outside of the shell and 0 inside.

We can then determine what conditions the gravitational constraints defined in Section 2.2.3 impose on the metric function R by integrating these constraints across the shell, and assuming both continuity of the (spatial) metric and finiteness of the gravitational momenta. One then finds the conditions

$$\Delta R' = -\frac{\bar{V}}{\hat{R}}, \quad \Delta\pi_L = -\frac{P}{\lambda}, \tag{3.11}$$

where $\bar{V} = \sqrt{P^2 + \bar{M}^2}$, $\bar{M} = \hat{M}\lambda$, and Δ indicates the jump of a quantity across the shell. By inspection, the metric function R defined in equation

(3.12) can be generalized as

$$R(r,t) = r - \frac{\epsilon}{X}\bar{V}\mathcal{G}\left(\frac{X-r}{\epsilon}\right), \tag{3.12}$$

for a function $\mathcal{G}$ having the same properties as in Section 2.2.4, i.e.

$$\lim_{z\to 0^+} \frac{d\mathcal{G}(z)}{dz} = 1 \tag{3.13}$$

$$\lim_{z\to 0^-} \frac{d\mathcal{G}(z)}{dz} = 0, \tag{3.14}$$

from which follows

$$\lim_{\epsilon\to 0} R'(X-\epsilon) = 1 + \frac{\bar{V}}{X} \tag{3.15}$$

$$\lim_{\epsilon\to 0} R'(X+\epsilon) = 1. \tag{3.16}$$

As can be expected from the form of the coordinate choice (3.1), the π_R term integrated over the deformation region will again give the only contribution to the pullback of the Liouville form:

$$\mathcal{F}_\lambda = P\boldsymbol{\delta}X + \int_{X-\epsilon}^X dr\, \pi_R \boldsymbol{\delta}R. \tag{3.17}$$

In the $\epsilon \to 0$ limit, we have, in the deformation region,

$$\pi_R = \frac{XR''}{\lambda\sqrt{\left(\frac{R'}{\lambda}\right)^2 - 1}} + \mathcal{O}(1), \tag{3.18}$$

which allows us to express the gravitational contribution to the Liouville form as

$$\int_{X-\epsilon}^X dr\, \pi_R\boldsymbol{\delta}R = X\boldsymbol{\delta}X \int_{X-\epsilon}^X dr\, \frac{R''\left(1-R'\right)}{\lambda\sqrt{\left(\frac{R'}{\lambda}\right)^2 - 1}} + \mathcal{O}(\epsilon). \tag{3.19}$$

We can then change the integration variable from r to $v = R'$, which yields

$$\int_{X-\epsilon}^X dr\, \pi_R\boldsymbol{\delta}R = \frac{X\boldsymbol{\delta}X}{\lambda} \int_1^{R'_-} dv\, \frac{(1-v)}{\sqrt{\left(\frac{v}{\lambda}\right)^2 - 1}} + \mathcal{O}(\epsilon), \tag{3.20}$$

with R'_- being R' evaluated just inside the shell. Integrating and rearranging then leads to

$$\boldsymbol{\delta X}\left[-P - X\lambda\sqrt{w} + X\left(\sqrt{1-\lambda^2} - \ln\left(1 + \sqrt{1-\lambda^2}\right)\right)\right.$$
$$\left. + X\ln\left(1 + \lambda\sqrt{w} + \frac{\bar{V}+P}{X}\right)\right] \qquad (3.21)$$

(plus terms that vanish as $\epsilon \to 0$), where we have used the definition

$$w \equiv \frac{1}{\lambda^2} - 1 + \frac{2H}{X}. \qquad (3.22)$$

This completes the calculation of $\mathcal{F}_\lambda$, the pullback of the full Liouville form $\mathcal{F}$ to $\bar{H}_\lambda$:

$$\mathcal{F}_\lambda = P_\lambda \boldsymbol{\delta X}, \qquad (3.23)$$

with the reduced canonical momentum evidently given by

$$\begin{aligned} P_\lambda = \;\; & - \;\; X\lambda\sqrt{w} + X\left[\sqrt{1-\lambda^2} - \ln\left(1 + \sqrt{1-\lambda^2}\right)\right] \\ & + \;\; X\ln\left(1 + \frac{\bar{V}+P}{X} + \lambda\sqrt{w}\right). \end{aligned} \qquad (3.24)$$

In the reduced phase space, the unreduced momentum P becomes a constrained function of H and X. One can obtain this function by inserting the gravitational momentum solutions away from the shell given by equation (3.10) into the jump equations (3.11) and squaring. We then find that P is constrained to solve

$$\lambda^2 H = \bar{V} + \frac{\bar{M}^2}{2X} - P\lambda\sqrt{w}. \qquad (3.25)$$

It is straightforward to check that this reduces to the previous case introduced in Chapter 2 when $\lambda = 1$.

3.3   Boundary Terms

In the previous Hamiltonian reduction, the boundary term we added to the initial reduced action was (very conveniently) equal to $-\int dt\, H$, with H being the ADM mass. Thus, the ADM mass was identified with the reduced Hamiltonian of the system. We will now demonstrate that this property holds for an arbitrary Painlevé family member.

As mentioned in Section 2.2.5, a nonzero boundary variation results from integrating by parts the term $\int dt_\lambda\, dr\, N^r L(\delta\pi_L)'$, which is part of

the momentum constraint. The boundary in this case is spatial infinity, and as $r \to \infty$ we now have $N^r \to \sqrt{1 - \lambda^2 f}/\lambda^2$, $N \to 1/\lambda$, and $\pi_L \to \sqrt{1/\lambda^2 - 1 + 2\mathcal{M}/r}$. It then readily follows that

$$\delta(\pi_L) \to \frac{\delta H}{\sqrt{\frac{1}{\lambda^2} - 1 + \frac{2\mathcal{M}}{r}}}, \tag{3.26}$$

and so $\delta(\pi_L)N^r L \to \delta H$. From this we can conclude that the variation of the boundary term is cancelled if we add to the action the term

$$I_{bdry} = -\int dt_\lambda \, H, \tag{3.27}$$

which has the same form as before, with the previous time t replaced by the Painlevé family member time t_λ.

We can then determine the reduced action associated with each family member by adding the boundary term to the action defined by $\mathcal{F}_\lambda$. The result is

$$I_{\lambda reduced} = \int dt_\lambda \left(P_\lambda \frac{dX}{dt_\lambda} - H \right), \tag{3.28}$$

with the reduced momentum now given by (3.24). As before, we can see from the form of the reduced action (3.28) that the ADM mass is the reduced Hamiltonian for an arbitrary Painlevé family member.

Let us now explicitly write the unreduced momentum P that satisfies the constraint (3.25). The result is a function of X, H, and λ:

$$P = \frac{\sqrt{1 - \lambda^2 f} h \pm \sqrt{h^2 - M^2 f}}{f}, \tag{3.29}$$

with $f = 1 - 2H/X$ and $h = H - M^2/2X$. One can easily confirm that this reduces to the previous case given by equation (2.52) when $\lambda = 1$.

Though the equations seem somewhat more complicated, they are still of the same form as before: P still obeys a quadratic equation, and the reduced canonical momentum can still be explicitly determined. This remarkable fact readily allows the previous calculations to be performed for arbitrary λ (for $0 < \lambda \leq 1$), so that one can straightforwardly investigate which properties of the system depend on the particular choice of coordinates.

3.4 Reduced Equations of Motion

In order to derive Hamilton's equations of motion for the reduced system, we will make use of the expression

$$P = X \sqrt{\left(\frac{\bar{V}}{X} + 1\right)^2 - \lambda^2} - X\sqrt{1 - \lambda^2 f}, \tag{3.30}$$

which results from the gravitational momentum solution π_L (3.10) and the second jump condition (3.11). With (3.30), along with the implicit relation (3.24), we can obtain

$$\dot{X} = \frac{\partial H}{\partial P_\lambda} = \frac{1}{\lambda^2}\left[\frac{P}{\bar{V}} - \sqrt{1 - \lambda^2 f}\right]. \tag{3.31}$$

Solving (3.31) for P and substituting into (3.30) yields

$$\frac{H\lambda}{M(X)} - \frac{M(X)\lambda}{2X} = \frac{1 - \left(\dot{X}\lambda^2 + \sqrt{1 - \lambda^2 f}\right)\sqrt{1 - \lambda^2 f}}{\sqrt{1 - \left(\dot{X}\lambda^2 + \sqrt{1 - \lambda^2 f}\right)^2}} \tag{3.32}$$

The line element (3.2) gives the relation between the proper time of the shell, τ, and the coordinate time, t_λ:

$$d\tau^2 = \frac{1}{\lambda^2}dt_\lambda^2 - \lambda^2\left(dr + \frac{1}{\lambda^2}\sqrt{1 - \lambda^2 f}dt_\lambda\right)^2, \tag{3.33}$$

from which it follows that

$$\frac{dt_\lambda}{d\tau} = \frac{1}{f}\left(\frac{dX}{d\tau}\sqrt{1 - \lambda^2 f} + \sqrt{\left(\frac{dX}{d\tau}\right)^2 + f}\right). \tag{3.34}$$

Using (3.34) to express $\dot{X}$ as $\dot{X} = \frac{dX}{d\tau}\frac{d\tau}{dt_\lambda}$ and rearranging relation (3.30), we find

$$\frac{H}{M(X)} - \frac{M(X)}{2X} = \sqrt{\left(\frac{dX}{d\tau}\right)^2 + f} \tag{3.35}$$

which is the correct classical equation of motion for the shell.

3.5   Transcendental Hamiltonian Approximations

Though it is not possible to solve the relation (3.24) for the Hamiltonian H when X is finite, in Chapter 2 we presented an approximate Hamiltonian (2.72) associated with the weak-field limit (large X) of the system defined by the canonical momentum (2.48). We will now derive this result as a special case of the results for arbitrary λ.

In the $X \to \infty$ limit (flat spacetime), the Hamiltonian is given exactly by

$$H = \frac{1}{1 - v_\infty^2}\left(-v_\infty P_\lambda + \sqrt{M(X)^2(1 - v_\infty^2) + P_\lambda^2} \right). \qquad (3.36)$$

For finite but large X, it is possible to obtain the Hamiltonian for small momentum P_λ. To this end, we choose the ansatz

$$H = H_0 + H_1 P_\lambda + H_2 P_\lambda^2 \qquad (3.37)$$

with some functions $H_0(X)$, $H_1(X)$, and $H_2(X)$. We substitute this ansatz into the relation (3.24) and expand for large X and small P_λ. Then we compare the coefficients for the various powers of P_λ and deduce for $\lambda = 1$

$$H_0 = M - \frac{M^2}{18X} + \frac{2M^3}{405X^2} + \mathcal{O}(1/X^3) \qquad (3.38)$$

$$H_1 = -\frac{2}{3}\sqrt{\frac{2M}{X}} - \frac{M^{3/2}}{135\sqrt{2}}\frac{1}{X^{3/2}} + \frac{161M^{5/2}}{48600\sqrt{2}X^{5/2}} + \mathcal{O}(1/X^{7/2}) \qquad (3.39)$$

$$H_2 = \frac{1}{2M} + \frac{1}{3X} + \frac{M}{270X^2} + \mathcal{O}(1/X^3). \qquad (3.40)$$

When the coordinate system corresponds to an observer with finite velocity at infinity, we find

$$H_0 \sim \frac{M}{\sqrt{1 - v_\infty^2}} - \frac{\sqrt{1 - v_\infty^2}\,M^3}{24v_\infty^2 X^2} \qquad (3.41)$$

$$H_1 \sim -\frac{v_\infty}{1 - v_\infty^2} - \frac{M}{2Xv_\infty\sqrt{1 - v_\infty^2}} + \frac{M^2}{6v_\infty^3 X^2} \qquad (3.42)$$

$$H_2 \sim \frac{1}{2M(1 - v_\infty^2)^{3/2}} + \frac{1}{2X(1 - v_\infty^2)} - \frac{3M}{16X^2 v_\infty^2 \sqrt{1 - v_\infty^2}}. \qquad (3.43)$$

Note that these asymptotic expansions do not have the correct limit for $v_\infty \to 0$. The reason for this is that for large X and finite v_∞, we have

$\sqrt{1 - \lambda^2 f} \sim 1/X$ (modulo a constant) whereas for vanishing v_∞, we find $\sqrt{1 - f} \sim 1/\sqrt{X}$. However, it is possible to find to the order to which we expanded the Hamiltonian an interpolating function. Specifically, a possible interpolating Hamiltonian is

$$H_0^{int} = \frac{M}{\sqrt{1 - v_\infty^2}} + A_0 \sqrt{v_\infty^4 + \frac{B_0}{X^2} + \frac{C_0}{X^3}} - A_0 v_\infty^2 \tag{3.44}$$

$$H_1^{int} = -A_1 - B_1 \sqrt{v_\infty^2 + \frac{C_1}{X(1 + v_\infty^2 E_1 X)}} + \frac{3 D_1 v_\infty^3}{2X}$$

$$- D_1 \left(v_\infty^6 + \frac{1}{X} \right)^{3/2} - \sqrt{v_\infty^2 + \frac{E_1}{X}} \tag{3.45}$$

$$H_2^{int} = -\frac{A_2}{2} - \frac{B_2 v_\infty^2}{2(1 + v_\infty^2 X)} - \frac{C_2}{2} \sqrt{v_\infty^4 + \frac{D_2}{X^2}} - \frac{1}{2} \sqrt{v_\infty^4 + \frac{E_2}{X^4}} \tag{3.46}$$

with the term zeroth-order in P_λ given explicitly by

$$\left\{ A_0 = -\frac{M}{27}, \quad B_0 = \frac{9 M^2}{4} \sqrt{1 - v_\infty^2}, \quad C_0 = -\frac{2 M^3}{5} \right\}, \tag{3.47}$$

the first-order coefficient given by

$$A_1 = v_\infty \left(-1 - \frac{M^{3/2} v_\infty^8}{135 \sqrt{2}} + \frac{1}{1 - v_\infty^2} + \frac{40(1 - v_\infty^2)^{3/2} \left(2\sqrt{2M} - 3\frac{\sqrt{M}}{(1 - v_\infty^2)^{1/4}} \right)^2}{M^{5/2}(\sqrt{2}(1 - v_\infty^2) + 30\sqrt{M}(1 - 4v_\infty^2))} \right) \tag{3.48}$$

$$B_1 = \frac{40(1 - v_\infty^2)^{7/2} \left(2\sqrt{2M} - 3\frac{\sqrt{m}}{(1 - v_\infty^2)^{1/4}} \right)^2 \left(90\sqrt{M} - (\sqrt{2} + 120\sqrt{M})(1 - v_\infty^2) \right)}{M^{5/2}(1 - v_\infty^2)^2(\sqrt{2}(1 - v_\infty^2) + 30\sqrt{M}(1 - 4v_\infty^2))^2} \tag{3.49}$$

$$C_1 = \frac{M^5 \left(\sqrt{2}(1 - v_\infty^2) + 30\sqrt{M}(1 - 4v_\infty^2) \right)^2}{14400(1 - v_\infty^2)^3 \left(2\sqrt{2M} - 3\frac{\sqrt{M}}{(1 - v_\infty^2)^{1/4}} \right)^2} \tag{3.50}$$

$$D_1 = \frac{M^{3/2}}{135 \sqrt{2}} \tag{3.51}$$

$$E_1 = \frac{M}{\sqrt{1 - v_\infty^2}}, \tag{3.52}$$

and the quadratic coefficient given by

$$A_2 = -\frac{1}{M\left(1 - v_\infty^2\right)^{3/2}} + v_\infty^2 \left(-1 + \frac{16\sqrt{1 - v_\infty^2}}{-27M + 48\sqrt{1 - v_\infty^2}}\right) \qquad (3.53)$$

$$B_2 = -\frac{2}{3} \qquad (3.54)$$

$$C_2 = \frac{16\sqrt{1 - v_\infty^2}}{3(9M - 16\sqrt{1 - v_\infty^2})} \qquad (3.55)$$

$$D_2 = \frac{M^2}{18225} \qquad (3.56)$$

$$E_2 = \frac{(9M - 16\sqrt{1 - v_\infty^2})^2}{64(1 - v_\infty^2)}. \qquad (3.57)$$

We now have all of the generalized asymptotics necessary to re-perform the interferometric calculations of Chapter 2, this time for an arbitrary member of the Painlevé-Gullstrand family of coordinate systems.

3.6 Interferometry in the Painlevé-Gullstrand Family

3.6.1 Flat Spacetime Limit

Before exploring the implications of our generalized coordinates for the self-gravitating system, let us see how the flat spacetime interferometer is affected. We will consider single-mode inputs, as in Chapter 2, for simplicity. In the flat spacetime limit our Hamiltonian takes the form (3.36), which we can then take the nonrelativistic limit of ($P_\lambda \to 0$) to obtain

$$H \sim \frac{\hat{M}}{\sqrt{1 - v_\infty^2}} - \frac{v_\infty}{1 - v_\infty^2} P_\lambda + \frac{1}{2\hat{M}\left(1 - v_\infty^2\right)^{3/2}} P_\lambda^2. \qquad (3.58)$$

Unlike the situation for finite X described in Section 3.5, this Hamiltonian has the correct behaviour as $v_\infty \to 0$ (or, equivalently, $\lambda \to 1$), and reproduces the nonrelativistic, flat spacetime Hamiltonian given in Section 2.3.3.

The (exact) momentum P_λ that corresponds to equation (3.36) is given by

$$P_\lambda = v_\infty H \pm \sqrt{H^2 - \hat{M}^2}. \qquad (3.59)$$

This expression has the usual flat spacetime momentum in the $v_\infty \to 0$ limit, and as $v_\infty \to 1$ ($\lambda \to 0$) leads to the "null observer" Hamiltonian

$$H = \frac{P_0^2 + \hat{M}^2}{2P_0}. \tag{3.60}$$

It should be noted that we still use the same symbol H here because the actual value of the (classical) Hamiltonian is the same, despite being expressed in terms of a different momentum. Perhaps unsurprisingly, in the null observer limit the exact momentum (3.59) is always positive for massive shells, regardless of whether the shell is ingoing or outgoing. In the coordinate representation, the operator $\hat{P}_0$ is represented as $-i\partial/\partial X$, so one might expect the inverse operator "$1/\hat{P}_0$" to be nonlocal. Whether or not a nonlocal Hamiltonian can produce an evolution that is equivalent (or perhaps just approximately equivalent) to a local Hamiltonian evolution is an open question.

We will also make use of the "WKB momentum," as in Section 2.3.4, which in this context is defined as the solution of (3.58) (treated as an equality) for P_λ:

$$\begin{aligned} P_{w\lambda} =& \hat{M} v_\infty \sqrt{1 - v_\infty^2} \\ & \pm \left(1 - v_\infty^2\right)^{3/4} \sqrt{2\hat{M} \left[H - \hat{M} \left(\frac{1 - \frac{1}{2} v_\infty^2}{\sqrt{1 - v_\infty^2}} \right) \right]}. \end{aligned} \tag{3.61}$$

For a small observer velocity v_∞, the special relativistic boost factors in the WKB momentum expression (3.61) are approximately unity, and we are left with

$$P_{w\lambda} \approx \hat{M} v_\infty \pm \sqrt{2\hat{M} \left(H - \hat{M} \right)}. \tag{3.62}$$

This is just as one might expect: the shell momentum defined with respect to our generalized Painlevé-Gullstrand coordinate system is given by the usual nonrelativistic expression, offset by a momentum $\hat{M} v_\infty$ that is attributed to the shell due to the infalling nature of the coordinates.

The null observer limit of the WKB momentum (3.61), however, is ill-defined. One can see from (3.58) that the quadratically truncated Hamiltonian has divergent terms as $v_\infty \to 1$. Thus, as we approach this limit we must use the exact momentum (3.59) in our WKB modes, to avoid pathological behaviour. As for the Hamiltonian, as we approach the null observer limit we should use the exact Hamiltonian, though for simplicity we will

expand in λ up to second order, such that

$$H \approx \frac{P_\lambda}{2} \left(1 + \frac{\lambda^2}{4} \right) + \frac{\hat{M}^2}{2P_\lambda} \left(1 - \frac{\hat{M}^2 \lambda^2}{4P_\lambda^2} \right). \tag{3.63}$$

The Hamiltonian (3.63) has a perfectly good limit as $\lambda \to 0$, but looks slightly unwieldy. Even with the inverse powers of the momentum, we can solve the corresponding Schrödinger equation in each section where $\hat{M}$ is constant (i.e. each side of the beam-splitter) by making use of the momentum representation. When gravitational corrections are added, however, inverse powers of X prevent us from avoiding a confrontation with nonlocal operators. We will keep this in mind when considering whether or not there are fundamental differences to the quantum evolution introduced by general relativity.

For much slower asymptotic observers, with v_∞ sufficiently less than unity, the Hamiltonian (3.58) is well-behaved, and leads to the (simpler) Schrödinger equation

$$i \frac{\partial}{\partial t_\lambda} \Psi = \frac{\hat{M}}{\sqrt{1 - v_\infty^2}} \Psi + \frac{i v_\infty}{1 - v_\infty^2} \Psi' - \frac{1}{2 \left(1 - v_\infty^2 \right)^{3/2}} \left(\frac{1}{\hat{M}} \Psi' \right)', \tag{3.64}$$

with Hermitian factor-ordering on the last term. As well as being continuous, one can immediately see by integrating (3.64) across the splitter at X_δ that the wavefunction Ψ obeys the same jump condition as in Section 2.3.3; namely,

$$\left[\frac{1}{\hat{M}} \Psi' \right]_\delta = 0, \tag{3.65}$$

with $[\cdot]_\delta$ indicating the jump of a quantity across X_δ. If we consider the simple scattering problem from the right,

$$\Psi = \begin{cases} \psi_{\lambda-+} + R_{\lambda\leftarrow} \psi_{\lambda++} & : X > X_\delta \\ T_{\lambda\leftarrow} \psi_{\lambda--} & : X < X_\delta \end{cases}$$

we realize that determination of the reflection and transmission amplitudes is trivial, because they obey the same relations as in Section 2.3.3:

$$\bar{R}_{\lambda\leftarrow} = \frac{M_- P_{\lambda-+} - M_+ P_{\lambda--}}{M_+ P_{\lambda--} - M_- P_{\lambda++}}, \quad \bar{T}_{\lambda\leftarrow} = \frac{M_- (P_{\lambda++} - P_{\lambda-+})}{M_- P_{\lambda++} - M_+ P_{\lambda--}}, \tag{3.66}$$

where now the momentum terms are given by (3.59), and the barred amplitudes are related to the unbarred amplitudes via

$$\bar{R}_{\lambda\leftarrow} \equiv \sqrt{\left| \frac{\frac{\partial E}{\partial P_{\lambda-+}}}{\frac{\partial E}{\partial P_{\lambda++}}} \right|} R_{\lambda\leftarrow}, \quad \bar{T}_{\lambda\leftarrow} \equiv \sqrt{\left| \frac{\frac{\partial E}{\partial P_{\lambda-+}}}{\frac{\partial E}{\partial P_{\lambda--}}} \right|} T_{\lambda\leftarrow}. \tag{3.67}$$

As with our previous definitions, the first set of plus/minuses indicate outgoing/ingoing, and the second set indicate $M_\pm$.

The same pattern occurs for scattering from the left, and the corresponding amplitudes are

$$\bar{R}_{\lambda\rightarrow} = \frac{M_- P_{\lambda++} - M_+ P_{\lambda+-}}{M_+ P_{\lambda--} - M_- P_{\lambda++}}, \quad \bar{T}_{\lambda\rightarrow} = \frac{M_+ (P_{\lambda+-} - P_{\lambda--})}{M_- P_{\lambda++} - M_+ P_{\lambda--}}, \quad (3.68)$$

using the similar definitions

$$\bar{R}_{\lambda\rightarrow} \equiv \sqrt{\left| \frac{\frac{\partial E}{\partial P_{\lambda+-}}}{\frac{\partial E}{\partial P_{\lambda--}}} \right|} R_{\lambda\rightarrow}, \quad \bar{T}_{\lambda\rightarrow} \equiv \sqrt{\left| \frac{\frac{\partial E}{\partial P_{\lambda+-}}}{\frac{\partial E}{\partial P_{\lambda++}}} \right|} T_{\lambda\rightarrow}. \quad (3.69)$$

The details of sending an initial state through the interferometer thus exactly parallel the nonrelativistic, flat spacetime case presented in Section 2.3.3. The reflection off of the inner and outer walls (X_- and X_+, respectively) is described by the same reflection coefficients

$$\bar{R}^{\lambda\rightarrow} = -e^{i(\phi_{\lambda++}+\phi_{\lambda-+})}, \quad \bar{R}^{\lambda\leftarrow} = -e^{i(\phi_{\lambda+-}+\phi_{\lambda--})}, \quad (3.70)$$

with the definitions $\phi_{\lambda\pm\pm} = \int_{X_\delta}^{X_\pm} dX P_{\lambda\pm\pm}$, $\phi_{\lambda\pm\mp} = \int_{X_\mp}^{X_\delta} dX P_{\lambda\pm\mp}$ (signs chosen together), and

$$\bar{R}^{\lambda\rightarrow} \equiv \sqrt{\left| \frac{\frac{\partial E}{\partial P_{\lambda++}}}{\frac{\partial E}{\partial P_{\lambda-+}}} \right|} R^{\lambda\rightarrow}, \quad \bar{R}^{\lambda\leftarrow} \equiv \sqrt{\left| \frac{\frac{\partial E}{\partial P_{\lambda--}}}{\frac{\partial E}{\partial P_{\lambda+-}}} \right|} R^{\lambda\leftarrow}. \quad (3.71)$$

The probability current J_λ still satisfies the continuity equation

$$\frac{\partial}{\partial t_\lambda} \left(|\Psi_\lambda|^2 \right) + \frac{\partial}{\partial X} J_\lambda = 0, \quad (3.72)$$

but this time the current is described by the generalized form (2.113), which in this case is

$$\begin{aligned} J_\lambda &= -\frac{v_\infty}{1 - v_\infty^2} |\Psi_\lambda|^2 + \frac{1}{2i\hat{M} \left(1 - v_\infty^2\right)^{3/2}} \left(\Psi_\lambda^* \Psi_\lambda' - \Psi_\lambda \Psi_\lambda^{*'} \right) \\ &= -\frac{v_\infty}{1 - v_\infty^2} |\Psi_\lambda|^2 + \frac{1}{\left(1 - v_\infty^2\right)^{3/2}} J_{\lambda s}. \end{aligned} \quad (3.73)$$

In the last line, we used $J_{\lambda s}$ to denote the standard (nonrelativistic) expression (2.91), evaluated with the λ-dependent WKB state Ψ_λ. Expression (3.73) implies that for real momenta, the input probability current is

$$J_{\lambda 0} = \frac{|\Psi_{\lambda 0}|^2}{1 - v_\infty^2} \left(\frac{P_{\lambda-+}}{M_+ \sqrt{1 - v_\infty^2}} - v_\infty \right), \quad (3.74)$$

56

(a) $E = 1.01$, $M_- = 1.0097$ (b) $E = 1.1$, $M_- = 1.0997$

Figure 3.1: Sample reflection and transmission coefficients for the initial beam-splitting using the exact flat spacetime momentum given by (3.59), for $M_+ = 1$ and different combinations of M_- and E. The coefficients are plotted against the asymptotic observer velocity, v_∞.

which certainly differs in form from the previous flat spacetime result (2.92). In this case the difference is superficial, because our initial WKB state $\Psi_{\lambda 0} = \psi_{\lambda -+}$ has a modulus-squared given by

$$|\Psi_{\lambda 0}|^2 = \left|\frac{\partial H}{\partial P_{\lambda -+}}\right|^{-1} = \left|\frac{P_{\lambda -+}}{M_+ (1 - v_\infty^2)^{3/2}} - \frac{v_\infty}{1 - v_\infty^2}\right|^{-1}, \qquad (3.75)$$

from which we can immediately deduce $J_{\lambda 0} = -1$.[5]

Let us take a moment to consider the reflection and transmission coefficients associated with the initial split. Since $|J_{\lambda 0}| = 1$, the reflection and transmission coefficients are given by $|J_{\lambda +}^{(i)}|$ and $|J_{\lambda -}^{(i)}|$ (respectively). A simple calculation then confirms that $|J_{\lambda +}^{(i)}| = |R_{\lambda \leftarrow}|^2$ and $|J_{\lambda -}^{(i)}| = |T_{\lambda \leftarrow}|^2$.

Figures 3.1 and 3.2 highlight the drastic differences in the reflection and transmission coefficients for the initial splitting, depending on whether one uses the exact momentum (3.59) or the WKB momentum (3.61). What's

---

[5]The previous initial current (2.92) is also equal to -1, although this was not explicitly mentioned.

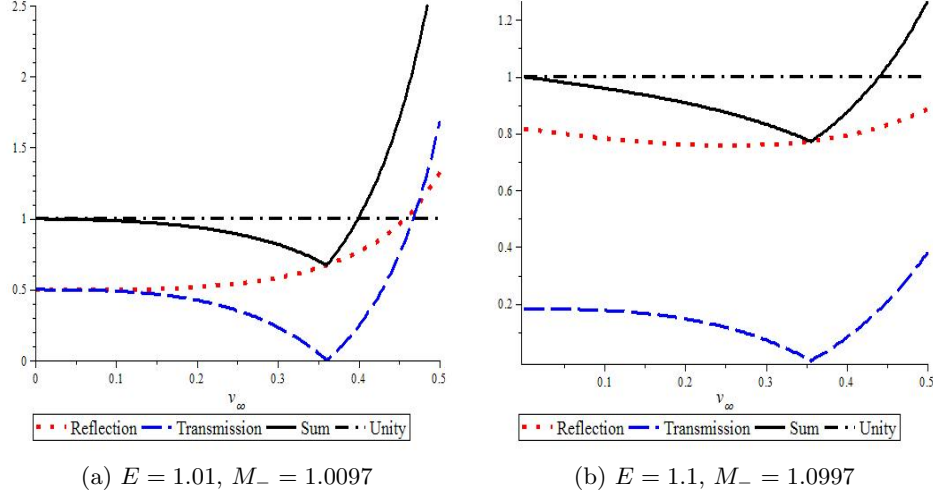(a) $E = 1.01$, $M_- = 1.0097$ (b) $E = 1.1$, $M_- = 1.0997$
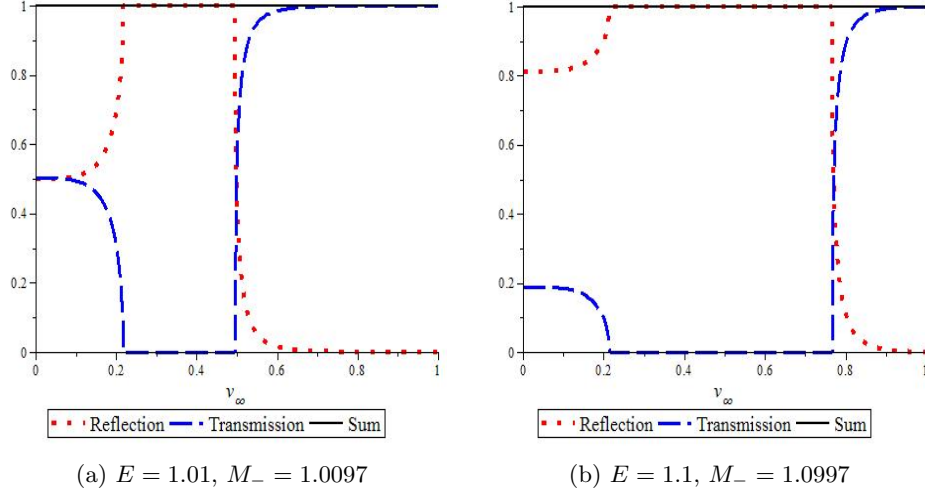
Figure 3.2: Sample reflection and transmission coefficients for the initial beam-splitting, using the flat spacetime WKB momentum given by (3.61), for $M_+ = 1$ and different combinations of E and M_-. The coefficients are plotted against the asymptotic observer velocity, v_∞.

happening here is that the discriminant from (3.61) is changing signs, and so the WKB momenta are taking on imaginary components. This is illustrated in Figure 3.3. In the process, for the first set of parameters Figure 3.2a shows that as v_∞ increases from 0, the splitter continuously goes from being a $50-50$ splitter, to totally reflecting, and then to totally transmitting. This is in stark contrast with the behaviour shown in Figure 3.1a for the same parameters, which shows the splitter smoothly transitioning from being a $50-50$ splitter for $v_\infty = 0$ to being somewhat more reflecting ($R_{\lambda\leftarrow} \to 1$) as the observer velocity reaches about half of the speed of light ($v_\infty = 1$). After this point, the shell momenta are too relativistic to be approximated by our probability current (which is conserved for Hamiltonians that are quadratic in momenta), resulting in a breakdown of the probabilistic interpretation of our reflection and transmission coefficients. Figure 3.3 depicts the ingoing and outgoing WKB momenta merging as the discriminant approaches zero, after which there cease to be real WKB momenta. The straight lines are the exact momenta, which continue (linearly) up to $v_\infty = 1$.

In the entire parameter range of v_∞, the sum of the reflection and transmission coefficients is identically 1 if we use only the WKB momenta in the expressions for $R_{\lambda\leftarrow}$ and $T_{\lambda\leftarrow}$ (we will demonstrate this in a more general context in the next section). If we use the exact momenta, we notice that the probability current is not quite conserved, as the current expression was derived for systems with Hamiltonians that are exactly quadratic in momentum. On the other hand, the phase in a WKB state is more accurately the momentum obtained from inverting a Hamiltonian $H(x,p)$ with respect to p than it is the momentum obtained from solving $H(x,p) \approx H_0(x) + H_1(x)p + H_2(x)p^2$ for p $(= p_w)$. Since phase information is crucial for interferometry, and at the same time probability conservation is crucial for a sensible interpretation of a quantum system, we will use the various momenta carefully.

It should be mentioned that in Figures 3.1 and 3.2, the initial probability current is equal to -1 for all $v_\infty \in [0,1]$, though the initial state is defined to be an ingoing WKB mode (with the same energy for each individual plot). Strictly speaking, since each choice of v_∞ defines a different coordinate system (and therefore a different notion of time), this means that the initial state is different for each value of v_∞ being plotted. We shouldn't be surprised, then, that the reflection and transmission probabilities vary with v_∞, because this is not an indication that the coordinates used to describe the initial scatter change these probabilities *for a given initial state*. We will address this issue in the following sections.

Let us focus now on the final interferometer outputs. In the generalized coordinates, we are no longer able to exploit the "identity" $\bar{R}_\leftarrow^2 + \frac{M_+ P_{--}}{M_- P_{-+}} \bar{T}_\leftarrow^2 = 1$, which led to the simple form of (2.104) and (2.105), since it is no longer valid in the new coordinates. Instead, we must calculate the final probability currents from the final output states defined by (2.101) and (2.100). Using the fact that for single-mode WKB states in flat spacetime the derivatives of the final states obey

$$\frac{d}{dX}\Psi_{\lambda\pm}^{(v)} = iP_{\lambda\pm\pm}\Psi_{\lambda\pm}^{(v)}, \tag{3.76}$$

we can write the term $J_{\lambda s}$ as

$$J_{\lambda s} = \frac{P_{\lambda\pm\pm}}{M_\pm}\left|\Psi_{\lambda\pm}^{(v)}\right|^2. \tag{3.77}$$

This means we can write the output currents as

$$J_{\lambda\pm}^{(v)} = \left|\Psi_{\lambda\pm}^{(v)}\right|^2\left(-\frac{v_\infty}{1-v_\infty^2} + \frac{1}{M_\pm\left(1-v_\infty^2\right)^{3/2}}P_{\lambda\pm\pm}\right) \tag{3.78}$$

59
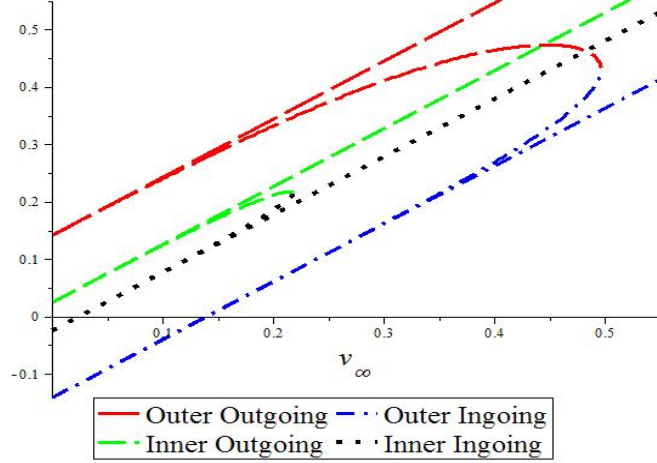
(a) WKB momenta and exact momenta for $M_- = 1.0097$, $E = 1.01$
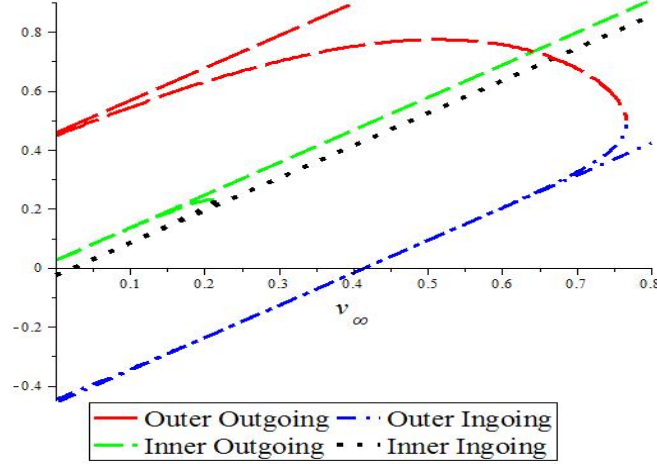
(b) WKB momenta and exact momenta for $M_- = 1.0997$, $E = 1.1$

Figure 3.3: Various WKB momenta in flat spacetime, for $M_+ = 1$ and different combinations of E and M_-, plotted against the asymptotic observer velocity, v_∞. The curved lines are WKB momenta which converge at the point where they become imaginary; at this point, they become significantly different from the exact momenta (straight lines), which are real and distinct for all regions of the parameter space. To avoid cluttering the y-axis with multiple labels, the y-values of the plots, which are various types of momenta, are specified in the legends.

which we can readily interpret to be

$$J_{\lambda\pm}^{(v)} = \left|\Psi_{\lambda\pm}^{(v)}\right|^2 \left(\frac{\partial H}{\partial P_\lambda}\right)_{\pm\pm}, \tag{3.79}$$

with the partial derivative evaluated at $P_{\lambda\pm\pm}$. The expression (3.79) makes intuitive sense: Hamilton's equation for $\dot{X}$ and the identification of the probability density ρ with $\left|\Psi_{\lambda\pm}^{(v)}\right|^2$ yield the familiar current relation

$$J = \rho\boldsymbol{v}, \tag{3.80}$$

where we have used $\boldsymbol{v} = \dot{X}$ to denote the shell velocity.

Taking the modulus-squared of the output states (2.101) gives us

$$\left|\Psi_{\lambda+}^{(v)}\right|^2 = \left|\frac{\partial H}{\partial P_{\lambda++}}\right|^{-1} \left(\bar{R}_{\lambda\leftarrow}^4 + \bar{T}_{\lambda\leftarrow}^2\bar{T}_{\lambda\rightarrow}^2 + 2\bar{R}_{\lambda\leftarrow}^2\bar{T}_{\lambda\leftarrow}\bar{T}_{\lambda\rightarrow}\cos 2\varphi_\lambda\right) \tag{3.81}$$

and

$$\left|\Psi_{\lambda-}^{(v)}\right|^2 = \left|\frac{\partial H}{\partial P_{\lambda-+}}\right|^{-1} \bar{T}_{\lambda\leftarrow}^2 \left(\bar{R}_{\lambda\leftarrow}^2 + \bar{R}_{\lambda\rightarrow}^2 + 2\bar{R}_{\lambda\leftarrow}\bar{R}_{\lambda\rightarrow}\cos 2\varphi_\lambda\right), \tag{3.82}$$

with the definition $\varphi_\lambda = (\phi_{\lambda++} + \phi_{\lambda-+} - \phi_{\lambda+-} - \phi_{\lambda--})$. Using (3.79), we can express the final reflected and transmitted probability currents as

$$J_{\lambda+}^{(v)} = \frac{\left(\frac{\partial H}{\partial P_{\lambda++}}\right)}{\left|\frac{\partial H}{\partial P_{\lambda-+}}\right|} \left(\bar{R}_{\lambda\leftarrow}^4 + \bar{T}_{\lambda\leftarrow}^2\bar{T}_{\lambda\rightarrow}^2 + 2\bar{R}_{\lambda\leftarrow}^2\bar{T}_{\lambda\leftarrow}\bar{T}_{\lambda\rightarrow}\cos 2\varphi_\lambda\right) \tag{3.83}$$

and

$$J_{\lambda-}^{(v)} = \frac{\left(\frac{\partial H}{\partial P_{\lambda--}}\right)}{\left|\frac{\partial H}{\partial P_{\lambda-+}}\right|} \bar{T}_{\lambda\leftarrow}^2 \left(\bar{R}_{\lambda\leftarrow}^2 + \bar{R}_{\lambda\rightarrow}^2 + 2\bar{R}_{\lambda\leftarrow}\bar{R}_{\lambda\rightarrow}\cos 2\varphi_\lambda\right). \tag{3.84}$$

These final output currents immediately determine the final reflection and transmission coefficients, since $R_{\lambda f} = |J_{\lambda+}^{(v)}|$ and $T_{\lambda f} = |J_{\lambda-}^{(v)}|$. Implicit in these expressions, as well as several other expressions in this section, is the assumption that the momenta are real. We will enforce this reality condition for the rest of this thesis, because apart from the above comments regarding the discriminant of the WKB momenta switching signs in some regions of the parameter space, we regard these imaginary components as an unnecessary (and in this case, unphysical) addition to the interferometric analysis.

How does the interference pattern in this case compare with the flat spacetime case presented in Chapter 2? If we use the WKB momenta, the final reflection and transmission coefficients take the simpler forms

$$R_{\lambda f} = \left[1 - 4\bar{R}^2_{\lambda\leftarrow}\left(1 - \bar{R}^2_{\lambda\leftarrow}\right)\sin^2\varphi_\lambda\right] \tag{3.85}$$

and

$$T_{\lambda f} = 4\bar{R}^2_{\lambda\leftarrow}\left(1 - \bar{R}^2_{\lambda\leftarrow}\right)\sin^2\varphi_\lambda, \tag{3.86}$$

which bear a striking resemblance to the previous flat spacetime expressions (2.104) and (2.105). Continuing the same steps as in Section 2.3.3 would lead us to the phase condition

$$\varphi_\lambda = 2L_+ P_{\lambda++} + 2L_- P_{\lambda--} = \frac{n\pi}{2} \tag{3.87}$$

(for $n \in \mathbb{Z}$), which is the generalized form of (2.109). We can then deduce the distance between nodes in the interference pattern to be

$$\Delta L_{\lambda n} = \frac{\pi}{4P_{\lambda++}}, \tag{3.88}$$

and again observe that coherence is fully present in the flat spacetime interferometer.

The node spacing (3.88) varies with the asymptotic observer velocity, but we should be careful what we conclude from this, because there is still the issue of a changing initial state to deal with. We will will see that the initial state problem in question presents us with a serious obstacle in our investigation of the coordinate dependence of our description of the interferometer: different coordinate choices define different notions of time, and different definitions of time evolution. We expected this to be the case because of (3.4)-(3.8), but we will see in Section 3.7 that the time transformation (3.6) has some very peculiar consequences indeed.

3.6.2 General Relativistic Corrections

We will worry about the initial state issue in the next section; first, let us use the generalized Hamiltonian asymptotics from Section 3.5 to determine the final output reflection and transmission coefficients for our shell interferometer by transforming the (tentative) input state accordingly. The Schrödinger equation for the arbitrary quadratic Hamiltonian (3.37) takes the form

$$i\frac{\partial}{\partial t_\lambda}\Psi = H_0\Psi - \frac{i}{2}\left(2H_1\Psi' + H_1'\Psi\right) - \left(H_2\Psi'\right)', \tag{3.89}$$

and upon integration across X_δ one obtains the jump condition

$$\left[H_2\Psi'\right]_\delta = -\frac{i}{2}\left[H_1\right]_\delta \Psi(X_\delta). \tag{3.90}$$

To calculate the reflection and transmission amplitudes for the initial scatter off of the beam-splitter, we consider the wavefunction

$$\Psi = \begin{cases} \psi_{\lambda-+} + R_{\lambda\leftarrow}\psi_{\lambda++} & : X > X_\delta \\ T_{\lambda\leftarrow}\psi_{\lambda--} & : X < X_\delta \end{cases}$$

If we apply continuity at X_δ and the jump condition (3.108) we can determine the reflection amplitude $R_{\lambda\leftarrow}$ and transmission amplitude $T_{\lambda\leftarrow}$. Making use of the notation

$$\Delta\left(\frac{\partial H}{\partial P_\lambda}\right) = \frac{1}{2}\left(\left(\frac{\partial H}{\partial P_\lambda}\right)_{++} - \left(\frac{\partial H}{\partial P_\lambda}\right)_{--}\right), \tag{3.91}$$

$$\Delta\left(H_2 P_\lambda\right)_\pm = \frac{1}{2}H_{2\pm}\left(P_{\lambda+\pm} - P_{\lambda-\pm}\right), \tag{3.92}$$

and

$$H_{2\pm} = \lim_{\epsilon\to 0} H_2\Big|_{X=X_\delta\pm\epsilon}, \tag{3.93}$$

we can express the barred amplitudes compactly as

$$\bar{R}_{\lambda\leftarrow} = \frac{2\Delta\left(H_2 P_\lambda\right)_+ - \Delta\left(\frac{\partial H}{\partial P_\lambda}\right)}{\Delta\left(\frac{\partial H}{\partial P_\lambda}\right)} \tag{3.94}$$

and

$$\bar{T}_{\lambda\leftarrow} = \frac{2\Delta\left(H_2 P_\lambda\right)_+}{\Delta\left(\frac{\partial H}{\partial P_\lambda}\right)}, \tag{3.95}$$

for scattering from the right. Similarly, we can express the barred amplitudes as

$$\bar{R}_{\lambda\to} = \frac{2\Delta\left(H_2 P_\lambda\right)_- - \Delta\left(\frac{\partial H}{\partial P_\lambda}\right)}{\Delta\left(\frac{\partial H}{\partial P_\lambda}\right)} \tag{3.96}$$

and

$$\bar{T}_{\lambda\to} = \frac{2\Delta\left(H_2 P_\lambda\right)_-}{\Delta\left(\frac{\partial H}{\partial P_\lambda}\right)}, \tag{3.97}$$

for scattering from the left.

Before working out the specific interferometric properties of our system in the Painlevé-Gullstrand family of coordinates, let us explore the general features of scattering with the Hamiltonian (3.37). We will assume, however, that the arbitrary quadratic Hamiltonian still has a discontinuity at X_δ, to serve as a beam-splitter. Dropping the λ subscript temporarily and solving (3.37) for P gives us the WKB momentum,

$$P = -\frac{H_1}{2H_2} \pm \sqrt{\frac{(H - H_0)}{H_2} + \left(\frac{H_1}{2H_2}\right)^2}. \qquad (3.98)$$

For brevity, we will denote this by $P = P_{0\pm} \pm P_\pm$, with the $\pm$ subscripts referring to which side of the splitter the quantity is evaluated at, and the other $\pm$ indicating outgoing/ingoing. We can then express the WKB P-derivatives as

$$\left(\frac{\partial H}{\partial P}\right)_{\pm\pm} = H_{1\pm} + 2H_{2\pm}P_{\pm\pm} = \pm 2H_{2\pm}P_\pm. \qquad (3.99)$$

We can tell from (3.99) that the WKB P-derivatives satisfy

$$\left|\frac{\partial H}{\partial P}\right|_{+\pm} = \left|\frac{\partial H}{\partial P}\right|_{-\pm}, \qquad (3.100)$$

which implies that $\bar{R}_\leftarrow = R_\leftarrow$, as well as $\bar{R}_\rightarrow = R_\rightarrow$, $\bar{R}^\rightarrow = R^\rightarrow$, and $\bar{R}^\leftarrow = R^\leftarrow$.

In the previous section it was pointed out that the initial probability current is -1, and that the reflection and transmission coefficients for the initial scatter off the beam-splitter are $R_{\lambda\leftarrow}^2$ and $T_{\lambda\leftarrow}^2$, respectively. We can notice that this remains true for arbitrary quadratic Hamiltonians, since to the order we are working at in $\hbar$, the derivative relation

$$\frac{d}{dX}\Psi_{\lambda\pm} = iP_{\lambda\pm\pm}\Psi_{\lambda\pm} \qquad (3.101)$$

holds, which in turn implies that the current relation

$$J_{\lambda\pm}^{(v)} = \left|\Psi_{\lambda\pm}^{(v)}\right|^2 \left(\frac{\partial H}{\partial P_\lambda}\right)_{\pm\pm} \qquad (3.102)$$

also holds. The aforementioned expressions for the reflection and transmission coefficients then directly follow.

Probability is conserved in this description of the initial split provided the reflection and transmission coefficients add up to 1, since by definition these coefficients give the splitting probabilities. Specifically, we find

$$
\begin{aligned}
R_\leftarrow^2 + T_\leftarrow^2 &= \left|\frac{\partial H}{\partial P}\right|_{-+}^{-1} \left(\bar{R}_\leftarrow^2 \left|\frac{\partial H}{\partial P}\right|_{++} + \bar{T}_\leftarrow^2 \left|\frac{\partial H}{\partial P}\right|_{--} \right) \\
&= \left|\frac{\partial H}{\partial P}\right|_{-+}^{-1} \left[\left(\frac{2\Delta\left(H_2 P\right)_+ - \Delta\left(\frac{\partial H}{\partial P}\right)}{\Delta\left(\frac{\partial H}{\partial P}\right)} \right)^2 \left|\frac{\partial H}{\partial P}\right|_{++} \right. \\
&\qquad \left. + \left(\frac{2\Delta\left(H_2 P\right)_+}{\Delta\left(\frac{\partial H}{\partial P}\right)} \right)^2 \left|\frac{\partial H}{\partial P}\right|_{--} \right] \\
&= \frac{8\Delta\left(H_2 P\right)_+^2 - 4\Delta\left(H_2 P\right)_+ \left(\frac{\partial H}{\partial P}\right)_{++} + \left(\frac{\partial H}{\partial P}\right)_{++} \Delta\left(\frac{\partial H}{\partial P}\right)}{\left|\frac{\partial H}{\partial P}\right|_{-+} \Delta\left(\frac{\partial H}{\partial P}\right)} \\
&= \frac{1}{\left(2H_{2+} P_+\right)\frac{1}{2}\left(2H_{2+} P_+ + 2H_{2-} P_-\right)} \left[8 P_+^2 H_{2+}^2 \right. \\
&\qquad \left. -2\left(2H_{2+} P_+\right)\left(2P_+\right) H_{2+} + H_{2+} P_+ \left(2H_{2+} P_+ + 2H_{2-} P_-\right) \right] \\
&= \frac{4 P_+^2 H_{2+} - 4 H_{2+} P_+^2 + P_+ \left(H_{2+} P_+ + H_{2-} P_-\right)}{P_+ \left(H_{2+} P_+ + H_{2-} P_-\right)} \\
&= 1, \tag{3.103}
\end{aligned}
$$

thus confirming that probability is conserved for the initial split, if we use the WKB momenta in our scattering expressions.

The final output states are determined by equations (2.101) and (2.100), which yield

$$
\begin{aligned}
\Psi_{\lambda+}^{(v)} &= \psi_{\lambda++} \left(R_{\lambda\leftarrow} e^{i\Phi_{\lambda++}} R^{\lambda\rightarrow} e^{i\Phi_{\lambda-+}} R_{\lambda\leftarrow} \right. \\
&\qquad \left. + T_{\lambda\leftarrow} e^{i\Phi_{\lambda--}} R^{\lambda\leftarrow} e^{i\Phi_{\lambda+-}} T_{\lambda\rightarrow} \right), \tag{3.104}
\end{aligned}
$$

and

$$
\begin{aligned}
\Psi_{\lambda-}^{(v)} &= \psi_{\lambda--} \left(R_{\lambda\leftarrow} e^{i\Phi_{\lambda++}} R^{\lambda\rightarrow} e^{i\Phi_{\lambda-+}} T_{\lambda\leftarrow} \right. \\
&\qquad \left. + T_{\lambda\leftarrow} e^{i\Phi_{\lambda--}} R^{\lambda\leftarrow} e^{i\Phi_{\lambda+-}} R_{\lambda\rightarrow} \right), \tag{3.105}
\end{aligned}
$$

with the mode functions $\psi_{\lambda\pm\pm}$ evaluated at $X = X_\delta + 0^\pm$.

Taking the modulus-squared of the final states (3.104) and (3.105) gives

us

$$
\left|\Psi_{\lambda+}^{(v)}\right|^2 = |\psi_{\lambda++}|^2 \left[\left| R_{\lambda\leftarrow}^2 \tilde{R}^{\lambda\rightarrow} \right|^2 + \left| T_{\lambda\leftarrow} T_{\lambda\rightarrow} \tilde{R}^{\lambda\leftarrow} \right|^2 \right.
$$
$$
\left. + 2\,\Re\left\{ R_{\lambda\leftarrow}^2 \tilde{R}^{\lambda\rightarrow} \left(T_{\lambda\leftarrow} T_{\lambda\rightarrow} \tilde{R}^{\lambda\leftarrow} \right)^* \right\} \right], \qquad (3.106)
$$

and

$$
\left|\Psi_{\lambda-}^{(v)}\right|^2 = |T_{\lambda\leftarrow}\psi_{\lambda--}|^2 \left[\left| R_{\lambda\leftarrow} \tilde{R}^{\lambda\rightarrow} \right|^2 + \left| R_{\lambda\rightarrow} \tilde{R}^{\lambda\leftarrow} \right|^2 \right.
$$
$$
\left. + 2\,\Re\left\{ R_{\lambda\leftarrow} \tilde{R}^{\lambda\rightarrow} \left(R_{\lambda\rightarrow} \tilde{R}^{\lambda\leftarrow} \right)^* \right\} \right], \qquad (3.107)
$$

where $\Re\{\cdot\}$ denotes the real part of a quantity and $(\cdot)^*$ denotes complex conjugation. We have also used the abbreviations $\tilde{R}^{\lambda\rightarrow} = R^{\lambda\rightarrow}e^{i(\Phi_{\lambda++}+\Phi_{\lambda-+})}$ and $\tilde{R}^{\lambda\leftarrow} = R^{\lambda\leftarrow}e^{i(\Phi_{\lambda--}+\Phi_{\lambda+-})}$, for brevity.

The same reasoning we used to establish that the probability is conserved for the initial split can be easily extended to show that the final interferometer output probabilities also sum to unity if the WKB momenta are used, but we will not belabour that point here. We will instead return to the task of determining the final output probabilities in the Painlevé-Gullstrand family of coordinates. The case $\lambda = 1$ was presented in Chapter 2, so we will restrict our attention to $0 < \lambda < 1$. Using the asymptotic Hamiltonian expressions (3.41)-(3.43), the jump condition (3.90) becomes

$$
\left[\left(\frac{1}{\lambda\hat{M}} + \frac{1}{X} \right) \Psi' \right]_\delta = \frac{i\lambda\Delta M}{v_\infty X_\delta} \Psi(X_\delta), \qquad (3.108)
$$

with $\Delta M = (M_+ - M_-)/2$. This parallels the previous gravitational jump condition (2.116), though we can see from the right hand side of (3.108) that the $v_\infty \to 0$ limit is ill-defined.

The reflection and transmission amplitudes for scattering from the right can be written as

$$
\bar{R}_{\lambda\leftarrow} = \frac{\frac{\lambda\Delta M}{v_\infty X_\delta} + \left(\frac{1}{\lambda M_-} + \frac{1}{X_\delta} \right) P_{\lambda--} - \left(\frac{1}{\lambda M_+} + \frac{1}{X_\delta} \right) P_{\lambda-+}}{-\frac{\lambda\Delta M}{v_\infty X_\delta} - \left(\frac{1}{\lambda M_-} + \frac{1}{X_\delta} \right) P_{\lambda--} + \left(\frac{1}{\lambda M_+} + \frac{1}{X_\delta} \right) P_{\lambda++}} \qquad (3.109)
$$

and

$$
\bar{T}_{\lambda\leftarrow} = \frac{\left(\frac{1}{\lambda M_+} + \frac{1}{X_\delta} \right) (P_{\lambda++} - P_{\lambda-+})}{-\frac{\lambda\Delta M}{v_\infty X_\delta} - \left(\frac{1}{\lambda M_-} + \frac{1}{X_\delta} \right) P_{\lambda--} + \left(\frac{1}{\lambda M_+} + \frac{1}{X_\delta} \right) P_{\lambda++}}. \qquad (3.110)
$$

which correspond to the previous gravitational reflection and transmission amplitudes (2.117) and (2.118). Similarly, for scattering from the left we have

$$\bar{R}_{\lambda\rightarrow} = \frac{\frac{\lambda\Delta M}{v_\infty X_\delta} + \left(\frac{1}{\lambda M_-} + \frac{1}{X_\delta}\right) P_{\lambda+-} - \left(\frac{1}{\lambda M_+} + \frac{1}{X_\delta}\right) P_{\lambda++}}{-\frac{\lambda\Delta M}{v_\infty X_\delta} - \left(\frac{1}{\lambda M_-} + \frac{1}{X_\delta}\right) P_{\lambda--} + \left(\frac{1}{\lambda M_+} + \frac{1}{X_\delta}\right) P_{\lambda++}} \qquad (3.111)$$

and

$$\bar{T}_{\lambda\rightarrow} = \frac{\left(\frac{1}{\lambda M_-} + \frac{1}{X_\delta}\right)(P_{\lambda+-} - P_{\lambda--})}{-\frac{\lambda\Delta M}{v_\infty X_\delta} - \left(\frac{1}{\lambda M_-} + \frac{1}{X_\delta}\right) P_{\lambda--} + \left(\frac{1}{\lambda M_+} + \frac{1}{X_\delta}\right) P_{\lambda++}}, \qquad (3.112)$$

which are the analogs of (2.119) and (2.120). Remarkably, as $v_\infty \rightarrow 0$, the transmission amplitudes from both the left and right approach zero, for any finite values of the remaining parameters. This does not reproduce the Painlevé-Gullstrand limit presented in the previous chapter, and so is clearly not the correct behaviour as $v_\infty \rightarrow 0$; the singular nature of the Hamiltonian asymptotics (3.41)-(3.43) is causing our WKB scattering approximation to break down.

To resolve this issue, we can use the interpolating Hamiltonian we derived in Section 3.5. Though the interpolating Hamiltonian has the correct limit as $v_\infty \rightarrow 0$, its use leads to some ugly expressions, which we will not present here. Nonetheless, even with the interpolating Hamiltonian, one still ends up with reflection and transmission probabilities that are λ-dependent, and it is unclear exactly how to interpret this, given the λ-dependence of the initial state.

A similar issue arises when using the reflection and transmission amplitudes to determine the node spacing in the interference pattern. The oscillatory part of the final reflection and transmission coefficients involves the phase

$$\bar{\varphi}_\lambda = \Phi_{\lambda++} + \Phi_{\lambda-+} - \Phi_{\lambda+-} - \Phi_{\lambda--}, \qquad (3.113)$$

with $\Phi_{\lambda\pm\tilde{\pm}} = \phi_{\lambda\pm\tilde{\pm}} - Ht_{\lambda\pm\tilde{\pm}}$ and $\phi_{\pm\tilde{\pm}} = \pm\tilde{\pm} \int_{X_\delta}^{X_{\tilde{\pm}}} dX\, P_{\lambda\pm\tilde{\pm}}$. Modulo a possible factor of 2, this means that if we fix all other system parameters and vary the outer interferometer arm length $L_+ = X_+ - X_\delta$, the node spacing in phase space for the nth node is given by $\bar{\varphi}_{\lambda(n+1)} - \bar{\varphi}_{\lambda n} = \pi$, for

$$\begin{aligned}
\bar{\varphi}_{\lambda n} &= \int_{X_\delta}^{X_{+n}} dX\, (P_{\lambda++} - P_{\lambda-+}) - \int_{X_-}^{X_\delta} dX\, (P_{\lambda+-} - P_{\lambda--}) \\
&\quad - H\left(t_{\lambda++} + t_{\lambda-+} - t_{\lambda+-} - t_{\lambda--}\right).
\end{aligned} \qquad (3.114)$$

If we make the assumption of equal travel times, i.e. we recombine the quantum states after a definite (shared) coordinate time has elapsed, then the node spacing condition becomes

$$\pi = \bar{\varphi}_{\lambda(n+1)} - \bar{\varphi}_{\lambda n} = \int_{X_{+n}}^{X_{+(n+1)}} dX \left(P_{\lambda++} - P_{\lambda-+} \right). \qquad (3.115)$$

We can further simplify the analysis by working in a regime where the node spacing is much smaller than the outer interferometer arm length; in this case we can use the definitions $\Delta L_n = L_{+(n+1)} - L_{+n}$, $L_{+n} = X_{+n} - X_\delta$, $\Delta(P_\lambda)_\pm = (P_{\lambda+\pm} - P_{\lambda-\pm})/2$, and $\Delta(P_\lambda)_{+n} = \Delta(P_\lambda)_+|_{X=X_{+n}}$ to approximate the integral in (3.115) as

$$
\begin{aligned}
\pi &= 2\int_{X_{+n}}^{X_{+n}+\Delta L_n} dX \, \Delta\left(P_\lambda\right)_+ \\
&\approx 2\Delta\left(P_\lambda\right)_{+n} \Delta L_n + \left(\frac{\partial \Delta\left(P_\lambda\right)_{+n}}{\partial \Delta L_n} \right) (\Delta L_n)^2. \qquad (3.116)
\end{aligned}
$$

When solved for the node spacing ΔL_n, the approximation (3.116) yields

$$\Delta L_n = \frac{-\Delta\left(P_\lambda\right)_{+n} \pm \sqrt{\left(\Delta\left(P_\lambda\right)_{+n}\right)^2 + \pi \left(\frac{\partial \Delta(P_\lambda)_{+n}}{\partial \Delta L_n} \right)}}{\left(\frac{\partial \Delta(P_\lambda)_{+n}}{\partial \Delta L_n} \right)}. \qquad (3.117)$$

As the outer interferometer arm length increases, the node spacing changes as

$$\frac{\partial \Delta L_n}{\partial L_{+n}} = \frac{\partial \Delta L_n}{\partial X_{+n}}, \qquad (3.118)$$

which clearly has a rather complicated dependence on λ.

3.7   Discussion

What can we conclude from the λ-dependence of this interference pattern? Since each λ specifies a coordinate choice, and this coordinate choice can be associated with a network of infalling observers, one might wonder if coherence itself could be observer-dependent. At first sight, this seems like quite an unintuitive possibility, but can we rule it out on consistency grounds? If a beam-splitter has a transmission probability of 50% according to one observer network, then that observer network could be used to make a series

of output measurements, and there would be roughly 50% recorded transmissions. Is this not an objective property of the beam-splitter, agreed upon by any other observer network?

To address these questions, let us return to the issue about the initial state mentioned earlier in the Chapter. In Chapter 2, we chose an initial (ingoing) WKB state of the form

$$\Psi_0 = \frac{e^{i \int dX \, P_{-+}}}{\sqrt{|\partial H/\partial P_{-+}|}} \equiv \psi_{-+}, \qquad (3.119)$$

evaluated at $H = E$, which we generalized in the previous section to

$$\Psi_{\lambda 0} = \psi_{\lambda-+}. \qquad (3.120)$$

The problem with this generalization is that although the states ψ_{-+} and $\psi_{\lambda-+}$ have the same energy, for $\lambda \neq 1$ they are, strictly speaking, different states. The time dependence of the generalized initial state, for instance, is defined by

$$\Psi_{\lambda-+} = \psi_{\lambda-+} e^{-iEt_\lambda}, \qquad (3.121)$$

with t_λ being related to the previous Painlevé-Gullstrand time by

$$t - t_\lambda = \int dX \, \frac{\sqrt{2E/X}}{f} - \int dX \, \frac{\sqrt{1 - \lambda^2 f}}{f} \qquad (3.122)$$

as a result of the transformations presented in Section 3.1. Here $f = 1 - 2E/X$, and the integration can be performed to obtain

$$
\begin{aligned}
t - t_\lambda \;=\; & 4E \left(\sqrt{\frac{X}{2E}} + \frac{1}{2} \ln \left| \frac{\sqrt{X/2E} - 1}{\sqrt{X/2E} + 1} \right| \right) \\
& - 4E \left[\frac{X}{4E} \sqrt{1 - \lambda^2 f} + \ln \left(\frac{\sqrt{f}}{1 + \sqrt{1 - \lambda^2 f}} \right) \right. \\
& \left. + \frac{\left(1 - \frac{\lambda^2}{2}\right)}{\sqrt{1 - \lambda^2}} \ln \left(\sqrt{\frac{X}{2E}} \left(\sqrt{1 - \lambda^2} + \sqrt{1 - \lambda^2 f} \right) \right) \right] \quad (3.123)
\end{aligned}
$$

One can then see that $t = 0$ corresponds to a generalized time t_λ that depends on the values of X and E, which implies that the (classical) transformation between the two definitions of time depends on the location in phase space. At the quantum level, the state of a system with respect to a particular coordinate choice at a specific value of the associated coordinate

time does not in general correspond to a system state with respect to a different coordinate choice at any individual value of the time associated with this other coordinate choice.[6]   The very notion of "initial state" therefore seems to be coordinate-dependent, which would potentially render the question of how the coordinate choice affects the propagation of a given initial state through the interferometer ill-defined.

To avoid this paradoxical conclusion, one could use an augmented family of coordinate systems that had equivalent constant-time hypersurfaces in the region where the initial state is defined, but were different everywhere else. For instance, one could have a family that were equal to Painlevé-Gullstrand coordinates ($\lambda = 1$) for $r > r_0$, but for $r < r_0$ the coordinate systems in this new family range from the $\lambda = 1$ to the $\lambda = 0$ coordinates of the original family. The different coordinate systems for $r < r_0$ then continuously connect to the same ($\lambda = 1$) coordinates for $r > r_0$, which enables us to define the same initial state for each member of the new family (in the $r > r_0$ region). This idea was suggested very recently (by Bill Unruh), and until it has been fully implemented we will have to accept that the analysis of coordinate dependence in our description of the self-gravitating interferometer is inconclusive.

---

[6]Given the connection between coordinate choices and observer networks, we might summarize this behaviour with the (somewhat Rovellian) maxim, "Everyone else's time is an operator except one's own."

Chapter 4

Superpositions of Clocks and Intrinsic Decoherence

4.1 Introduction

Time dilation is one of the most profound consequences of relativity theory. In classical systems, time dilation effects are fairly well understood, but in quantum systems there are still many questions that remain unanswered. One such question is how to properly incorporate the effects of time dilation into the quantum evolution of composite systems, either in the limit of flat spacetime or in situations where gravitational effects are significant.

In a series of papers by Pikovski et al. [12]-[14], for instance, a "universal" decoherence mechanism was proposed for composite general relativistic systems, due to gravitational time dilation. In [12], Pikovski et al. present an approximate quantum description of such a composite system that as a whole behaves as a point particle (located at the center-of-mass of the system) with a well-defined proper time, with internal degrees of freedom that are defined in the rest frame of the system. The system is placed in the gravitational field of the earth, and the authors postulate that the quantum evolution of the system with respect to a laboratory frame on the surface of the earth should be given by a Schrödinger equation of the form $i\frac{D}{D\tau}\Psi = H_{rest}\Psi$, with τ being the proper time of the system (treated as a point particle), and H_{rest} being the rest-frame Hamiltonian. Expressing the proper time derivative in terms of the lab-frame time t induces a coupling between the internal degrees of freedom and the center-of-mass coordinate, and if one only keeps track of the center-of-mass dynamics, tracing out over the internal degrees of freedom leads to a novel form of the "third-party decoherence" described in Chapter 1. It is this effect, and variations on the theme, that we focus on in this chapter.

It is unclear whether any inconsistencies result from simply replacing the usual time derivative in the Schrödinger equation with a proper time derivative for the system's center-of-mass, since this is not the standard

procedure for quantizing general relativistic systems. Rather than make use of the same model used by Pikovski et al., we will explore similar ideas with a model that generalizes the self-gravitating spherical perfect fluid shell introduced in Chapter 2. Whereas the original model was introduced to study the consequences of general relativity on massive interferometers, here we extend the model to include an "internal" harmonic oscillator, to analyze the quantum structure of composite relativistic systems. By "internal," we mean that the harmonic oscillator is described by an internal coordinate q that oscillates in an abstract space that is not part of the spacetime; such an internal degree of freedom could represent the values of a single spherically symmetric mode of an oscillating field confined to the surface of the shell, for instance. The internal coordinate oscillates harmonically with respect to the proper time of the (external) shell position, and therefore the oscillator serves as a clock, evolving based on the local flow of time determined by the external motion. Unlike the postulated evolution in [12], however, our internal coordinates evolve *classically* according to the proper time of the shell, and then a Hamiltonian H is defined with respect to a coordinate time t, which then allows us to quantize the system with a standard Schrödinger equation $i\frac{\partial}{\partial t}\Psi = H\Psi$. This avoids any extra postulates about how such systems evolve quantum-mechanically.

We should keep in mind that the internal oscillator contributes to the external shell dynamics as well, which in turn affects the spacetime; in other words, the very ticking of our clock influences the manner in which it ticks. This is especially relevant in the quantized system, because uncertainties in clock readings become intimately connected with uncertainties in spacetime geometry.

We will explore some of the ambiguities associated with the quantum theory of this generalized shell system in reduced phase space, and then relate an approximate form of our reduced Hamiltonian with the Hamiltonian presented in [12]. We exploit this parallel to demonstrate time dilation decoherence in our system, and observe that when the fluid pressure is nonzero, the (external) shell position decoheres even in the (gravity-free) limit of flat spacetime, because of the acceleration caused by the pressure. This indicates that the proposed effect results from proper time differences alone, and as such is not necessarily related to gravity.

Further, we can use our generalized shell model to include self-interaction corrections to the time dilation decoherence, such that the decoherence is altered by the manner in which our shell and its clock influence the state of their own geometry. We find that even without pressure, the self-gravitation of the shell leads to the nonzero acceleration required to produce the time di-

lation decoherence. We interpret this "self-decoherence" as a fundamentally gravitational effect.

4.2 Classical Action

For context, before adding an internal oscillator, the self-gravitating spherical perfect fluid shell model introduced in Chapter 2 is described by the action $I_x + I_G$, where I_x is the shell action

$$I_x = -\int d\lambda \sqrt{-g_{\mu\nu} \frac{dx^\mu}{d\lambda} \frac{dx^\nu}{d\lambda}} M(R), \qquad (4.1)$$

with all quantities evaluated on the shell history, and I_G is the Einstein-Hilbert action

$$I = \frac{1}{16\pi} \int d^4x \sqrt{-g^{(4)}} \, \mathcal{R}^{(4)}. \qquad (4.2)$$

Here superscripts on the metric determinant g and the Ricci scalar $\mathcal{R}$ indicate that these are constructed from the full $(3+1)$-dimensional spacetime metric components $\{g_{\mu\nu}\}$. We make use of the ADM form of the metric in spherical symmetry,

$$g_{\mu\nu} dx^\mu dx^\nu = -N^2 dt^2 + L^2 \left(dr + N^r dt\right)^2 + R^2 d\Omega^2, \qquad (4.3)$$

where N is the lapse function, N^r is the radial component of the shift vector, and L^2 and R^2 are the only nontrivial components of the spatial metric [54]. It is then clear that R is the "radius" of the shell, obtained from the area $4\pi R^2$ of symmetry two-spheres. The shell contribution I_x is analogous to a free relativistic particle action, except with a mass M that depends on the position-dependent metric function R; the function $M(R)$ serves to parametrize the relationship between the density $\sigma = M(R)/4\pi R^2$ and pressure $P_\sigma = -M'(R)/8\pi R$ of the fluid.

We add an internal oscillator to our shell with the action

$$I_q = \frac{1}{2} \int d\tau \left[m \left(\frac{dq}{d\tau}\right)^2 - kq^2 \right], \qquad (4.4)$$

with τ being the proper time evaluated on the shell history, and q being an internal coordinate that does not take values in the (external) spacetime. The quantity k is related to ω_0, the natural frequency of the oscillator, via $k = m\omega_0^2$. The action (4.4) is manifestly invariant under coordinate transformations, as it only makes use of the proper time of the shell.

It simplifies the description to parametrize the shell history with the co-ordinate time t, such that the classical shell motion is defined by a trajectory $r = X(t)$. We can use the shell 4-velocity $u^\mu = (dt/d\tau)(1, \dot{X}, 0, 0)$ to express the proper time differentials as

$$d\tau = -u_\mu dx^\mu = \dot{\tau} dt \tag{4.5}$$

and

$$\frac{dq}{d\tau} = -u^\mu \partial_\mu q = \dot{\tau}^{-1} \frac{dq}{dt}. \tag{4.6}$$

Now q is being treated as a function solely of coordinate time t, to reflect our choice of parametrization. The 4-velocity normalization $u^\mu u_\mu = -1$ then implies that one can express the derivative of the proper time with respect to the coordinate time as

$$\begin{aligned}
\dot{\tau} &= \int dr \sqrt{N^2 - L^2 (N^r + \dot{X})^2} \delta(r - X) \\
&= \sqrt{\hat{N}^2 - \hat{L}^2 (\hat{N}^r + \dot{X})^2}.
\end{aligned} \tag{4.7}$$

An overhat denotes that a quantity is to be evaluated on the shell history; likewise, it is understood that the overdots denote coordinate-time deriva-tives along the shell trajectory.

If we define the original shell Lagrangian as

$$\begin{aligned}
\mathcal{L}_x &= -\int dr \sqrt{N^2 - L^2 (N^r + \dot{X})^2} M(R) \delta(r - X) \\
&= -\dot{\tau} \hat{M}
\end{aligned} \tag{4.8}$$

and the oscillator Lagrangian as

$$\begin{aligned}
\mathcal{L}_q &= \frac{1}{2} \int dr \, \dot{\tau} \left[m \left(\frac{\dot{q}}{\dot{\tau}} \right)^2 - kq^2 \right] \delta(r - X) \\
&= \frac{1}{2} \left(m \frac{\dot{q}^2}{\dot{\tau}} - k\dot{\tau} q^2 \right),
\end{aligned} \tag{4.9}$$

then the shell-oscillator action is given by

$$I_{shell} = \int dt \, \mathcal{L} = \int dt \, (\mathcal{L}_x + \mathcal{L}_q). \tag{4.10}$$

4.3   Hamiltonianization

We can Hamiltonianize the shell-oscillator system with the Legendre transformation $\mathcal{H} = P\dot{X} + p\dot{q} - \mathcal{L}$. The momentum p conjugate to the internal coordinate q is given by

$$p \equiv \frac{\partial \mathcal{L}}{\partial \dot{q}} = m \int dr \, \frac{\dot{q}}{\dot{\tau}} \delta(r - X) = m \frac{\dot{q}}{\dot{\tau}}, \tag{4.11}$$

and that the momentum conjugate to the shell position X is given by

$$
\begin{aligned}
P &\equiv \frac{\partial \mathcal{L}}{\partial \dot{X}} = -\hat{M} \frac{\partial \dot{\tau}}{\partial \dot{X}} - \frac{1}{2} m \left(\frac{\dot{q}}{\dot{\tau}} \right)^2 \frac{\partial \dot{\tau}}{\partial \dot{X}} - \frac{1}{2} k q^2 \frac{\partial \dot{\tau}}{\partial \dot{X}} \\
&= -\frac{\partial \dot{\tau}}{\partial \dot{X}} \left(\hat{M} + \frac{p^2}{2m} + \frac{1}{2} k q^2 \right) \\
&= -\frac{\partial \dot{\tau}}{\partial \dot{X}} \left(\hat{M} + H_q \right),
\end{aligned}
\tag{4.12}
$$

where the internal "clock" Hamiltonian $H_q = p^2/2m + kq^2/2$ takes the form of a (free) harmonic oscillator. Introducing the notation $\tilde{M} = \hat{M} + H_q$, one can observe that our shell-oscillator system becomes very similar to the shell system without the oscillator, subject to the transformation $\hat{M} \to \tilde{M}$.

More explicitly, the shell momentum P can be expressed as

$$P = \int dr \, \frac{L^2 \left(N^r + \dot{X} \right) \tilde{M}}{\sqrt{N^2 - L^2 \left(N^r + \dot{X} \right)^2}} \delta(r - X), \tag{4.13}$$

from which we can solve for $\dot{X}$ to obtain

$$
\begin{aligned}
\dot{X} &= \int dr \left(\frac{NP}{L\sqrt{P^2 + L^2 \tilde{M}^2}} - N^r \right) \delta(r - X) \\
&= \frac{\hat{N} P}{\hat{L} \sqrt{P^2 + \hat{L}^2 \tilde{M}^2}} - \hat{N}^r.
\end{aligned}
\tag{4.14}
$$

The Legendre transformation then gives us the Hamiltonian

$$\mathcal{H} = P\dot{X} + p\dot{q} - \mathcal{L} = \int dr \, (N H_t^s + N^r H_r^s), \tag{4.15}$$

with the definitions

$$
\begin{aligned}
H_t^s &= \sqrt{L^{-2} P^2 + \tilde{M}^2} \delta(r - X), \\
H_r^s &= -P\delta(r - X).
\end{aligned}
\tag{4.16}
$$

We remind the reader that $\tilde{M} = \hat{M} + H_q$, so our clock Hamiltonian adds to the (position-dependent) shell mass $\hat{M}$ to alter the Hamiltonian constraint from the form it took in Chapters 2 and 3.

Hamiltonianizing the gravitational sector as well, as in Chapter 2, leads to the total action

$$I = \int dt \left(P\dot{X} + p\dot{q} \right)$$
$$+ \int dt\, dr \left(\pi_R \dot{R} + \pi_L \dot{L} - N H_t - N^r H_r \right), \qquad (4.17)$$

for $H_t = H_t^s + H_t^G$ and $H_r = H_r^s + H_r^G$, such that

$$
\begin{aligned}
H_t^G &= \frac{L\pi_L^2}{2R^2} - \frac{\pi_L \pi_R}{R} + \left(\frac{RR'}{L} \right)' - \frac{(R')^2}{2L} - \frac{L}{2}, \\
H_r^G &= R'\pi_R - L\pi_L'.
\end{aligned}
\qquad (4.18)
$$

4.4 Reduced Phase Space Quantization

Since we are working in spherical symmetry, the metric itself has no actual degrees of freedom, because although there are only two gravitational constraints ($H_t = 0$ and $H_r = 0$), there are also only two independent metric functions (L and R). Accordingly, one can obtain an unconstrained description of the system by making a coordinate choice, solving the constraints for the corresponding gravitational momenta, and inserting the solutions into the Liouville form $\mathcal{F}$ on the full phase space,

$$\mathcal{F} = P\boldsymbol{\delta}X + p\boldsymbol{\delta}q + \int dr \left(\pi_L \boldsymbol{\delta}L + \pi_R \boldsymbol{\delta}R \right). \qquad (4.19)$$

This amounts to a pullback of the full Liouville form to the representative hypersurface defined by the coordinate choice. From the Liouville pullback, denoted by $\tilde{\mathcal{F}}$, we can deduce the canonical structure of the reduced phase space, which only depends on the shell-oscillator variables X and q (and their momenta).

To solve the gravitational constraints, first consider the following linear combination of the constraints, away from the shell:

$$-\frac{R'}{L}H_t - \frac{\pi_L}{RL}H_r = \mathcal{M}', \qquad (4.20)$$

for

$$\mathcal{M}(r) = \frac{\pi_L^2}{2R} + \frac{R}{2} - \frac{R(R')^2}{2L^2}. \qquad (4.21)$$

The quantity $\mathcal{M}(r)$ corresponds to the ADM mass H when evaluated outside of the shell, and vanishes inside the shell. We can now solve for the gravitational momenta π_L, π_R away from the shell. The result is

$$\pi_L = \pm R\sqrt{\left(\frac{R'}{L}\right)^2 - 1 + \frac{2\mathcal{M}}{R}}, \quad \pi_R = \frac{L}{R'}\pi_L'. \tag{4.22}$$

Assuming a continuous metric and singularity-free gravitational momenta, we can integrate the gravitational constraints ($H_t = 0$ and $H_r = 0$) across the shell, from which we obtain the jump conditions

$$\Delta R' = -\frac{\tilde{V}}{\hat{R}}, \quad \Delta \pi_L = -\frac{P}{\hat{L}}, \tag{4.23}$$

where $\tilde{V} = \sqrt{P^2 + \tilde{M}^2}$. We use Δ to denote the jump of a quantity across the shell (at $r = X(t)$).

The coordinates we will use resemble the Painlevé-Gullstrand coordinates $\{L = 1, R = r\}$, though the jump conditions force us to include a deformation region ($X - \epsilon < r < X$) near the shell. By inspection, the required metric function R can be generalized as

$$R(r,t) = r - \frac{\epsilon}{X}\tilde{V}\mathcal{G}\left(\frac{X - r}{\epsilon}\right), \tag{4.24}$$

for a function $\mathcal{G}$ having the properties

$$\lim_{z \to 0^+} \frac{d\mathcal{G}(z)}{dz} = 1 \tag{4.25}$$

$$\lim_{z \to 0^-} \frac{d\mathcal{G}(z)}{dz} = 0, \tag{4.26}$$

from which it follows that

$$\lim_{\epsilon \to 0} R'(X - \epsilon) = 1 + \frac{\tilde{V}}{X} \tag{4.27}$$

$$\lim_{\epsilon \to 0} R'(X + \epsilon) = 1. \tag{4.28}$$

By inserting the gravitational momentum solutions (4.22) associated with the coodinate choice (4.24) into the jump equations (4.23) and squaring, one finds

$$H = \sqrt{P^2 + \tilde{M}^2} + \frac{\tilde{M}^2}{2X} - P\sqrt{\frac{2H}{X}}. \tag{4.29}$$

This implies that the unreduced momentum P is implicitly defined as a function of the reduced phase space quantities X, q, p, and H: one can easily solve (4.29) to obtain

$$P = \frac{1}{1 - \frac{2H}{X}}\left(\sqrt{\frac{2H}{X}\left(H - \frac{\tilde{M}^2}{2X}\right)}\right) \tag{4.30}$$

$$\pm \frac{1}{1 - \frac{2H}{X}}\left(\sqrt{\left(H - \frac{\tilde{M}^2}{2X}\right)^2 - \tilde{M}^2\left(1 - \frac{2H}{X}\right)}\right).$$

The $\pm$ in (4.30) indicates whether the shell is outgoing (+) or ingoing (-), with respect to our choice of coordinates.

Let us now calculate the pullback of the full Liouville form to the representative hypersurface defined by our coordinate choice. The condition $L = 1$ and the fact that $R = r$ outside of the deformation region implies that

$$\tilde{\mathcal{F}} = P\boldsymbol{\delta}X + p\boldsymbol{\delta}q + \int_{X-\epsilon}^{X} dr\, \pi_R \boldsymbol{\delta}R. \tag{4.31}$$

We can then simplify the remaining integral by changing the integration variable from r to $v = R'$, which yields

$$\int_{X-\epsilon}^{X} dr\, \pi_R \boldsymbol{\delta}R = X\boldsymbol{\delta}X \int_{1}^{R'_-} dv\, \frac{(1-v)}{\sqrt{v^2 - 1}} + \mathcal{O}(\epsilon), \tag{4.32}$$

with R'_- being R' evaluated just inside the shell. Now the integration is trivial, and we can easily obtain the desired Liouville form pullback,

$$\mathcal{F} = P_c\boldsymbol{\delta}X + p\boldsymbol{\delta}q, \tag{4.33}$$

with the reduced canonical momentum for the shell position satisfying

$$P_c = -\sqrt{2HX} + X\ln\left(1 + \frac{\tilde{V} + P}{X} + \sqrt{\frac{2H}{X}}\right). \tag{4.34}$$

This expression gives an implicit definition of the Hamiltonian H on the reduced phase space, as a function of the shell-oscillator variables (X and q), along with the momenta that are conjugate to them in the reduced phase space (P_c and p, respectively).

Just as the expressions (2.47) and (2.48) from Chapter 2 were shown to be equivalent, the expression (4.34) for the reduced canonical shell momentum

P_c is equivalent to

$$P_c = -\sqrt{2HX} - X \ln\left(\frac{X + \tilde{V} - P - \sqrt{2HX}}{X}\right),\qquad (4.35)$$

despite the different minus sign placement.

To gain some intuition for how the presence of the oscillator alters the reduced dynamics, let us consider the flat spacetime limit of the system defined by (4.35). Keeping in mind the similarities with the relativistic-particle-like structure of our shell system, it should be unsurprising that in this limit (4.35) becomes

$$P_c = \pm\sqrt{H^2 - \tilde{M}^2} = \pm\sqrt{H^2 - \left(\hat{M} + H_q\right)^2},\qquad (4.36)$$

and therefore the Hamiltonian is given by

$$H = \sqrt{P_c^2 + \tilde{M}^2} = \sqrt{P_c^2 + \left(\hat{M} + H_q\right)^2}.\qquad (4.37)$$

In the nonrelativistic regime (i.e. small P_c), the Hamiltonian can then be expressed as

$$\begin{aligned} H &\approx \hat{M} + H_q + \frac{P_c^2}{2\left(\hat{M} + H_q\right)} \\ &= \hat{M} + \frac{1}{2}kq^2 + \frac{p^2}{2m} + \frac{P_c^2}{2\left(\hat{M} + \frac{1}{2}kq^2 + \frac{p^2}{2m}\right)}. \end{aligned}\qquad (4.38)$$

The last term in this approximate Hamiltonian is an effective coupling between the internal oscillator variables (q and p) and the external shell variables (X and P_c). The coupling is of course produced by the fact that the internal "clock" oscillates harmonically with the shell's proper time, the flow of which is influenced by the external variables.

Even in the flat spacetime nonrelativistic limit, one can tell from the appearance of the clock Hamiltonian H_q in the denominator of the last term in (4.38) that exact quantization will require nonstandard techniques. The Hamiltonian (4.38) leads to the following Schrödinger equation, in the coordinate basis:

$$\begin{aligned} i\frac{\partial}{\partial t}\Psi &= \left(\hat{M} + \frac{1}{2}kq^2 - \frac{1}{2m}\frac{\partial^2}{\partial q^2}\right)\Psi \\ &\quad -\frac{1}{2}\frac{\partial}{\partial X}\left[\frac{1}{\hat{M} + \frac{1}{2}kq^2 - \frac{1}{2m}\frac{\partial^2}{\partial q^2}}\right]\frac{\partial}{\partial X}\Psi. \end{aligned}\qquad (4.39)$$

79

The factor-ordering in the last term of (4.39) was chosen to make the differential operator Hermitian, but there is still some ambiguity in the meaning of the bracketed factor between the X-derivatives, since the formal expression has q-derivatives in the denominator.

To formulate a more tractable problem, let us consider the following approximation to the Hamiltonian (4.38):

$$
\begin{aligned}
H &= \hat{M} + H_q + \frac{P_c^2}{2\hat{M}\left(1 + \frac{H_q}{\hat{M}}\right)} \\
&\approx \hat{M} + H_q + \frac{P_c^2}{2\hat{M}}\left(1 - \frac{H_q}{\hat{M}}\right),
\end{aligned}
\tag{4.40}
$$

which should be valid as long as the shell mass $\hat{M}$ is sufficiently larger than the clock energy H_q. In this case the system decomposes into a more standard form

$$
H = H_0 + H_{xq} = H_x + H_q + H_{xq},
\tag{4.41}
$$

with the approximate shell Hamiltonian $H_x = \hat{M} + P_c^2/2\hat{M}$, the internal "clock" Hamiltonian $H_q = p^2/2m + kq^2/2$, and the interaction

$$
H_{xq} = -\frac{P_c^2}{2\hat{M}^2}H_q,
\tag{4.42}
$$

which is induced by the clock oscillation being defined with respect to the proper time of the shell.

4.5 Time Dilation Decoherence

The decomposition (4.41) is of the same form as the one used recently by Pikovski et al. [12] to demonstrate decoherence due to gravitational time dilation for composite systems, though the interpretation of the system variables is different. In the (gravity-free) limit of flat spacetime, the main difference is simply that the "external" coordinate of our system is the shell radius instead of the (somewhat ill-defined) center-of-mass coordinate. In the next section, however, the self-gravitation of the shell-plus-clock system is taken into account, so both the shell and the clock influence the spacetime geometry, which is therefore no longer fixed. Nonetheless, we can exploit the similarity enough to demonstrate a decoherence effect in our system analogous to that described by Pikovski et al., as will become clear in what follows.

Represented by a density operator, the full state ρ obeys the von Neumann equation,

$$\dot{\rho} = -i\,[H, \rho]\,. \tag{4.43}$$

We can then change the frame to primed coordinates, as in [12], which are defined by $\rho'(t) = e^{it(H_0+h)}\rho(t)e^{-it(H_0+h)}$, for $h(X, P_c) = Tr_q\,[H_{xq}\rho_q(0)]$. We are assuming that the initial state of the system is of the product form $\rho(0) = \rho_x(0)\rho_q(0)$, i.e. initially uncorrelated. Denoting the average clock energy $Tr_q\,[H_q\rho_q(0)]$ by $\bar{E}_q$ and the shell part of the interaction by $\Gamma = -P_c^2/2\hat{M}^2$, we obtain the expression $h = \Gamma(X, P_c)\bar{E}_q$. The transformed von Neumann equation is

$$
\begin{aligned}
\dot{\rho}'(t) &= i\left[H_0'(t) + h'(t), \rho'(t)\right] - i\left[H_0'(t) + H_{xq}'(t), \rho'(t)\right] \\
&= -i\left[H_{xq}'(t) - h'(t), \rho'(t)\right],
\end{aligned} \tag{4.44}
$$

with $h'(t) = h(X'(t), P_c'(t))$. If we integrate and iterate equation (4.44), we are led to the integro-differential equation

$$
\begin{aligned}
\dot{\rho}'(t) &= -i\left[H_{xq}'(t) - h'(t), \rho'(0)\right] \\
&\quad - \int_0^t ds\,\left[\tilde{h}(t), \left[\tilde{h}(s), \rho'(s)\right]\right],
\end{aligned} \tag{4.45}
$$

using the definition $\tilde{h}(t) = H_{xq}'(t) - h'(t)$. At this point Pikovski et al. trace over the internal variables, which for us describe the clock, and make use of the Born part of the Born-Markov approximation, keeping only terms up to second order in the interaction Hamiltonian H_{xq}, and replacing the $\rho'(s)$ in the integral by $\rho_x'(s)\rho_q'(0)$. This application of the Born approximation assumes weak coupling, but in contrast to the full Born-Markov it does not ignore memory effects. For a detailed discussion of this approximation, see [71]. The reduced equation for the external shell evolution is then given by

$$
\begin{aligned}
\dot{\rho}_x'(t) &= Tr_q\left[\dot{\rho}'(t)\right] \\
&\approx -\int_0^t ds\,Tr_q\left\{\left[\tilde{h}(t), \left[\tilde{h}(s), \rho'(s)\right]\right]\right\} \\
&= -\int_0^t ds\,Tr_q\left\{(H_q - \bar{E}_q)^2\left[\Gamma'(t), \left[\Gamma'(s), \rho'(s)\right]\right]\right\} \\
&= -(\Delta E_q)^2 \int_0^t ds\,\left[\Gamma'(t), \left[\Gamma'(s), \rho_x'(s)\right]\right],
\end{aligned} \tag{4.46}
$$

with $\Gamma'(s) = \Gamma(X'(s), P_c'(s))$ and

$$(\Delta E_q)^2 = Tr_q\left[(H_q - \bar{E}_q)^2\,\rho_q(0)\right]. \tag{4.47}$$

One can then transform back to the unprimed frame, whereby the substitution $s \to t - s$ leads to the expression

$$\dot{\rho}_x(t) = -i \left[H_x + \Gamma \bar{E}_q, \rho_x(t) \right] \tag{4.48}$$
$$- (\Delta E_q)^2 \int_0^t ds \, \left[\Gamma, e^{-isH_x} \left[\Gamma, \rho_x(t-s) \right] e^{isH_x} \right].$$

In general, the reduced evolution equation (4.48) exhibits decoherence due to the nonunitary contribution of the last term on the right. Under some special circumstances this term vanishes, leaving the reduced system to evolve unitarily; for example, such a circumstance occurs for initial states that are eigenstates of the internal (clock) Hamiltonian, of course then the oscillator is not much of a clock, as it never changes with time (modulo a phase).

4.6 Discussion

In the last section, we demonstrated intrinsic decoherence due to time dilation, in the (gravity-free) limit of flat spacetime. In the system described by Pikovski et al. [12], which includes spacetime curvature caused by the external gravitational field of the earth, the time dilation decoherence should vanish in the absence of the earth's gravitational influence: without the earth, the center-of-mass coordinate they use defines the origin of an inertial frame, and in that frame the proper time associated with the center-of-mass coordinate is equal to the coordinate time.[7] However, in our system, decoherence (in the position basis) is present even without an external gravitational field, because of the nonzero acceleration of the shell due to the position dependence of the mass ($\hat{M} = M(X)$). We are then led to conclude that the time dilation decoherence proposed in [12] is not necessarily related to gravity, but produced by proper time differences in composite systems with nonzero accelerations.

The preceding analysis can be extended to include self-interaction effects, by making use of the Hamiltonian asymptotics derived in Chapter 3, along with the transformation $\hat{M} \to \tilde{M}$. We then find that the components H_x

---

[7] Of course, quantum fluctuations of the center-of-mass motion will still produce decoherence in the momentum basis for the reduced system, but coherence will remain for the center-of-mass position itself; similarly, for our shell system in the absence of both gravity and pressure, the effective interaction 4.42 will lead to decoherence in the momentum basis of the reduced system, but coherence will remain for the (external) shell position.

and Γ of the decomposition (4.41) generalize to

$$H_x \to \left(\hat{M} + \frac{P_c^2}{2\hat{M}} \right) + \left[\frac{P_c^2}{3X} - \frac{2}{3}\sqrt{\frac{2\hat{M}}{X}}P_c - \frac{\hat{M}^2}{18X} \right] \qquad (4.49)$$

and

$$\Gamma \to \left(-\frac{P_c^2}{2\hat{M}^2} \right) + \left[-\frac{\hat{M}}{9X} - \frac{1}{3\hat{M}}\sqrt{\frac{2\hat{M}}{X}}P_c \right], \qquad (4.50)$$

to second order in $1/\sqrt{X}$. The bracketed term in each of these expressions originates from self-gravitation. From this we can observe that even in the constant $\hat{M}$ limit, where the fluid pressure vanishes, (4.48) (with the generalized components H_x and Γ) indicates that the time dilation decoherence remains present, in this case because the self-gravitation produces a nonzero acceleration of the shell position. Conceptually, such an effect should occur for any composite general relativistic system that has internal motion that (classically) evolves according to the proper time associated with the system's external motion, since the alteration of the local flow of time caused by the system's influence on its own spacetime geometry induces an effective coupling between the internal and external degrees of freedom. It is *this* effect that is fundamentally gravitational in nature, as it is present even in the absence of any other interactions.

We have therefore arrived at a type of intrinsic decoherence similar to the "third-party" decoherence described by Stamp [15], though in contrast to the use of the earth as the third party as proposed by Pikovski et al. [12], we have bootstrapped the idea by incorporating gravitational self-interaction, effectively producing third-party decoherence without the third party.

Chapter 5

Denouement

5.1 Reflections and Resolutions

In the preceding chapters, we have explored some of the consequences of forming superpositions of quantum states that correspond to different space-time geometries, in the context of a general relativistic model of a self-gravitating spherical perfect fluid shell. It has long been argued by Penrose (and others) that there is an inherent ambiguity associated with forming such superpositions [9], [10]. However, if the corresponding spacetime geometries are nearly identical, we know from standard quantum mechanics that there is effectively a well-defined notion of time evolution. When such an effective structure exists (as it does in almost every conceivable quantum system within technological reach), it has been extensively confirmed experimentally that quantum coherence is possible, which enables interference between distinct elements of a superposition.

When the spacetime geometries are sufficiently different, Penrose argues that the effective structure of quantum-mechanical time evolution ceases to be well-defined, at least with the current interpretation given to how we usually apply our quantization techniques. Penrose speculates that this sufficient difference in spacetime geometries leads to an instability that causes the interference between the corresponding quantum states to decay, though it is unclear from his work whether the system undergoes a "collapse" or just an intrinsic form of gravitational decoherence. Since the former possibility seems to necessarily require altering the foundations of quantum theory, this thesis focused on the possibility that a suitably-interpreted quantum description of time evolution in an idealized general relativistic system can exhibit this intrinsic form of gravitational decoherence, without the addition of any exotic or untested physics. Accordingly, we worked within canonical quantum gravity; for simplicity, as well as practicality, we restricted our attention to minisuperspace, and used the reduced phase space approach to quantization.

We used our self-gravitating fluid shell model to perform an interferometric analysis in Chapter 2 for single-mode input states, but ended up

concluding that even though the classical model was general-relativistically correct, we did not observe any limitations on the coherence of the system attributable to gravity. This outcome does not necessarily imply that our model is incapable of producing such a limitation, as discussed in Section 2.4, though it does mean that our approximation scheme did not capture the essential features necessary to confirm Penrose's proposed decoherence effect.

The fact that we did not observe any limitation on the coherence of our self-gravitating interferometer could also be explained if Penrose's argument about the ill-definedness of time evolution for superpositions of geometries is avoided by the very structure of canonical quantum gravity itself. Penrose recognizes this possibility, as well as the fact that superpositions of 3-geometries are ubiquitous in canonical quantum gravity, but considers the picture one ends up with insufficient to describe the physics *within* such a superposition of spaces [10]. Rather than being this dismissive, the perspective we have entertained in this thesis is that canonical quantum gravity is precisely the arena to obtain a resolution of the issues Penrose raises, and perhaps the resolution entails no fundamental decoherence whatsoever, by providing a well-defined description not only of how superpositions of 3-geometries behave, but also of what this implies for the physics within such a superposition.

To understand how this could be the case, let's recall the details of the single-mode analysis. We followed the standard quantum mechanical prescription, and assumed that the system evolves according to a time evolution operator $\partial/\partial t$ that is the same for both components of our superposition. Penrose's argument suggests that it is exactly this identification that is inherently ambiguous, since by "$\partial/\partial t$" we do not mean the timelike Killing vector associated with any specific spacetime; how, then, can we justify the use of a single operator for both components?

A natural possibility is that once a coordinate choice is made that defines a physical time evolution, one can construct a quantum theory that reflects the geometric structure in the (physical) Hamiltonian operator, while treating the associated time as a parameter that is no longer endowed with nontrivial geometric meaning. In our shell system, then, the position dependence and non-polynomial form of our Hamiltonian encodes the geometric content about spacetime, while using the coordinate time t as a parameter that flows forward independent of the quantum state of the geometry, thus defining an operator $\partial/\partial t$ that acts in the same way on any particular state. As long as we take into account how the Hamiltonian operates differently on states corresponding to different geometries, we could potentially escape Penrose's argument by construction, since the time evolution has a unique

definition once a particular coordinate choice is made that fixes the meaning of the Hamiltonian.

Regardless of what the true theoretical explanation is, there are experimental investigations already underway to test for signatures of gravity-induced intrinsic decoherence in various optical systems [72]. These experiments generalize the infamous Colella-Overhauser-Werner (COW) experiment [73]-[75], which measures the gravitational phase shift experienced by neutrons in an interferometer that has one path at a different gravitational potential than the other. The original COW experiment was the first experiment to include both quantum and gravitational effects, though it only required Newtonian gravity to describe it. The more recent experiments, such as the efforts to observe macroscopic superposition effects in optomechanical systems [76], [77], intend to test the role of general relativity in quantum systems. There are many technical obstacles to overcome to minimize the effects of standard environmental decoherence, which obscures the desired behaviour, but there is hope that these types of experiments will bear fruit within the next decade [78].

One of the remaining questions from the analysis presented in Chapter 2 is about the role of our coordinate choice on the properties of the interference pattern: does our approximation scheme describe coherence in a coordinate-invariant manner, or are our conclusions about the coherence of the system dependent on the coordinates used? In Chapter 3, we attempted to answer this question by re-performing the previous analysis, this time using an infinite family of similar coordinate systems. We interpreted these family members as different networks of infalling observers, each with a different asymptotic velocity. Upon doing so, we encountered some perplexing obstacles due to the nebulous connection between quantizations associated with different family members. The main problem was that the very concept of an "initial state" seemed to be coordinate-dependent, which directly impeded our ability to compare the interference patterns we obtained using different coordinate choices.

Another issue worth mentioning is the identification of travel times for the two interferometer paths ($t_{\lambda++} + t_{\lambda-+} = t_{\lambda--} + t_{\lambda+-}$). We enforced this identification for our interferometric analysis in both Chapter 2 and Chapter 3, but a difficulty arises when we consider the time transformation defined by equation (3.123): if the travel times are equal in one coordinate system, the dependence of the transformation on the Hamiltonian H and the shell position X makes it unlikely that the travel times will remain equal in another coordinate system. This difficulty therefore must also be overcome before any conclusive statements can be made about the coordinate

dependence of our interferometer.

So, though we have found indications that the interferometric coherence might be "observer-dependent," and speculated about the implications of the difficulties we encountered trying to obtain a concrete determination of the possible observer-dependence, we are ultimately forced to accept that the investigation of coordinate dependence in our interferometer is inconclusive (at least tentatively).

It is also possible that the only way to describe the coherence of a general relativistic interferometer in a coordinate-independent way is to in some way define the quantum evolution with respect to a physical clock that is embedded within the system. An initial realization of this idea was explored by Page and Wooters [79], and later extended by Gambini, Porto and Pullin [80], [18] by incorporating a generalization of the relational interpretation of quantum mechanics put forward by Rovelli [81], [82]. There have even been experimental proposals to test the validity of the relational interpretation of quantum evolution [83], though nothing concrete has yet been produced to this end. The main contention of these approaches is that one should formulate quantum time evolution using conditional probabilities, such that instead of determining the probability that an observable takes on a particular value at a coordinate time "t", one should determine the probability that an observable takes on a particular value, given the condition that the clock observable takes on a particular value. It is this *conditional* probability, in these proposals, that yields a physically meaningful description of the evolution of quantum predictions.

In Chapter 4, we explored the effects of adding such a "clock" degree of freedom to our shell system, in the form of an internal oscillator. Upon analysis of the combined system, we obtained a clear picture of some direct consequences of forming superpositions of geometries, though rather than attempting to formulate the evolution using conditional probabilities (which it is not clear we should necessarily do), we applied the same quantization techniques used in the previous chapters. We first showed that time dilation induces an effective coupling between the external variables (that describe the shell's motion) and the internal (clock) variables, and identified a regime where the reduced Hamiltonian of our system has the same form as the Hamiltonian used in a recent proposal of a "universal" decoherence mechanism due to gravitational time dilation [12]. For the situation where only the external variables are observed, one can follow the calculation presented in [12], and trace out the clock variables. This leads to an interesting form of intrinsic decoherence called "third-party" decoherence [15], which we showed in Section 4.5 in the (gravity-free) limit of flat spacetime.

Since the proposed time dilation decoherence effect was present even in the flat spacetime limit of our system, we concluded that the effect was not necessarily related to gravity. Though the specific application of the effect mentioned in [12] was gravitational, with the role of the "third-party" played by the earth, the effect relies only on proper time differences. Our shell system generally has tangential pressure that produces acceleration, and this alone leads to time dilation decoherence, even without gravity.

As a variation on this theme of time dilation decoherence, we then considered what happens when one takes into account the gravitational self-interaction of the shell. We found that the same calculation, with suitably generalized components, provided us with a demonstration that the time dilation decoherence still remains present when there is no tangential pressure whatsoever (or any other interactions), by virtue of the quantum consequences of self-gravitation. We interpreted this example of "third-party decoherence without the third party" to be a manifestly gravitational effect.

One can then connect this gravitational "self-decoherence" to the ideas brought up by Penrose: conceptually, tracing out the clock variables effectively averages the contribution of the internal oscillation to the ADM mass of the spacetime (as indicated by the appearance of $\bar{E}_q$ in equation 4.48), while producing a nonunitary contribution to the (external) evolution of the reduced density matrix that is proportional to the square of the clock energy uncertainty. Thus, the reduced dynamics associated with the external degree of freedom experiences an averaged geometry due to our ignorance of the internal evolution, and also decoheres due to the resulting uncertainty in the spacetime geometry. In this way, we see that the fundamentally gravitational form of intrinsic decoherence we demonstrated captures the spirit of Penrose's ideas, though it requires the additional structure of a local clock to do so.

Bibliography

[1] C. Gooding and W. G. Unruh, "Self-gravitating interferometry and intrinsic decoherence," Phys. Rev. D **90**, 044071 (2014).

[2] S. W. Hawking, "Particle Creation by Black Holes," Comm. Math. Phys. **43** 199 (1975).

[3] J. M. Bardeen, B. Carter, and S. W. Hawking, "The Four Laws of Black Hole Mechanics," Comm. Math. Phys. **31** 161 (1973).

[4] J. D. Bekenstein, "Black Holes and Entropy," Phys. Rev. D. **7** 2333 (1973).

[5] T. Jacobson, "Thermodynamics of Spacetime: The Einstein Equation of State," Phys. Rev. Lett. **75** 1260 (1995).

[6] I. Ruo Berchera, I. P. Degiovanni, S. Olivares, M. Genovese, "Quantum Light in Coupled Interferometers for Quantum Gravity Tests," Phys. Rev. Lett. **110**, 213601 (2013).

[7] I. Pikovski, M. R. Vanner, M. Aspelmeyer, M. S. Kim, and C. Brukner, "Probing Planck-scale physics with quantum optics," Nature Phot. **8**, 393 (2012).

[8] B. Lamine, R. Hervé, A. Lambrecht, and S. Reynaud, "Ultimate Decoherence Border for Matter-Wave Interferometry," Phys. Rev. Lett. **96**, 050405 (2006).

[9] R. Penrose, "Gravity and state vector reduction," In "Quantum Concepts in Space and Time," Penrose & Isham (eds.), Oxford: Clarenden, Oxford Science Publications, 129 (1986).

[10] R. Penrose, "On gravity's role in quantum state reduction," Gen. Rel. Grav. **28**, 581 (1996).

[11] K. Banaszek, P. Horodecki, M. Karpiński, and C. Radzewicz, "Quantum mechanical which-way experiment with an internal degree of freedom," Nature Comm. **4**, 2594 (2013).

[12] I. Pikovski, M. Zych, F. Costa, and Č. Brukner, "Universal decoherence due to gravitational time dilation," [arXiv:quant-ph/1311.1095] (2013).

[13] M. Zych, F. Costa, I. Pikovski, and Č. Brukner, "Quantum interferometric visibility as a witness of general relativistic proper time," Nat. Commun. **2**, 505 (2011). [arXiv:quant-ph/1105.4531v2]

[14] M. Zych, F. Costa, I. Pikovski, T.C. Ralph and Č. Brukner, "General relativistic effects in quantum interference of photons," Class. Quantum Grav. **29**, 224010 (2012). [arXiv:quant-ph/1206.0965v2]

[15] P. C. E. Stamp, "The decoherence puzzle," Stud. in Hist. and Phil. of Mod. Phys. **37**, 467 (2006).

[16] L. Diosi, "Intrinsic time-uncertainties and decoherence: comparison of 4 models," Braz. J. Phys. **35**, 260 (2005). [arXiv:quant-ph/0412154v2]

[17] C. Anastopoulos and B. L. Hu, "Intrinsic and Fundamental Decoherence: Issues and Problems," Class. Quant. Grav. **25**, 154003 (2008).

[18] R. Gambini, R. A. Porto, and J. Pullin, "Fundamental decoherence from quantum gravity: a pedagogical review," Gen. Rel. Grav. **39**, 1143 (2007).

[19] G. J. Milburn, "Intrinsic decoherence in quantum mechanics," Phys. Rev. A **44**, 5401 (1991).

[20] G. J. Milburn, "Lorentz invariant intrinsic decoherence," New J. Phys. **8**, 96 (2006).

[21] I. C. Percival, "Quantum spacetime fluctuations and primary state diffusion," Proc. R. Soc. Lond. A **451**, 503 (1995).

[22] S. Weinberg, "Precision tests of quantum mechanics," Phys. Rev. Lett. **62**, 485 (1989).

[23] S. Weinberg, "Testing quantum mechanics," Ann. Phys. **194**, 336 (1989).

[24] I. M. Moroz, R. Penrose, and P. Tod, "Spherically-symmetric solutions of the Schrödinger-Newton equations," Class. Quant. Grav. **15**, 2733 (1998).

[25] J. Polchinski, "Weinberg's Nonlinear Quantum Mechanics and the Einstein-Podolsky-Rosen Paradox," Phys. Rev. Lett. **66**, 397 (1991).

[26] P. C. E. Stamp, "Environmental decoherence versus intrinsic decoherence," Phil. Trans. R. Soc. A **370**, 4429 (2012).

[27] C. H-T. Wang, R. Bingham, and J. T. Mendonça, "Quantum gravitational decoherence of matter waves," Class. Quantum Grav. **23**, L59-L65 (2006).

[28] B. L. Hu, "Gravitational Decoherence, Alternative Quantum Theories, and Semiclassical Gravity," To appear in J. Phys. (Conf. Ser.). [arXiv:gr-qc/1402.6584v1] (2014).

[29] B. S. DeWitt, "Quantum Theory of Gravity. I. The Canonical Theory," Phys. Rev. **160**, 1113 (1967).

[30] M. Visser, "Quantum wormholes," Phys. Rev. D **43**, 402 (1991).

[31] K. Kuchǎr, "Canonical Quantization of Cylindrical Gravitational Waves," Phys. Rev. D **4**, 955 (1971).

[32] S. W. Hawking, "Quantum gravity and path integrals," Phys. Rev. D **18**, 6 (1978).

[33] J. J. Halliwell, "Derivation of the Wheeler-DeWitt equation from a path integral for minisuperspace models," Phys. Rev. D **38**, 2468 (1988).

[34] A. Stern, Y. Aharonov, and Y. Imry, "Phase uncertainty and loss of interference: A general picture," Phys. Rev. A **41**, 3436 (1990).

[35] B.-G. Englert, "Fringe visibility and which-way information: An inequality," Phys. Rev. Lett. **77**, 2154 (1996).

[36] T. Banks, L. Susskind, and M. E. Peskin, "Difficulties for the evolution of pure states into mixed states," Nucl. Phys. B **244**, 125 (1984).

[37] W. G. Unruh and R. M. Wald, "On Evolution Laws Taking Pure States to Mixed States in Quantum Field Theory," Phys. Rev. D**52**, 2176 (1995).

[38] P. C. E. Stamp, "Influence of Paramagnetic and Kondo Impurities on Macroscopic Quantum Tunneling in SQUID's," Phys. Rev. Lett. **61**, 2905 (1988).

[39] N. V. Prokof′ev and P. C. E. Stamp, "Theory of the spin bath," Rep. Prog. Phys. **63**, 669 (2000).

[40] W. G. Unruh, "Decoherence without dissipation," Phil. Trans. Roy. Soc. A **370**, 4454 (2012). [arXiv:quant-ph/1205.6750]

[41] K. Lochan, K. Parattu, and T. Padmanabhan, "Quantum Evolution Leading to Classicality: A Concrete Example," [arXiv:gr-qc/1404.2605v3] (2014).

[42] G. Gangopadhyay, M. S. Kumar, and S. Dattagupta, "On dissipationless decoherence," J. Phys. A: Math. Gen. **34**, 5485 (2001).

[43] C. Rovelli and M. Smerlak, "Unruh effect without trans-horizon entanglement," Phys. Rev. D **85**, 124055 (2012).

[44] P. Langlois, "Causal particle detectors and topology," Annals Phys. **321**, 2027 (2006). [arXiv:gr-qc/0510049]

[45] J. M. M. Senovilla, "Particle production from marginally trapped surfaces of general spacetimes," [arXiv:gr-qc/1409.6044v2] (2014).

[46] A. Raval, B. L. Hu, and D. Koks, "Near-thermal radiation in detectors, mirrors, and black holes: A stochastic approach," Phys. Rev. D **55**, 4795 (1997).

[47] A. Einstein, "On a Stationary System With Spherical Symmetry Consisting of Many Gravitating Masses," Ann. Math. **40**, 4, 922 (1939).

[48] B. K. Berger, D. M. Chitre, V. E. Moncrief, and Y. Nutjku, "Hamiltonian Formulation of Spherically Symmetric Gravitational Fields," Phys. Rev. D **5**, 2467 (1972).

[49] W. G. Unruh, "Notes on black-hole evaporation," Phys. Rev. D **14**, 870 (1976).

[50] P. Kraus and F. Wilczek, "Self-Interaction Correction to Black Hole Radiance," Nucl. Phys. B **433**, 403 (1995). [arXiv:gr-qc/9408003v1]

[51] P. Kraus and F. Wilczek, "Some Applications of a Simple Stationary Line Element for the Schwarzschild Geometry," Mod. Phys. Lett. A **9**, 3713 (1994). [arXiv:gr-qc/9406042v2]

[52] P. Kraus and F. Wilczek, "Effect of Self-Interaction on Charged Black Hole Radiance," Nucl. Phys. B **437**, 231 (1995). [arXiv:hep-th/9411219v1]

[53] W. Israel, "Singular Hypersurfaces and Thin Shells in General Relativity," Nuovo Cimento B **44**, 1 (1966).

[54] R. L. Arnowitt, S. Deser, and C. W. Misner, "Canonical Variables for General Relativity," Phys. Rev. **117**, 1595 (1960). [arXiv:gr-qc/0405109]

[55] B. F. Schutz, Jr., "Perfect Fluids in General Relativity: Velocity Potentials and a Variational Principle," Phys. Rev. D **2**, 2762 (1970).

[56] J. Crisostomo and R. Olea, "Hamiltonian Treatment of the Gravitational Collapse of Thin Shells," Phys. Rev. D **69**, 104023 (2004). [arXiv:hep-th/0311054v2]

[57] J. L. Friedman, J. Louko, and S. N. Winters-Hilt, "Reduced phase space formalism for spherically symmetric geometry with a massive dust shell," Phys. Rev. D **56**, 7674 (1997).

[58] F. Fiamberti and P. Menotti, "Reduced Hamiltonian for intersecting shells," Nucl. Phys. B **794**, 512 (2008). [arXiv:hep-th/0708.2868v1]

[59] T. Regge and C. Teitelboim, "Role of surface integrals in the Hamiltonian formulation of general relativity," Ann. Phys. **88**, 286 (1974).

[60] W. G. Unruh and R. M. Wald, "Time and the interpretation of canonical quantum gravity," Phys. Rev. D **40**, 2598 (1989).

[61] S. W. Hawking, "The unpredictability of Quantum Gravity," Comm. Math. Phys. **87**, 395 (1982).

[62] J. Ellis, S. Mohanty, and D. V. Nanopoulos, "Quantum gravity and the collapse of the wavefunction," Phys. Lett. B **221** 2, 113 (1989).

[63] J. Sucher, "Relativistic Invariance and the Square-Root Klein-Gordon Equation," J. Math. Phys. **4**, 1 (1962).

[64] C. Lämmerzahl, "The pseudodifferential operator square root of the Klein-Gordon equation," J. Math. Phys. **34**, 9 (1993).

[65] P. Garbaczewski and V. Stephanovich, "Lévy flights and nonlocal quantum dynamics," J. Math. Phys. **54**, 072103 (2013).

[66] P. Garbaczewski and M. Żaba, "Nonlocally-induced (quasirelativistic) bound states: Harmonic confinement and the finite well," [arXiv:quant-ph/1405.4724] (2014).

[67] P. Hjek and J. Kijowski, "Spherically symmetric dust shell and the time problem in canonical relativity," Phys. Rev. D **62**, 044025 (2000).

[68] K. Martel and E. Poisson, "Regular coordinate systems for Schwarzschild and other spherical spacetimes," Am. J. Phys. **69**, 476 (2001). [arXiv:gr-qc/0001069v4]

[69] R. Penrose, "Gravitational Collapse and Space-Time Singularities," Phys. Rev. Lett. **14**, 57 (1965).

[70] P. Malkiewicz, "Multiple choices of time in quantum cosmology," [arXiv:gr-qc/1407.3457] (2014).

[71] D. Walls and G. Milburn, "Quantum Optics," Springer-Verlag, Berlin (1994).

[72] A. Brodutch, A. Gilchrist, T. Guff, A. R. H. Smith, and D. Terno, "Post-Newtonian gravitational effects in quantum interferometry," [arXiv:quant-ph/1412.2440v1] (2014).

[73] R. Colella, A. W. Overhauser, and S. A. Werner, "Observation of Gravitationally Induced Quantum Interference," Phys. Rev. Lett. **34** 23 (1975).

[74] D. M. Greenberger and A. W. Overhauser, "Coherence effects in neutron diffraction and gravity experiments," Rev. Mod. Phys. **51** 43 (1979).

[75] J. L. Staudenmann, S. A. Werner, R. Colella, and A. W. Overhauser, "Gravity and inertia in quantum mechanics," Phys. Rev. A **21** 5 (1980).

[76] W. Marshall, C. Simon, R. Penrose, and D. Bouwmeester, "Towards quantum superpositions of a mirror," Phys. Rev. Lett. **91**, 130401 (2003).

[77] D. Kleckner, I. Pikovski, E. Jeffrey, L. Ament, E. Elie, J. van den Brink, and D. Bouwmeester, "Creating and verifying a quantum superposition in a micro-optomechanical system," New J. Phys. **10**, 095020 (2008).

[78] R. Penrose, "On the Gravitization of Quantum Mechanics 1: Quantum State Reduction," Found. Phys. **44**, 557 (2014).

[79] D. N. Page and W. K. Wootters, "Evolution without evolution: Dynamics described by stationary observables," Phys. Rev. D **27**, 2885 (1983).

[80] R. Gambini, R. A. Porto, J. Pullin, and S. Torterolo, "Conditional probabilities with Dirac observables and the problem of time in quantum gravity," Phys. Rev. D **79** 041501 (R) (2009).

[81] C. Rovelli, "Time in quantum gravity: An hypothesis," Phys. Rev. D **43**, 442 (1991).

[82] C. Rovelli, "Relational Quantum Mechanics," Int. J. of Theor. Phys. **35**, 1637 (1996).

[83] E. Moreva, G. Brida, M. Gramegna, V. Giovannetti, L. Maccone, and M. Genovese, "Time from quantum entanglement: an experimental illustration," Phys. Rev. A **89**, 052122 (2014).

[84] W. K. Wootters and W. H. Zurek, "Complementarity in the double-slit experiment: Quantum nonseparability and a quantitative statement of Bohr's principle," Phys. Rev. D **19** 2 (1979).

[85] L. Li, N. Liu, and S. Yu, "Duality relations in a two-path interferometer with an asymmetric beam splitter," [arXiv:quant-ph/1202.3326v1] (2012).

[86] T. Baumgratz, M. Cramer, and M. B. Plenio, "Quantifying Coherence," Phys. Rev. Lett. **113** 140401 (2014).

[87] S. Wehner and A. Winter, "Entropic uncertainty relations - A survey," New J. Phys. **12**, 025009 (2010).

[88] P. J. Coles, J. Kaniewski, and S. Wehner, "Equivalence of wave-particle duality to entropic uncertainty," Nature Comm. **5** 5814 (2014).

[89] These words were written by Fermat in his copy of the ancient text Arithmetica by Diophantus, in reference to what is now known as "Fermat's Last Theorem."

Appendix A

Probability Current Conservation

A.1 Standard Nonrelativistic Quantum Mechanics

Throughout this thesis, we make use of the concept of a *probability current*. In nonrelativistic quantum mechanics, the probability current takes the form

$$J(x,t) = \frac{1}{2im} \left[\psi^* \psi' - \psi \left(\psi^* \right)' \right],\tag{A.1}$$

where the prime indicates differentiation with respect to x (we'll restrict our attention to one dimension, for simplicity). In Dirac notation, this can also be expressed as

$$J(x) = \frac{1}{2im} \left[\langle \psi | x \rangle \langle x | \hat{p} | \psi \rangle + \langle x | \psi \rangle \left(\langle x | \hat{p}^\dagger | \psi \rangle \right)^* \right],\tag{A.2}$$

from which we can deduce, provided the momentum operator $\hat{p}$ is Hermitian [8], that the current $J(x)$ is the expectation value of a simple operator:

$$J(x,t) = \langle \psi | \hat{J}(x) | \psi \rangle,\tag{A.3}$$

for the operator

$$\hat{J}(x) = \frac{1}{2m} \left(|x\rangle\langle x|\hat{p} + \hat{p}^\dagger |x\rangle\langle x| \right).\tag{A.4}$$

Note that in these expressions, a hat denotes an operator, in contrast with the majority of this thesis, in which a hat indicates that a quantity is evaluated along the shell trajectory.

---

[8]Note that in this appendix, we are denoting the momentum operator by $\hat{p}$, which corresponds to the classical momentum p. This should not be confused with our use of p in other parts of the thesis to denote pressure.

The utility of the probability current (A.1) comes from the fact that it satisfies the continuity equation,

$$\frac{\partial \rho(x,t)}{\partial t} + \frac{\partial J(x,t)}{\partial x} = 0, \tag{A.5}$$

with $\rho(x,t) = |\psi|^2$ being the probability density. This can be established straightforwardly using the standard nonrelativistic Schrödinger equation,

$$i\frac{\partial}{\partial t}|\psi\rangle = \hat{H}|\psi\rangle = \left(\frac{\hat{p}^2}{2m} + \hat{V}\right)|\psi\rangle, \tag{A.6}$$

and its dual-space counterpart

$$-i\frac{\partial}{\partial t}\langle\psi| = \langle\psi|\hat{H}^\dagger, \tag{A.7}$$

where $\hat{H}$ is the Hamiltonian operator and $\hat{V}$ is the potential energy operator. Taking the time derivative of the probability density yields

$$
\begin{aligned}
\frac{\partial}{\partial t}|\psi|^2 &= \frac{\partial \psi^*}{\partial t}\psi + \psi^*\frac{\partial \psi}{\partial t} \\
&= i\langle\psi|\hat{H}^\dagger|x\rangle\langle x|\psi\rangle - i\langle\psi|x\rangle\langle x|\hat{H}|\psi\rangle \\
&= i\left(\frac{1}{2m}\langle\psi|(\hat{p}^\dagger)^2|x\rangle + \langle\psi|\hat{V}^\dagger|x\rangle\right)\langle x|\psi\rangle \\
&\quad -i\langle\psi|x\rangle\left(\frac{1}{2m}\langle x|\hat{p}^2|\psi\rangle + \langle x|\hat{V}|\psi\rangle\right) \\
&= i\left(\frac{-1}{2m}(\psi^*)'' + \psi^* V(x)\right)\psi - i\psi^*\left(\frac{-1}{2m}\psi'' + V(x)\psi\right) \\
&= i\frac{1}{2m}\left[\psi^*\psi'' - (\psi^*)''\psi\right] \\
&= -\frac{\partial}{\partial x}\left(\frac{1}{2im}\left[\psi^*\psi' - \psi(\psi^*)'\right]\right), \tag{A.8}
\end{aligned}
$$

which demonstrates that the probability current defined by (A.1) indeed solves the continuity equation (A.5).

It will also be useful to consider an analogy between an approximate general relativistic probability current (derived in the next section) and the probability current for a (nonrelativistic) charged scalar particle in $(3+1)$ dimensional flat spacetime. Suppose we have this charged scalar particle in an electromagnetic field defined by a vector potential $\mathbf{A}(\mathbf{r},t)$ and a scalar potential $\phi(\mathbf{r},t)$. In this case the effect of the potentials on our particle

Hamiltonian is to replace the momentum $\mathbf{p}$ by the *kinetic* momentum $\mathbf{P} = \mathbf{p} - q\mathbf{A}(\mathbf{r}, t)$, with q being the particle charge. The total Hamiltonian is then given by

$$\hat{H} = \frac{1}{2m} \left(\hat{\mathbf{p}} - q\hat{\mathbf{A}} \right)^2 + q\hat{\phi} = \frac{\hat{\mathbf{P}}^2}{2m} + q\hat{\phi}, \tag{A.9}$$

and a calculation analogous to (A.8) proceeds as

$$
\begin{aligned}
\frac{\partial}{\partial t} |\psi|^2 &= \frac{\partial \psi^*}{\partial t} \psi + \psi^* \frac{\partial \psi}{\partial t} \\
&= i\langle\psi|\hat{H}^\dagger|\mathbf{r}\rangle\langle\mathbf{r}|\psi\rangle - i\langle\psi|\mathbf{r}\rangle\langle\mathbf{r}|\hat{H}|\psi\rangle \\
&= i\left(\frac{1}{2m}\langle\psi|(\hat{\mathbf{P}}^2)^\dagger|\mathbf{r}\rangle + q\langle\psi|\hat{\phi}^\dagger|\mathbf{r}\rangle \right)\langle\mathbf{r}|\psi\rangle \\
&\quad - i\langle\psi|\mathbf{r}\rangle\left(\frac{1}{2m}\langle\mathbf{r}|\hat{\mathbf{P}}^2|\psi\rangle + q\langle\mathbf{r}|\hat{\phi}|\psi\rangle \right) \\
&= \frac{1}{2im}\left(\psi^*\langle\mathbf{r}|\hat{\mathbf{P}}^2|\psi\rangle - \langle\psi|(\hat{\mathbf{P}}^2)^\dagger|\mathbf{r}\rangle\psi \right).
\end{aligned} \tag{A.10}
$$

In the coordinate basis, we can represent the operator $\hat{\mathbf{P}}$ by $-i(\nabla - iq\mathbf{A})$, and the calculation continues as

$$
\begin{aligned}
\frac{\partial}{\partial t} |\psi|^2 &= -\frac{1}{2im}\left(\psi^*\left[(\nabla - iq\mathbf{A})^2 \psi \right] - \left[(\nabla + iq\mathbf{A}^*)^2 \psi^* \right]\psi \right) \\
&= -\nabla \cdot \left(\frac{1}{2im}\left[\psi^*\nabla\psi - \psi\nabla(\psi^*) \right] \right) \\
&\quad + \frac{q}{2m}\psi^*\left[\nabla \cdot (\mathbf{A}\psi) + \mathbf{A} \cdot \nabla\psi \right] \\
&\quad + \frac{q}{2m}\left[\nabla \cdot (\mathbf{A}^*\psi^*) + \mathbf{A}^* \cdot \nabla\psi^* \right]\psi.
\end{aligned} \tag{A.11}
$$

At this point it is common to simplify the expressions by working in a particular gauge. We will be most interested in the Coulomb gauge, $\nabla \cdot \mathbf{A} = 0$, which for real $\mathbf{A}$ leads to

$$
\begin{aligned}
\frac{\partial}{\partial t} |\psi|^2 &= -\nabla \cdot \left(\frac{1}{2im}\left[\psi^*\nabla\psi - \psi\nabla(\psi^*) \right] \right) \\
&\quad + \frac{q}{m}\left(\psi^*\mathbf{A} \cdot \nabla\psi + \psi\mathbf{A} \cdot \nabla\psi^* \right) \\
&= -\nabla \cdot \left[\mathbf{J}_s - \frac{q}{m}\mathbf{A}|\psi|^2 \right],
\end{aligned} \tag{A.12}
$$

where we have denoted the standard (3+1)-dimensional nonrelativistic probability current by

$$\mathbf{J}_s = \frac{1}{2im}\left[\psi^*\nabla\psi - \psi\nabla(\psi^*) \right]. \tag{A.13}$$

The total probability current operator is therefore given by

$$
\begin{aligned}
\hat{\mathbf{J}}(\mathbf{r}) &= \frac{1}{2m}\left(|\mathbf{r}\rangle\langle\mathbf{r}|\hat{\mathbf{p}} + \hat{\mathbf{p}}^\dagger|\mathbf{r}\rangle\langle\mathbf{r}|\right) - \frac{q}{m}|\mathbf{r}\rangle\hat{\mathbf{A}}\langle\mathbf{r}| \\
&= \frac{1}{2m}\left(|\mathbf{r}\rangle\langle\mathbf{r}|\hat{\mathbf{P}} + \hat{\mathbf{P}}^\dagger|\mathbf{r}\rangle\langle\mathbf{r}|\right),
\end{aligned}
\tag{A.14}
$$

and the associated continuity equation takes the form

$$
\frac{\partial\rho(\mathbf{r},t)}{\partial t} + \nabla\cdot\mathbf{J}(\mathbf{r},t) = 0.
\tag{A.15}
$$

A.2 General Systems Quadratic in Momenta

Now suppose our system is effectively $(1+1)$-dimensional, and has a Hamiltonian given by

$$
H = H_0(x) + H_1(x)p + H_2(x)p^2,
\tag{A.16}
$$

where $\{H_i(x)\}$ are (for now) arbitrary functions of x. We will order the operators in the quantum Hamiltonian as in Section 2.3.2, in an attempt to enforce Hermiticity. For this Hamiltonian, calculation of the time derivative of the probability density becomes

$$
\begin{aligned}
\frac{\partial}{\partial t}|\psi|^2 &= i\langle\psi|\hat{H}^\dagger|x\rangle\langle x|\psi\rangle - i\langle\psi|x\rangle\langle x|\hat{H}|\psi\rangle \\
&= i\langle\psi|[(1/2)(\hat{H}_1\hat{p} + \hat{p}\hat{H}_1) + \hat{p}\hat{H}_2\hat{p}]^\dagger|x\rangle\psi \\
&\quad -i\psi^*\langle x|[(1/2)(\hat{H}_1\hat{p} + \hat{p}\hat{H}_1) + \hat{p}\hat{H}_2\hat{p}]|\psi\rangle \\
&= i\psi\left[\frac{i}{2}\frac{\partial}{\partial x}(H_1\psi^*) + \frac{i}{2}H_1\frac{\partial\psi^*}{\partial x} - \frac{\partial}{\partial x}\left(H_2\frac{\partial\psi^*}{\partial x}\right)\right] \\
&\quad -i\psi^*\left[-\frac{i}{2}H_1\frac{\partial\psi}{\partial x} - \frac{i}{2}\frac{\partial}{\partial x}(H_1\psi) - \frac{\partial}{\partial x}\left(H_2\frac{\partial\psi}{\partial x}\right)\right] \\
&= -\frac{\partial}{\partial x}\left(H_1|\psi|^2\right) - \frac{\partial}{\partial x}\left(\frac{1}{i}H_2\left[\psi^*\psi' - \psi(\psi^*)'\right]\right).
\end{aligned}
\tag{A.17}
$$

Thus, our system possesses a probability current of the same form as (A.12), given by

$$
J(x,t) = H_1|\psi|^2 + \frac{1}{i}H_2\left[\psi^*\psi' - \psi(\psi^*)'\right],
\tag{A.18}
$$

from which we can deduce the probability current operator

$$
\hat{J}(x) = |x\rangle\hat{H}_1\langle x| + \hat{H}_2|x\rangle\langle x|\hat{p} + \hat{p}^\dagger|x\rangle\langle x|\hat{H}_2.
\tag{A.19}
$$

We can gain a different perspective on the result (A.19) by considering the Hamiltonian (A.16) to be the second-order truncation of a Taylor series expansion of a general Hamiltonian in powers of p (provided such a thing exists for a given Hamiltonian). Indeed, this is the context in which (A.16) is used in this thesis. The coefficient functions that multiply powers of p can then be interpreted as

$$H_0(x) = H|_{p=0}, \quad H_1(x) = \left(\frac{\partial H}{\partial p} \right) \bigg|_{p=0}, \quad H_2(x) = \frac{1}{2} \left(\frac{\partial^2 H}{\partial p^2} \right) \bigg|_{p=0}. \quad \text{(A.20)}$$

This enables us to express the probability current as

$$J(x,t) = \psi^* \left(\frac{\partial H}{\partial p} \right)_0 \psi + \frac{1}{2} \psi^* \left(\frac{\partial^2 H}{\partial p^2} \right)_0 (\hat{p}\psi) + \frac{1}{2} (\hat{p}\psi)^* \left(\frac{\partial^2 H}{\partial p^2} \right)_0 \psi, \quad \text{(A.21)}$$

where the subscript 0 indicates an evaluation at $p = 0$, and it is understood that the action of the operator $\hat{p}$ on the coordinate-space wavefunction ψ is given by $\hat{p}\psi = -i\partial\psi/\partial x$. Since the general p-derivative of the truncated Hamiltonian (A.16) is

$$\left(\frac{\partial H}{\partial p} \right) = \left(\frac{\partial H}{\partial p} \right) \bigg|_{p=0} + \left(\frac{\partial^2 H}{\partial p^2} \right) \bigg|_{p=0} p, \quad \text{(A.22)}$$

we can re-express the probability current operator (A.19) as

$$\hat{J}(x) = |x\rangle \left(\widehat{\frac{\partial H}{\partial p}} \right) \langle x|, \quad \text{(A.23)}$$

as long as we make sure to symmetrize the term linear in momentum, to maintain consistency with (A.21). Keeping in mind Hamilton's equation for the time evolution of x (i.e. $dx/dt = \partial H/\partial p$), we arrive at an intuitive expression for the probability current operator:

$$\hat{J}(x) = |x\rangle \hat{v} \langle x|, \quad \text{(A.24)}$$

with $\hat{v}$ being an operator version of the velocity $v = dx/dt$. Taking the expectation value yields the corresponding probability current,

$$J(x,t) = \psi^* \hat{v} \psi, \quad \text{(A.25)}$$

with the action of the operator $\hat{v}$ understood to be in the coordinate basis. This has the same form as the current for a charged scalar particle (A.14), since the kinetic momentum is connected to the particle velocity via $\mathbf{P} = m\mathbf{v}$.

Appendix B

Multi-mode Interferometry

B.1 General Relativistic Wave-packets

Here we consider the properties of our self-gravitating interferometer with multi-mode input states, to explore whether or not having a superposition of ADM masses could affect the conclusions of the single-mode analysis. We will form localized wave-packets as initial states by taking a Gaussian distribution of energies as weighting factors of the previously introduced ingoing WKB modes. We emphasize that since we are superposing WKB modes with different energies, we are actually superposing states that correspond to spacetime geometries with different ADM masses (recall that the classical value of our Hamiltonian was found to be equal to the ADM mass of the associated geometry). We are not, then, merely doing quantum mechanics on a fixed curved spacetime; even in the single-mode analysis we were working with a superposition of geometries, because each path through the interferometer (classically) defined a different geometry. For single-mode input states, however, the corresponding spacetimes had the same ADM mass, and therefore beyond the outer reflector of the interferometer the spacetimes we superposed were equivalent. With multi-mode input states, this will no longer be the case. The purpose of this appendix is to identify possible ways that evidence of intrinsic gravitational decoherence could manifest itself in the behaviour of the multi-mode system.

Suppose that our wave-packets are much narrower than the interferometer arm lengths - this allows us to treat each element of the interferometer separately, mode by mode, as we did in the single-mode analysis. The initial wave-packet will first encounter the splitter, at which point each mode in the wave-packet will transform into a reflected mode with a factor $R_{\leftarrow}$ and a transmitted mode with a factor $T_{\leftarrow}$. We remind the reader that subscripts are used here because the reflection/transmission coefficients depend on the direction each mode of the wave-packet encounters the splitter from.

The split wave-packets will then perfectly reflect off of the outer/inner reflectors, and travel back towards one another at the beam-splitter. Upon recombination there will be splitting of each set of modes coming from each

direction of the splitter, which produces two outputs (one going in each direction from the splitter) that are themselves composed of two parts.

It is clear that we will not observe interference in the multi-mode interferometer unless the wave-packets travelling on each of the interferometer arms reach the splitter for recombination at approximately the same time; there must be sufficient overlap of the parts of the output states associated with the two paths through the interferometer in order for cancellation of either of the final outputs to be possible. There is some parameter freedom left in this system, so let us attempt to make use of this freedom to make the (classical) travel times along the interferometer arms be the same. From equation (2.56), we find that the time can be found as a function of H and X:

$$
\begin{aligned}
t &= \int dX \left(\frac{dt}{dX} \right) = \int dX \left(\dot{X}^{-1} \right) \\
&= \int dX \left(\frac{\sqrt{\frac{2H}{X}}}{f} \pm \frac{h}{f \sqrt{h^2 - \hat{M}^2 f}} \right),
\end{aligned}
\tag{B.1}
$$

with $h = H - \hat{M}^2/2X$ and $f = 1 - 2H/X$. The first term is independent of whether the shell is outgoing or ingoing, and can be integrated exactly as

$$
\begin{aligned}
\int dX \, \frac{\sqrt{\frac{2H}{X}}}{f} &= 4H \left(\sqrt{\frac{X}{2H}} - \operatorname{arctanh} \sqrt{\frac{X}{2H}} \right) \\
&= 4H \left(\sqrt{\frac{X}{2H}} - \frac{1}{2} \ln \left| \frac{1 + \sqrt{\frac{X}{2H}}}{1 - \sqrt{\frac{X}{2H}}} \right| \right).
\end{aligned}
\tag{B.2}
$$

Let us denote the term (B.2) by t_0. The second term in (B.1), which gives a contribution that we will denote by $t_\pm$, depends both on whether the shell is outgoing or ingoing as well as on the mass function $\hat{M}$. For weak-field regions of constant $\hat{M}$, we can expand the integrand in inverse powers of $\sqrt{X}$ and integrate term-by-term to obtain the asymptotic contribution

$$
\begin{aligned}
t_\pm \sim \pm \frac{1}{\sqrt{H^2 - \hat{M}^2}} \Bigg(HX + \frac{\left(4H^4 + \hat{M}^4 - 6\hat{M}^2 H^2 \right)}{2 \left(H^2 - \hat{M}^2 \right)} \ln \left(\frac{X}{2H} \right) \\
+ \frac{H \left(9\hat{M}^6 - 60H^2\hat{M}^4 + 80H^2\hat{M}^4 - 32H^6 \right)}{8X \left(H^2 - \hat{M}^2 \right)^2} \Bigg).
\end{aligned}
\tag{B.3}
$$

The total travel time for the path through the interferometer that initially reflects from the beam-splitter is given by $t_{++} + t_{-+}$, and the time for the path that initially transmits is $t_{--} + t_{+-}$. We then have

$$
\begin{aligned}
t_{++} + t_{-+} &= t_+(X_+) - t_+(X_{\delta+}) + t_-(X_{\delta+}) - t_-(X_+) \\
&= 2t_+(X_+) - 2t_+(X_{\delta+}),
\end{aligned}
\tag{B.4}
$$

as well as

$$
\begin{aligned}
t_{--} + t_{+-} &= t_-(X_-) - t_-(X_{\delta-}) + t_+(X_{\delta-}) - t_+(X_-) \\
&= 2t_+(X_-) - 2t_+(X_{\delta-}),
\end{aligned}
\tag{B.5}
$$

with $X_{\delta\pm} = \lim_{\epsilon \to 0} (X_\delta \pm \epsilon)$. The difference in travel times can then be expressed as

$$
\begin{aligned}
\Delta t &= \frac{1}{2} \left((t_{++} + t_{-+}) - (t_{--} + t_{+-}) \right) \\
&= t_+(X_+) - t_+(X_{\delta+}) - t_+(X_-) + t_+(X_{\delta-}).
\end{aligned}
\tag{B.6}
$$

In the flat spacetime, nonrelativistic limit, we have

$$
\dot{X}_{\pm\tilde{\pm}} = \frac{P_{\pm\tilde{\pm}}}{M_{\tilde{\pm}}} = \pm \frac{\sqrt{2M_{\tilde{\pm}} \left(E - M_{\tilde{\pm}} \right)}}{M_{\tilde{\pm}}},
\tag{B.7}
$$

and so equating the travel times ($\Delta t = 0$) gives us the following condition for the lengths of the interferometer arms:

$$
L_+ \sqrt{\frac{M_+}{E - M_+}} = L_- \sqrt{\frac{M_-}{E - M_-}}.
\tag{B.8}
$$

Here, the interferometer arm lengths are defined such that $L_\pm \equiv \pm(X_\pm - X_\delta)$, and the use of $\pm$ and $\tilde{\pm}$ above is to remind us that the signs can be chosen independently.

The arm length condition (B.8) (or its relativistic generalization) can be applied for a single mode, but for a wave-packet all we can do is apply the condition for the peak energy (or expectation value, perhaps), and try to keep the energy variance small enough that the deviations from equal travel times for different energy modes will be negligible. We also want to keep the energy variance small so that the travel time will be less than the coherence time for the wave-packet, to make sure that dispersion will not significantly affect the interference pattern.

B.2 Localize, Normalize, Propagate

We imagine an initial state for the shell to be a superposition of ingoing WKB modes, with a Gaussian distribution in energy:

$$\Psi_0 = N \int dE \, e^{i\tilde{X}(E-E_0)} e^{\frac{-(E-E_0)^2}{4\sigma_E^2}} \psi_{-+}. \tag{B.9}$$

Here the parameter $\tilde{X}$ has been used to control the peak location in X-space.

Before propagating the initial state through the interferometer, we should determine the relationship between the peak location parameter $\tilde{X}$ and the true peak location in X-space. Since the relevant mode function is given by

$$\psi_{-+} = (E_{,-+})^{-1/2} \, e^{i \int dX \, P_{-+}}, \tag{B.10}$$

the integral in (B.9) is no longer just a Gaussian. However, if we suppose that the Gaussian prefactor to the mode function varies on a broader energy scale than the mode function itself, we can approximate the integral by evaluating the square root term at the peak energy E_0 and expanding the WKB phase to linear order in $(E - E_0)$. The resulting Gaussian can be easily integrated, and in flat spacetime one obtains

$$\Psi_0 = 2\sigma_E \sqrt{\frac{\pi M_+}{P_+}} \tilde{N} e^{-\frac{(X-X_0)^2}{4\sigma_X^2}}, \tag{B.11}$$

with X-variance σ_X^2 and peak location X_0 given by

$$\sigma_X^2 = \sqrt{\frac{2(E_0 - M_+)}{M_+}} \frac{1}{4\sigma_E^2}, \tag{B.12}$$

$$X_0 = \sqrt{\frac{2(E_0 - M_+)}{M_+}} \tilde{X} - \frac{i(E_0 - M_+)}{\sigma_E^2}. \tag{B.13}$$

Note that the "physical" peak location in X-space is given by the real part of X_0, and we have absorbed irrelevant factors into $\tilde{N}$ coming from constants of integration. If we normalize the state such that $\langle \Psi_0 | \Psi_0 \rangle = 1$, the factor $\tilde{N}$ is found to be given by

$$\left| \tilde{N} \right|^{-2} = \sqrt{2\pi} \sigma_X e^{\frac{\sqrt{2M_+}(E_0 - M_+)^{3/2}}{\sigma_E^2}}. \tag{B.14}$$

The general relativistic initial state can be similarly analyzed. It simplifies matters to further approximate the WKB phase by expanding in inverse

powers of $\sqrt{X}$. Performing the X-integration term by term then leads to terms that diverge as $X \to \infty$, so at this point we can safely neglect inverse powers of $\sqrt{X}$ when we evaluate the Gaussian energy integral. The fully integrated initial state then has an exponential with a bi-quadratic structure in $\sqrt{X}$,[9] so we can complete the square to obtain the peak location

$$\tilde{X}_0 \sim \frac{2\left(E_0^2 - M_+^2\right)}{E_0} \left(1 + \sqrt{1 + \frac{\hat{X}}{2\sqrt{E_0^2 - M_+^2}}}\right)^2 , \qquad (B.15)$$

with

$$\hat{X} \equiv \tilde{X} - \ln X \frac{\partial}{\partial E_0} \left(\frac{\left(E_0^2 - M_+^2/2\right) E_0}{\sqrt{E_0^2 - M_+^2}}\right). \qquad (B.16)$$

In the flat spacetime limit, this reduces to the real part of the previous result:

$$X_0 = \frac{\sqrt{E_0^2 - M_+^2}\,\tilde{X}}{E_0}. \qquad (B.17)$$

Let us use our initial wave-packet to calculate the initial probability current. For simplicity, we will work in the flat spacetime, nonrelativistic limit. Using the standard expression (2.91), as well as the definition $\tilde{X}_0 \equiv \tilde{X}\sqrt{2(E_0 - M_+)/M_+}$, one can express the current associated with the approximate X-Gaussian (B.11) as

$$J_0 = -\sigma_E \sqrt{\frac{2}{\pi}} \left(\frac{2(E_0 - M_+)}{M_+}\right)^{1/4} e^{\frac{-(X - \tilde{X}_0)^2}{2\sigma_X^2}}. \qquad (B.18)$$

Actually, we can simplify things more than that for arbitrary peak widths by taking advantage of the fact that we only care about what happens as $X \to X_\delta$: if we take the lower integration boundary for X-integrals to be $X = X_\delta$, then as $X \searrow X_\delta$, we have

$$\Psi_0 = N \int dE \frac{e^{i\tilde{X}(E - E_0)} e^{\frac{-(E - E_0)^2}{4\sigma_E^2}}}{\sqrt{\left|\frac{\partial E}{\partial P_{-+}}\right|}}. \qquad (B.19)$$

---

[9]Actually, there is a term logarithmic in X, but for the purpose of finding an approximate peak location we ignore the variation of this logarithm compared to $\sqrt{X}$ and X, since we work in the weak-field ($X \to \infty$) limit.

Let us change variables to $z = (1/2\sigma_E)(E - E_0 - 2i\sigma_E^2 \tilde{X})$. We can then express the initial state as

$$\Psi_0 = 2N\sigma_E\sqrt{\pi}e^{-\sigma_E^2\tilde{X}^2}e^{\frac{1}{4}\frac{d^2}{dz^2}}\left[\left|\frac{\partial E}{\partial P_{-+}}\right|^{-1/2}\right], \qquad (B.20)$$

evaluated at $z = 0$. We can similarly express the initial derivative (with respect to X) as

$$
\begin{aligned}
\Psi_0' &= 2iN\sigma_E e^{-\sigma_E^2\tilde{X}^2}\int dz P_{-+}\left|\frac{\partial E}{\partial P_{-+}}\right|^{-1/2}e^{-z^2} \\
&= iN_0 e^{\frac{1}{4}\frac{d^2}{dz^2}}\left[P_{-+}\left|\frac{\partial E}{\partial P_{-+}}\right|^{-1/2}\right], \qquad (B.21)
\end{aligned}
$$

for $N_0 \equiv 2N\sigma_E\sqrt{\pi}e^{-\sigma_E^2\tilde{X}^2}$.

We are then led to the probability current J_0 as $X \searrow X_\delta$ given by

$$J_0 = \frac{|N_0|^2}{M_+}\Re\left(N_+^*\tilde{N}_+\right), \qquad (B.22)$$

where $\Re$ indicates the real part and we have made the definitions

$$N_+ \equiv e^{\frac{1}{4}\frac{d^2}{dz^2}}\left|\frac{\partial E}{\partial P_{-+}}\right|^{-1/2} \qquad (B.23)$$

and

$$\tilde{N}_+ \equiv e^{\frac{1}{4}\frac{d^2}{dz^2}}\left(P_{-+}\left|\frac{\partial E}{\partial P_{-+}}\right|^{-1/2}\right). \qquad (B.24)$$

The initial current expression (B.22) is valid for arbitrary wave-packet widths, and can be generalized easily to include gravity. If our wave-packet is highly-peaked about a particular energy E_0, then the probability current takes the simpler form

$$J_{00} = -|N_0|^2. \qquad (B.25)$$

Now that we have parametric control over the localization of the initial state, we can propagate this state mode by mode through the interferometer. Each mode transforms in the same way as described in Chapter 2, and so one finds the final output states

$$\begin{pmatrix} \Psi_+^{(v)} \\ \Psi_-^{(v)} \end{pmatrix} = \int dE\, N_E \begin{pmatrix} \psi_+^{(v)} \\ \psi_-^{(v)} \end{pmatrix}, \qquad (B.26)$$

with the definitions

$$
N_E \;=\; Ne^{i(E-E_0)\tilde{X}}e^{\frac{-(E-E_0)^2}{4\sigma_E^2}}\,, \tag{B.27}
$$

$$
\psi_+^{(v)} \;=\; \psi_{++}\left(R_\leftarrow e^{i\Phi_{++}} R^\rightarrow e^{i\Phi_{-+}} R_\leftarrow \right.
$$
$$
\left. + T_\leftarrow e^{i\Phi_{--}} R^\leftarrow e^{i\Phi_{+-}} T_\rightarrow\right), \tag{B.28}
$$

$$
\psi_-^{(v)} \;=\; \psi_{--}\left(R_\leftarrow e^{i\Phi_{++}} R^\rightarrow e^{i\Phi_{-+}} T_\leftarrow \right.
$$
$$
\left. + T_\leftarrow e^{i\Phi_{--}} R^\leftarrow e^{i\Phi_{+-}} R_\rightarrow\right). \tag{B.29}
$$

Here, the mode functions are evaluated at X_δ.

How do the probability currents transform at the beam-splitter? The reflected and transmitted probability currents for the initial split can be calculated in the same way as the initial current, and the reflection and transmission coefficients can be written as

$$
\left| \frac{J_+^{(i)}}{J_0} \right| = \frac{\Re\left(N_+^{(i)*}\tilde{N}_+^{(i)}\right)}{\Re\left(N_+^*\tilde{N}_+\right)} \tag{B.30}
$$

and

$$
\left| \frac{J_-^{(i)}}{J_0} \right| = \frac{M_+}{M_-}\frac{\Re\left(N_-^{(i)*}\tilde{N}_-^{(i)}\right)}{\Re\left(N_+^*\tilde{N}_+\right)}, \tag{B.31}
$$

using the definitions

$$
N_+^{(i)} \;\equiv\; e^{\frac{1}{4}\frac{d^2}{dz^2}}\left(R_\leftarrow \left|\frac{\partial E}{\partial P_{++}}\right|^{-1/2}\right) \tag{B.32}
$$

$$
\tilde{N}_+^{(i)} \;\equiv\; e^{\frac{1}{4}\frac{d^2}{dz^2}}\left(R_\leftarrow P_{++} \left|\frac{\partial E}{\partial P_{++}}\right|^{-1/2}\right) \tag{B.33}
$$

$$
N_-^{(i)} \;\equiv\; e^{\frac{1}{4}\frac{d^2}{dz^2}}\left(T_\leftarrow \left|\frac{\partial E}{\partial P_{--}}\right|^{-1/2}\right) \tag{B.34}
$$

$$
\tilde{N}_-^{(i)} \;\equiv\; e^{\frac{1}{4}\frac{d^2}{dz^2}}\left(T_\leftarrow P_{--} \left|\frac{\partial E}{\partial P_{--}}\right|^{-1/2}\right). \tag{B.35}
$$

In the limit that our initial wave-packet is highly-peaked about an energy E_0, the reflection and transmission coefficients take the simpler forms

$$
\left| \frac{J_+^{(i)}}{J_0} \right|_0 = R_\leftarrow^2, \quad \left| \frac{J_-^{(i)}}{J_0} \right|_0 = T_\leftarrow^2. \tag{B.36}
$$

It is then easy to demonstrate that $R_{\leftarrow}^2 + T_{\leftarrow}^2 = 1$.

For arbitrary peak widths, things are not so simple. The time dependence of the probability currents implies that the output currents do not balance *at each point in time*, as they did in the stationary (single-mode) case. Thus, the continuity equation does not imply probability current conservation, and this makes our single-mode analysis inappropriate for the multi-mode system.

B.3   Fringe Visibility and Path Retrodiction

Unlike the probability current, the *total probability* is still conserved (in principle), even if our approximations break down in some regions of the parameter space and indicate otherwise. What will prove useful, then, in this time-dependent setting, are the "inner" and "outer" output probabilities, which are defined in the obvious way: the inner output probability (denoted by $\mathcal{P}_-$) is the probability of finding the shell on the inner side of the splitter ($X_- < X < X_\delta$) after recombination, and the outer output probability (denoted by $\mathcal{P}_+$) is the probability of finding the shell on the outer side of the splitter ($X_\delta < X < X_+$). To calculate $\mathcal{P}_-$ and $\mathcal{P}_+$, we can use the output states (B.26), except rather than evaluating the mode functions in the outputs at X_δ, we will need to integrate the magnitude-squared outputs in their respective regions:

$$\mathcal{P}_\pm = \pm \int_{X_\delta}^{X_\pm} dX \left| \Psi_\pm^{(v)} \right|^2 . \tag{B.37}$$

One must be careful, of course, to make sure enough time has elapsed after recombination so that all of the wave that will eventually transmit has transmitted, and similarly for the final reflected part.

How can we extract information about the coherence of the multi-mode system from these output probabilities? A simple approach is to use an analogy with a Mach-Zehnder interferometer: as we vary a system parameter (outer arm length, for instance), there is a phase shift induced between the different interferometric paths, and this affects how the waves interfere upon recombination [14]. Let us call this (generalized) phase shift $\delta\Phi$. We can then quantify the coherence in the system with a quantity $\mathcal{V}$, which is defined as the amplitude of the oscillation of $\mathcal{P}_+$ (or, equivalently, $\mathcal{P}_-$) as $\delta\Phi$ is varied. The quantity $\mathcal{V}$ is referred to as the "fringe visibility" (or just "visibility") of the interference pattern. Since the inner and outer output probabilities $\mathcal{P}_\pm$ necessarily take values between 0 and 1, the visibility $\mathcal{V}$ is

bounded from below by 0 (no visibility of the interference fringes) and from above by 1 (full visibility of the interference fringes).

In the version of the Mach-Zehnder described in [14], an internal degree of freedom is added to the particle used in the interferometer. Just as in Chapter 4, the evolution of the internal degree of freedom is defined with respect to the proper time of the particle, and therefore serves as a local clock. Without the internal degree of freedom, the standard Mach-Zehnder has maximal visibility ($\mathcal{V} = 1$), but after the internal degree of freedom is added the visibility is reduced due to the proper time evolution accumulating information about which path was taken through the interferometer. As the proper time evolutions of different interferometer paths become more and more dissimilar, the visibility goes down; however, another quantity, called the "distinguishability" and denoted by $\mathcal{D}$, goes up. The distinguishability quantifies the "which-way" information known about a system, in the sense of providing a measure of the probability of correctly predicting which path was taken through the interferometer (i.e. path retrodiction). Hence, there is a natural trade-off between path retrodictability and visibility of the interference pattern, and this is generally considered to be a manifestation of wave-particle duality.

For the Mach-Zehnder with an added internal degree of freedom, for instance, one can demonstrate that a *duality relation* holds, of the form $\mathcal{V}^2 + \mathcal{D}^2 = 1$. Duality relations like this one have been around at least as far back as the 1970s [84], and there have been various extensions, such as broadening the applicability to include asymmetric beam-splitting [85]. Still, even though some work has gone into quantifying coherence in a unified way (for a recent analysis, see [86]), there has been much confusion on the true meaning of the duality relations, and their connections to different forms of uncertainty principles. In particular, it is often claimed that the duality between visibility and distinguishability is conceptually distinct from the Heisenberg uncertainty principle (HUP), since several derivations of such duality relations existed in the literature that did not assume that the HUP holds.

Very recently, however, it was demonstrated that there was indeed a common conceptual origin of both the duality relations and the HUP [87], [88]. It was discovered that one can derive the various duality relations, as well the HUP, from a generalized uncertainty relation defined in terms of entropies. This so-called "entropic uncertainty" relation provides the conceptual link between the duality relations and the HUP that was previously absent in the literature.

A possible implication of this link is that it could potentially fill in the

gap in Penrose's argument between the time uncertainty induced by superposing geometries and the resulting decoherence, since it is currently unclear exactly how they are connected. An in-depth analysis of this possibility is beyond the scope of this appendix, and is the subject of future work.

Appendix C

The Exact WKB Phase

To facilitate the approximation schemes used in this thesis, it was necessary to use several asymptotic forms of the reduced phase space canonical momentum. The exact expression,

$$P_{\pm\tilde{\pm}} = -\sqrt{2HX} - X \ln\left(1 - \sqrt{\frac{2H}{X}} + \frac{\beta_{\pm\tilde{\pm}}}{X}\right), \qquad \text{(C.1)}$$

with the definitions

$$\beta_{\pm\tilde{\pm}} = \frac{h_{\tilde{\pm}} \mp \sqrt{h_{\tilde{\pm}}^2 - M_{\tilde{\pm}}^2 f}}{1 + \sqrt{\frac{2H}{X}}}, \qquad \text{(C.2)}$$

$h_{\tilde{\pm}} = H - \frac{M_{\tilde{\pm}}^2}{2X}$, and $f = 1 - 2H/X$, is often difficult to work with. For instance, the WKB state we make use of,

$$\psi_{\pm\tilde{\pm}} = \frac{e^{iI_{\pm\tilde{\pm}}}}{\sqrt{\left|\frac{\partial H}{\partial P_{\pm\tilde{\pm}}}\right|}}, \qquad \text{(C.3)}$$

has a phase (the "WKB phase") that involves the integral of the reduced canonical momentum:

$$I_{\pm\tilde{\pm}} = \int dX\, P_{\pm\tilde{\pm}}. \qquad \text{(C.4)}$$

We remind the reader that the first set $\pm$ indicates outgoing (for $+$) or ingoing (for $-$), whereas the second set $\tilde{\pm}$ indicates which side of the splitter location X_δ one is considering.

Rather than finding asymptotic expressions for the WKB phase, let us see how far we can get towards a more explicit exact expression. After integrating the square root term in (C.1) and applying some simple algebraic

manipulations we can write the WKB phase (C.4) as

$$I_{\pm\bar{\mp}} = -\frac{2}{3}X\sqrt{2HX} + \int dX\, X \ln\left(1 + \sqrt{\frac{2H}{X}}\right)$$

$$- \int dX\, X \ln\left(1 - \frac{2H}{X} + \frac{\left(h_\pm \mp \sqrt{h_\pm^2 - M_\pm^2 f}\right)}{X}\right). \quad (C.5)$$

One can notice that the first two terms on the right hand side of this equation are independent of the shell mass, and represent non-perturbative contributions to the WKB phase. The second of these two terms can be straightforwardly integrated to obtain

$$\int dX\, X \ln\left(1 + \sqrt{\frac{2H}{X}}\right) = \left(\frac{1}{2}X^2 - 2H^2\right)\ln\left(\sqrt{X} + \sqrt{2H}\right) - \frac{1}{2}XH$$

$$+ \left(H + \frac{1}{6}X\right)\sqrt{2HX} - \frac{1}{4}X^2 \ln X, \quad (C.6)$$

but the last term in expression (C.5) requires a bit more work. First we will separate out some factors of X in the argument of the logarithm, to get rid of inverse powers of X; then we can separate the logarithms and integrate the part that came from the factors of X. Suppressing indices for the moment, the remaining part involves the integral

$$\int dX\, X \ln\left(X^2 f + X\left(h \mp \sqrt{h^2 - M^2 f}\right)\right). \quad (C.7)$$

If we integrate by parts, this becomes

$$\frac{1}{2}X^2 \ln\mathcal{F} - \frac{1}{2}\int dX\, \frac{X^2 \frac{d\mathcal{F}}{dX}}{\mathcal{F}}, \quad (C.8)$$

for a function $\mathcal{F}$ defined by

$$\mathcal{F} = X^2 f + X\left(h \mp \sqrt{h^2 - M^2 f}\right). \quad (C.9)$$

Putting all the pieces together, we are led to the following expression for the WKB phase:

$$I = \sqrt{2HX}\left(H - \frac{X}{2}\right) - \frac{1}{2}XH - \frac{1}{4}X^2 + \left(\frac{1}{2}X^2 - 2H^2\right)\ln\left(\sqrt{X} + \sqrt{2H}\right)$$

$$+ \frac{1}{2}X^2 \ln\left(\frac{X^{3/2}}{\mathcal{F}}\right) + \frac{1}{2}\int dX\, \frac{X^2 \frac{d\mathcal{F}}{dX}}{\mathcal{F}}. \quad (C.10)$$

The terms are arranged such that the first line of (C.10) contributes to the phase in the same way as a massless dust shell, whereas the second line completely encodes the information about the special equation of state we make use of for the interferometry presented in several chapters of this thesis.

In the flat spacetime limit, the function $\mathcal{F}$ simplifies to

$$\mathcal{F} \to X^2 + X\,(H - P)\,, \tag{C.11}$$

with $P = \pm\sqrt{H^2 - M^2}$, and the last unevaluated integral in the WKB phase (C.10) is found to be

$$\int dX \, \frac{X^2 \frac{d\mathcal{F}}{dX}}{\mathcal{F}} \to X^2 + (H - P)\left[(H - P)\ln\left(X + H - P\right) - X\right]. \tag{C.12}$$

Of course, if we only care about the flat spacetime limit, we can start from the momentum $P = \pm\sqrt{H^2 - M^2}$, which immediately yields the phase $I = \pm\sqrt{H^2 - M^2}X$, or, for nonrelativistic speeds, $I \approx \pm\sqrt{2M(H - M)}X$. The utility of (C.12) presents itself when we search for approximations to the WKB phase that are more accurate than the usual perturbative approximations we were forced to use in this thesis for practical reasons; in other words, using our previous perturbation approach to correct (C.12) and inserting it into (C.10) provides us with a better approximation to the exact behaviour than would be obtained by exclusively using the perturbation approach.

If we really wish to be accurate, we can go one step further and perform the (somewhat challenging) integral (C.12) exactly. This is possible, and has been done (by the author), but will not be presented here due to the lengthy and unenlightening form of the result.[10]

---

[10] "I have discovered a truly remarkable proof of this proposition that this margin is too small to contain." [89]